LECTURE 2: NUCLEAR DEFORMATION

NUCLEAR STRUCTURE
STUDIED WITH
SPECTROSCOPY AND REACTIONS

A. Obertelli

CEA Saclay

TU Darmstadt, IKP, February 2017

Lecture 2: Nuclear Deformation

- **Deformation & nuclear shapes**
  - Symmetry breaking and nuclear shapes
  - The deformed harmonic oscillator and Nilsson models
  - Configuration mixing approaches
  - Observables: rotational models and quadrupole moments

- **Ground state deformation from hyperfine structure**

- **Low-energy Coulomb excitation**
  - First order calculation, second order and re-orientation effect
  - Physics case: **shape coexistence** in light Kr isotopes

- **Intermediate-energy Coulomb excitation**
  - Semi-classical description
  - Physics case: **island of inversion** and ^{32}Mg

- **Extreme quadrupole deformations**
  - Superdeformation and hyperderformation

- **higher order multipole moments**
  - Octahedral and thetrahedral shapes
  - Physics case: **octupole deformation** in ^{220}Ra

Symmetry breaking and deformation

- A symmetry is an **invariance** of H and observables under a given **transformation**
  Ex. spherical symmetry / rotation, isospin symmetry / proton-neutron exchange

- Nuclear deformation is a **spontaneous symmetry breaking**
  i.e. the Hamiltonian is invariant but the physical states are not (different from « explicite » SB)

- **Most nuclei are deformed**: deformation = correlations = gain in energy

- **(electric) quadrupole** (elongated) shape is the most encountered

Ellipsoide: $\left(\frac{x}{R_\perp}\right)^2 + \left(\frac{y}{R_\perp}\right)^2 + \left(\frac{z}{R_z}\right)^2 = 1$

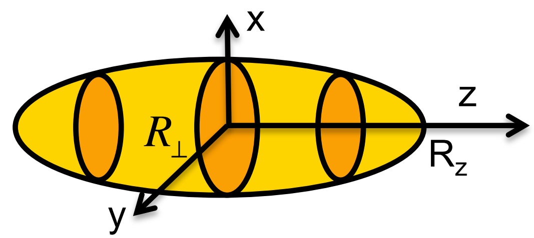

$$Q_0 = \frac{2}{5} Z e^2 \left(R_z^2 - R_\perp^2\right)$$

The intrinsic quadrupole moment Q_0 measures the deviation of an elliptical shape from a sphere

- Q moment of long-lived states can be measured from hyperfine spectroscopy
- Q moment of long & short-lived states can be measured from **low-energy Coulomb excitation**

- A nucleus with intrinsic deformation can **rotate**
  Its **spectrocopy** characterizes its collectivity and deformation

Parameterization of nuclear shapes

Generic nuclear shapes can be described by a development of spherical harmonics

$$R(\vartheta,\phi) = R_0\left[1 + \sum_{\lambda}\sum_{\mu=-\lambda}^{+\lambda} a_{\lambda\mu}\, Y_{\lambda\mu}(\vartheta,\phi)\right]$$

quadrupole $\quad a_{20} = \beta_2 \cos\gamma \qquad a_{22} = a_{2\,-2} = \frac{1}{\sqrt{2}}\beta_2 \sin\gamma$

$\mathbf{a_{\lambda\mu}}$: deformation parameters

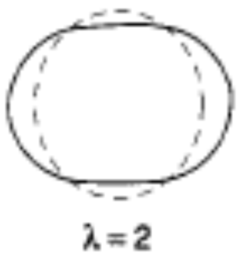

octupole

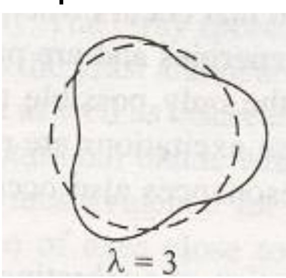

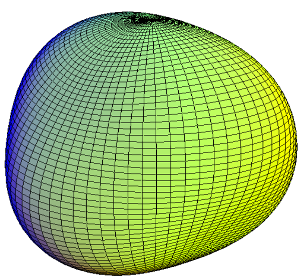

hexadecapole

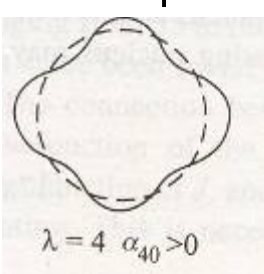

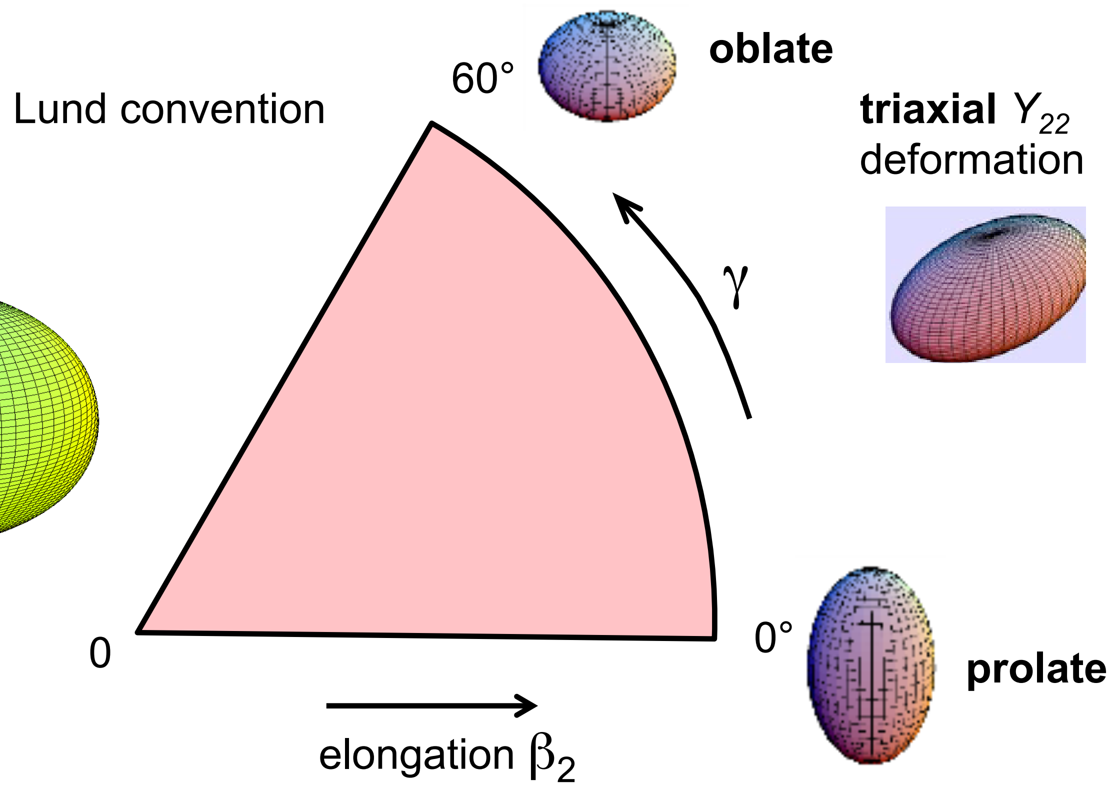

Spectroscopic quadrupole moment

Experiments measure the **maximum projection of the intrinsic electric quadrupole moment** along the quantization axis, which is different from the intrinsic electric Qpole

$$Q_s = Q_0 P_2(\cos\theta)_{m=I}$$

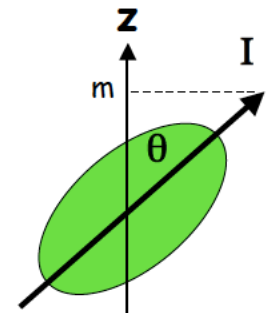

$Q>0$ $Q=0$ $Q<0$

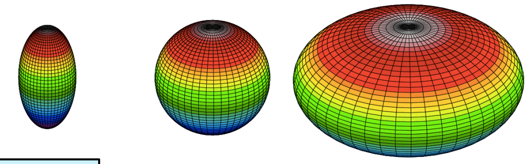

- By use of angular momentum algebra: $$\boxed{Q_s = Q_0 \frac{3K^2 - I(I+1)}{(I+1)(2I+3)}}$$

- K is the projection along the symmetry axis of the nuclear spin I.
  For spin I=0 and I=1/2 Qs vanishes even if the intrinsic shape is deformed

- The intrinsic moment Q_0 can be related to the elongation parameter β_2 :

$$Q_0 \approx \frac{3Zr_0^2}{\sqrt{5\pi}} \langle \beta^2 \rangle (1 + 0.36 \langle \beta^2 \rangle)$$

Quadrupole deformation

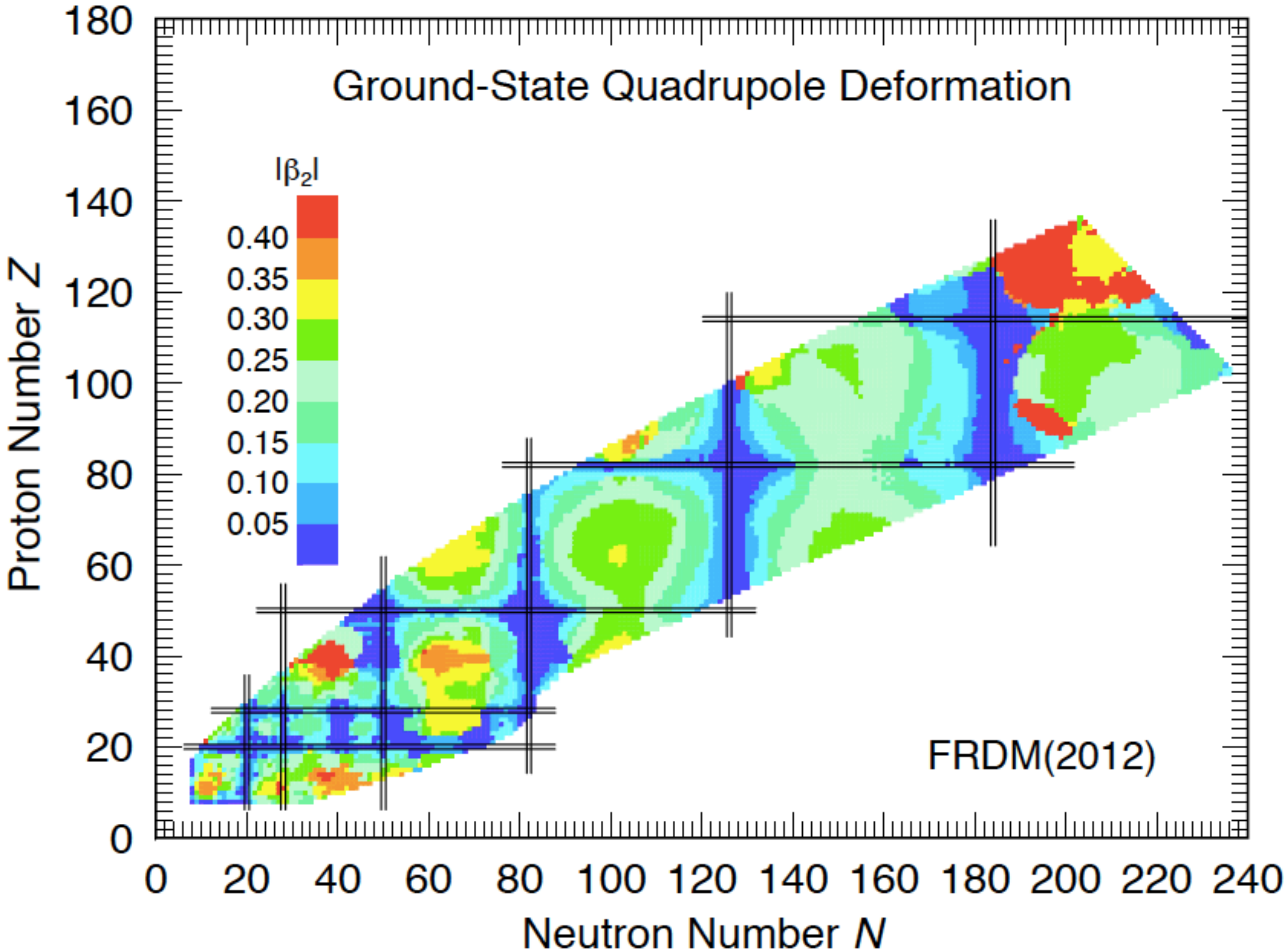

Macroscopic-microscopic model by P. Möller

Deformed harmonic oscillator potential

- axial symmetry:

$$\omega_\perp = \omega_0 e^{\alpha}, \quad \omega_z = \omega_0 e^{-2\alpha}$$

$$h = -\frac{\hbar^2}{2m}\Delta + \frac{m}{2}\omega_\perp^2(x^2+y^2) + \frac{m}{2}\omega_z^2 z^2$$

$\alpha>0$: prolate, $\alpha<0$:oblate

- Quantum numbers: $(n_\perp, n_z)$
- Degeneracy: $2(n_\perp+1)$
- Total energy of the system:

$$E(\alpha) = \sum_{i=1}^{N_F} \varepsilon_\Lambda^i(\alpha)$$

I. Hammamoto and B.R. Mottelson, PRC 79, 034317 (2009)
[Well bound nuclei, one type of fermions, no spin-orbit, no pairing]

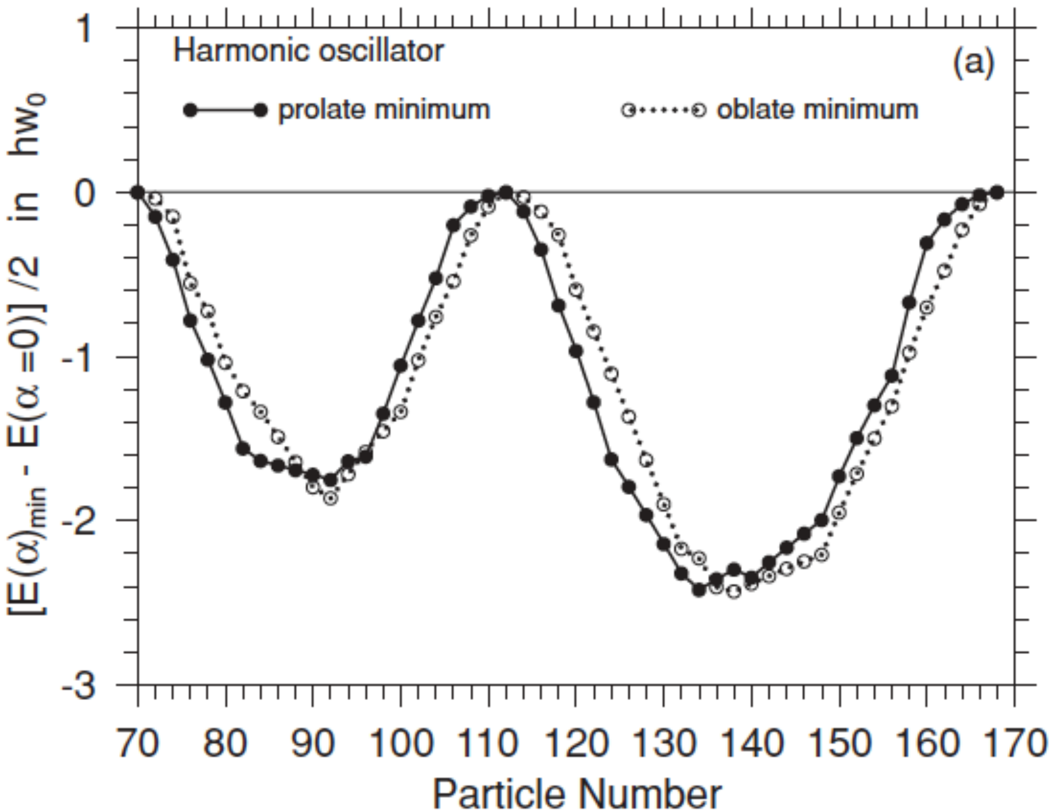

For Harmonic Oscillator, as many oblate that prolate ground states

Nilsson Hamiltonian: anisotropic one-body potential

- **Single-particle orbitals** in an **axially deformed potential** (z symmetry axis)

$$h = -\frac{\hbar^2}{2m}\Delta + \frac{m}{2}\omega_\perp^2(x^2+y^2) + \frac{m}{2}\omega_z^2 z^2 + C\vec{\ell}.\vec{s} + D\vec{\ell}^2$$

- Energy depends on the orientation (**projection of angular momentum**) of the wavefunction

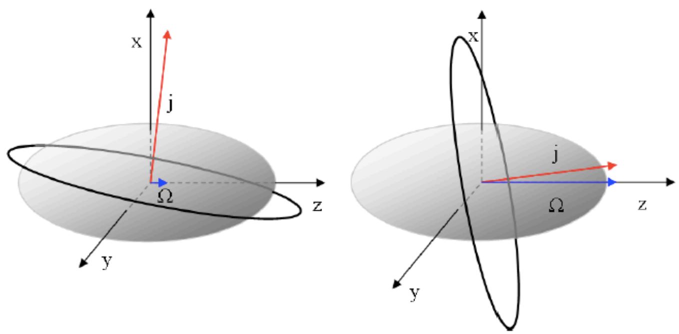

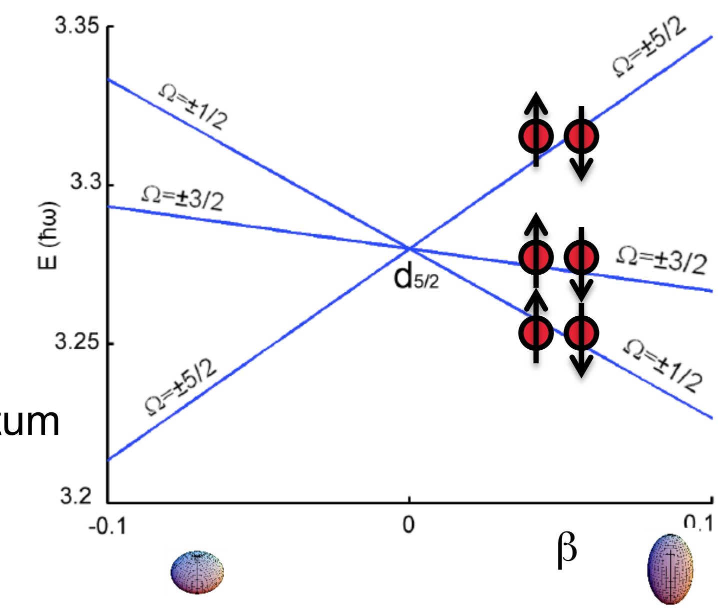

- At β≠0 total angular momentum is not a good quantum number, its projection Ω and parity π are.

- **Orbitals are indexed by Ωπ [Nn_zm_l]**.
  $\Omega = m_l + m_s = m_l \pm 1/2$
  N, n_z, m_l: **asymptotic quantum numbers** of axially-deformed harmonic oscillator

- **No crossing of two levels with same quantum numbers** (mixing)

Prolate dominance

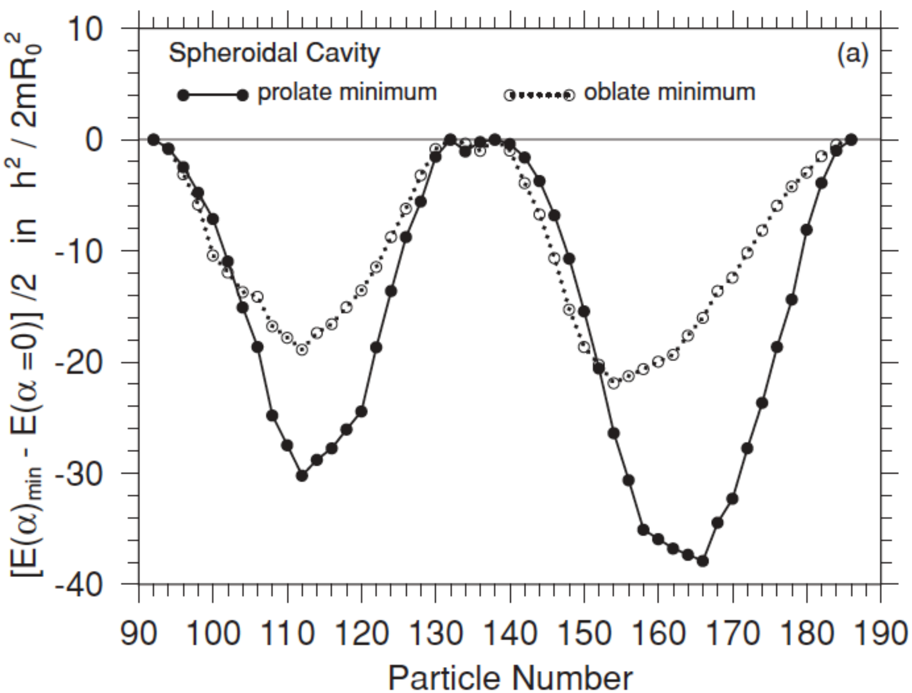

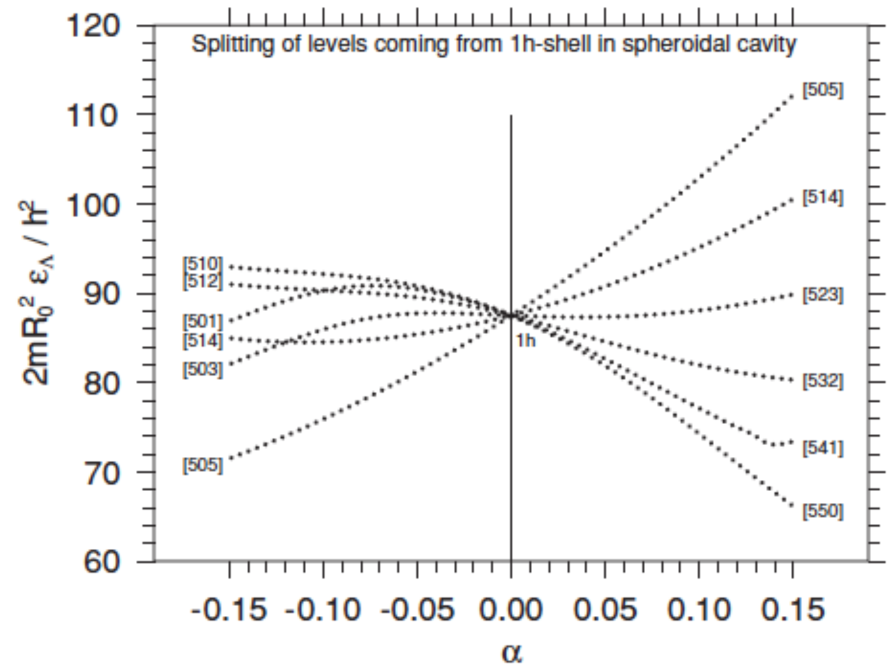

- ❑ **Prolate dominance due to sharp nuclear surface**
- ❑ Prolate dominance may be questioned for drip line or very heavy nuclei with softer surface

EDF and configuration mixing approaches

- **Variational approach** based on an **effective hamiltonian H**
- Ansatz for the wavefunction, *ex.* Slater determinants or quasiparticle vacuum

$$\varepsilon[\phi] = \frac{\langle\phi|H|\phi\rangle}{\langle\phi|\phi\rangle} - \lambda_Q \langle\phi|Q|\phi\rangle - \lambda_N \langle N\rangle - \lambda_Z \langle Z\rangle$$

$$Minimization:\ \delta\varepsilon[\phi] = 0$$

- **Projection method**, important quantum numbers: N,Z,J,P

Ex. $$P^N|\phi\rangle = \frac{1}{2\pi}\int_0^{2\pi} d\phi\, e^{i\phi(\hat{N}-N)}|\phi\rangle$$

- **Configuration Mixing** (multireference EDF)

$$Set\ \Omega_I \equiv \{|\phi(Q)\rangle\}$$ e.g. Q= collective coordinates

$$|\psi_\varepsilon^{JMNZP}\rangle = \int dQ \sum_{K=-J}^{J} f_\varepsilon^{JMNZP}(Q) P^N P^Z P^J_{MK} |\phi(Q)\rangle$$

$$Minimization:\ \delta\frac{\langle\psi|H|\psi\rangle}{\langle\psi|\psi\rangle} = 0$$ Hill-Wheeler equations

Hill-Wheeler equations

- The weight are determined by imposing $$\frac{\delta E}{\delta f^*} = 0$$

- Hill-Wheeler equation

$$\boxed{\int dQ' h(Q,Q') f_\varepsilon(Q') = E_\varepsilon \int dQ' n(Q,Q') f(Q')}$$

with $$n(Q,Q') = \left\langle \phi(Q) \middle| \phi(Q') \right\rangle$$ norm overlaps

and $$h(Q,Q') = \left\langle \phi(Q) \middle| H \middle| \phi(Q') \right\rangle$$

- The choice of the generating coordinates Q depends on the physics to be described
- Typically Q is a multipole moment of the mass distribution (quadrupole deformation $Q_{2\lambda}$)
- Resolution of HW equations by discretization of Q

- Approximation to HW equation: Bohr Hamiltonian and Gaussian Overlap Approximation

Deformed mean-field

Calculations and figures by Tomàs R. Rodriguez

Example: ^{32}Mg triaxial+TRSC

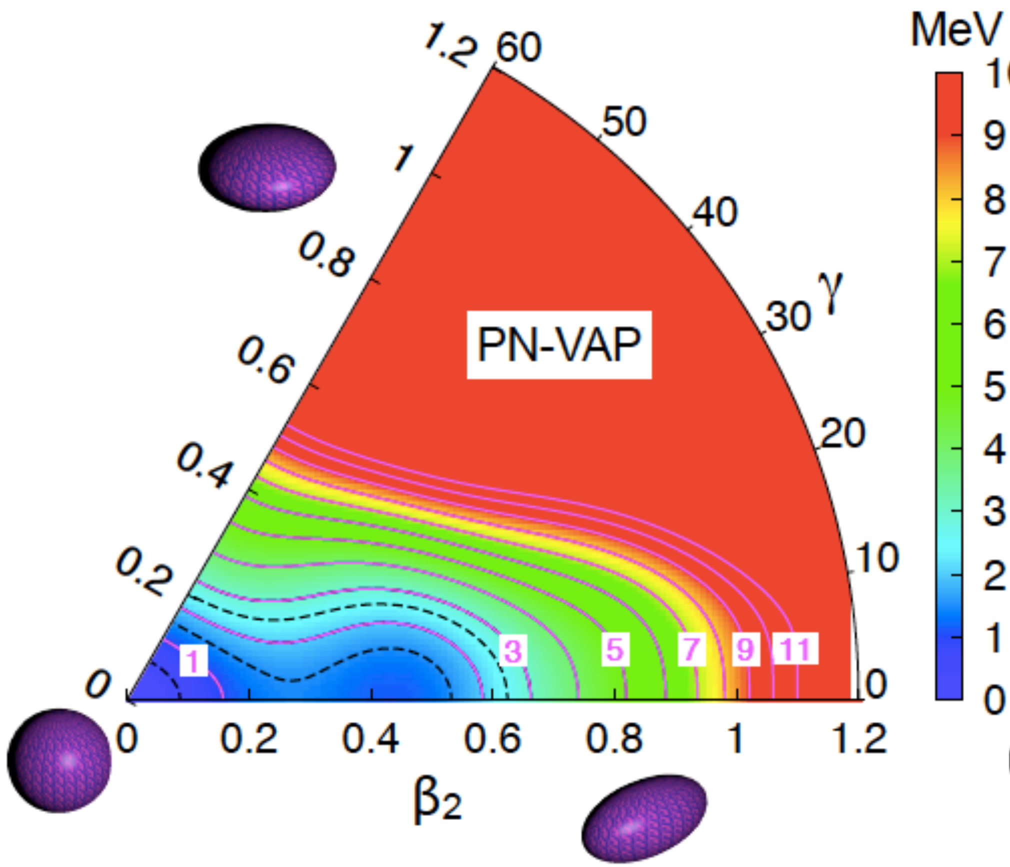

Potential energy surface

Collective wavefunctions and levels

Calculations and figures by Tomàs R. Rodriguez

Example: ^{32}Mg triaxial+TRSC

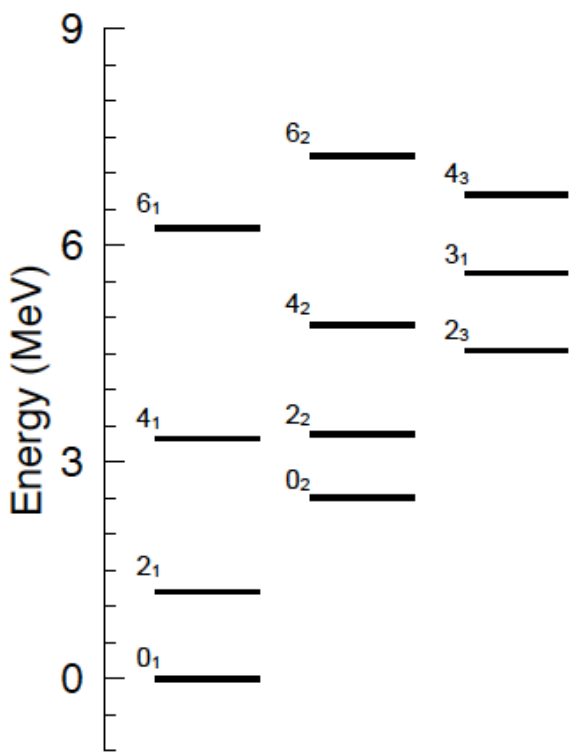

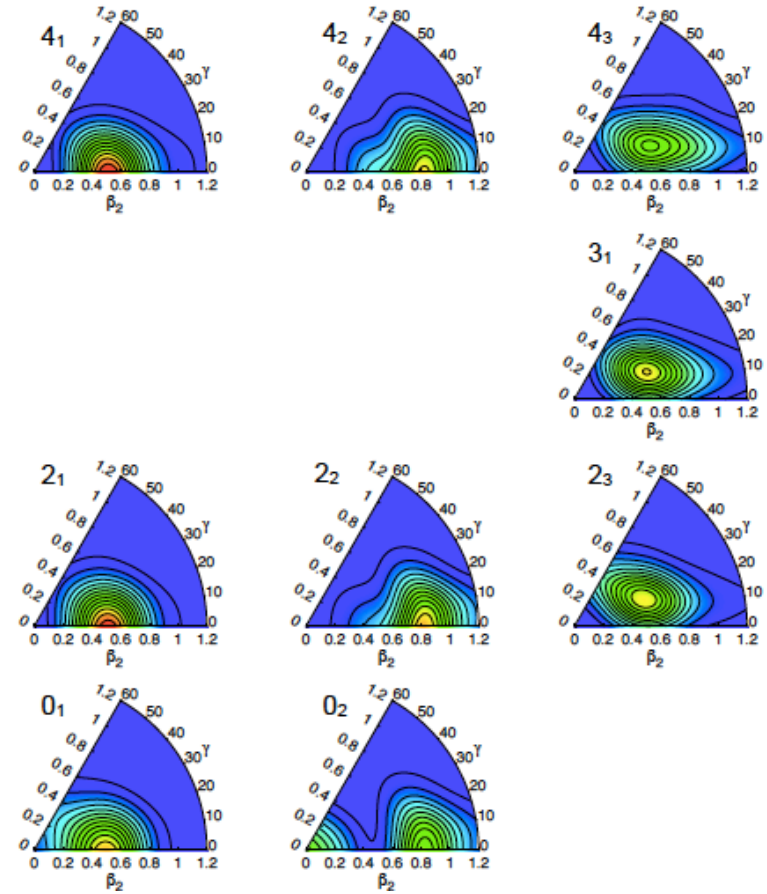

- level scheme, collective wavefunctions accessible
- further improvement: state-dependent moment of inertia (cranked states)

Magnesium isotopes

Calculations and figures by Tomàs R. Rodriguez

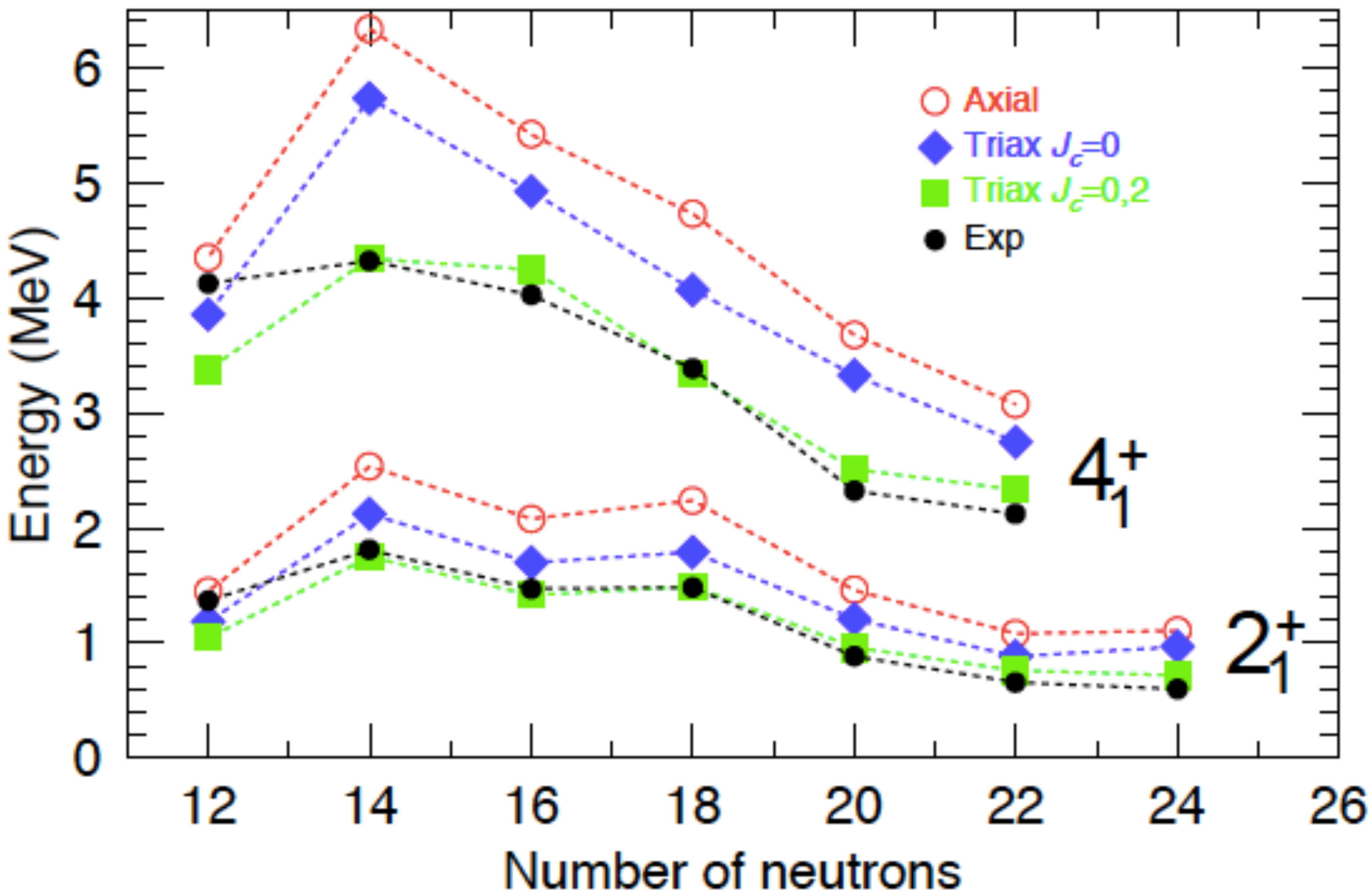

Dominance of prolate deformation over oblate

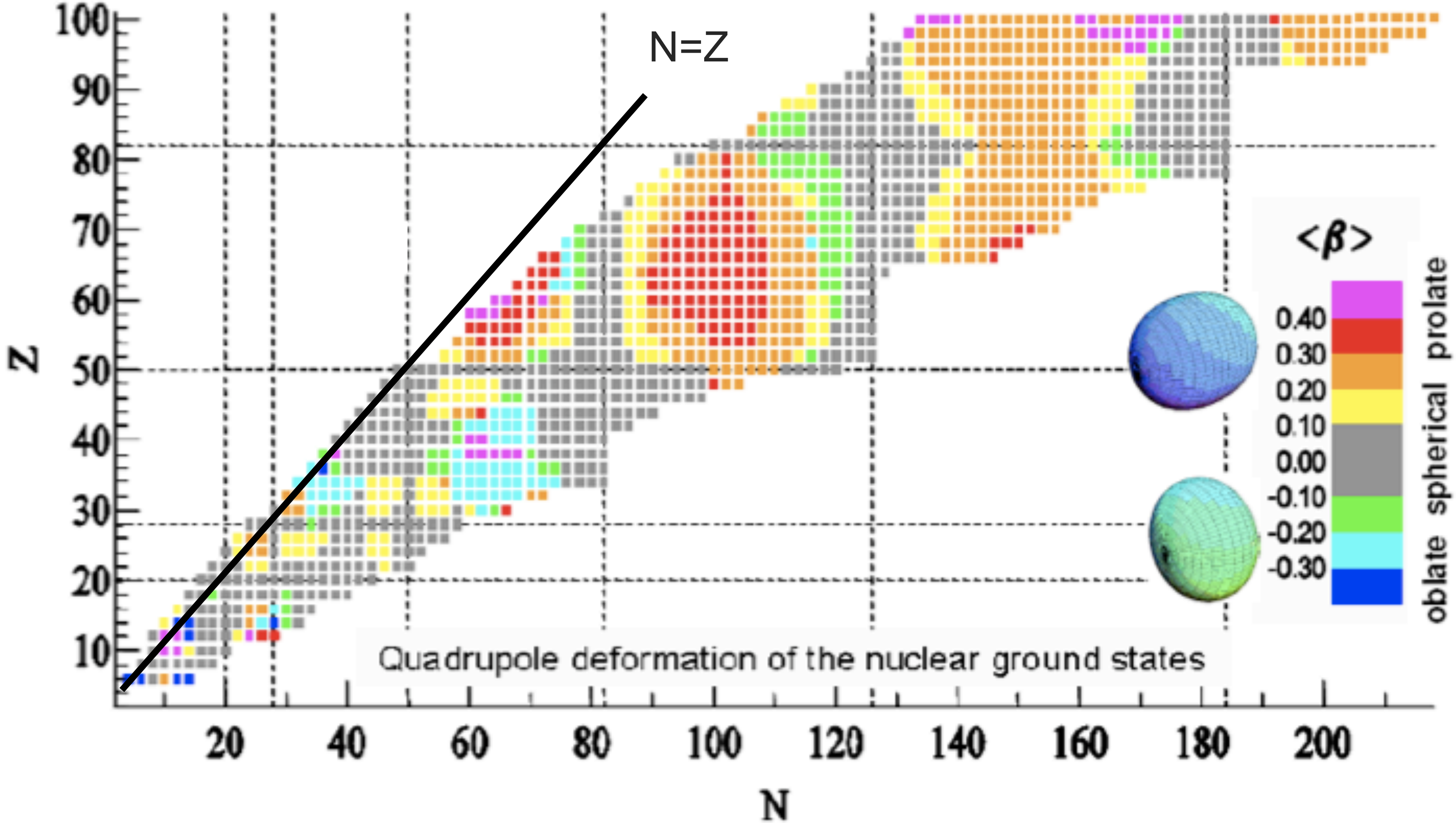

Mean-field calculations with the Gogny D1S effective interaction, M. Girod (CEA)

Hyperfine interaction in free atoms

- Hyperfine interaction = the interaction of nuclear magnetic and electric moments with electromagnetic fields

We will consider the fields created by an atomic orbit of spin J

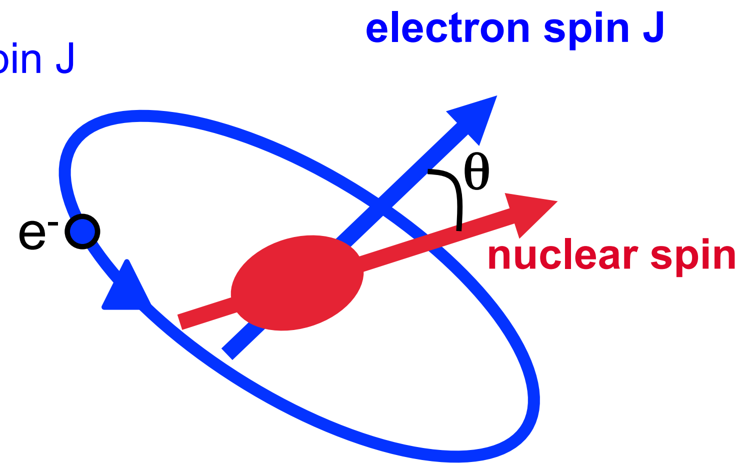

The atomic and nuclear spins couple to form
The total angular momentum **F**

$$\vec{F} = \vec{I} + \vec{J}$$

Each state **J** has several **F** substates

$$|I - J| \leq F \leq I + J$$

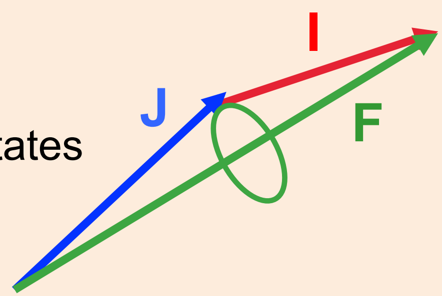

The energy shift caused by the interaction depends on the angle θ, thus for the same **I** and **J**, the different **F** states have slightly different energies

Magnetic dipole interaction $-\vec{\mu}.\vec{B}$ **Electric quadrupole interaction** $\frac{e}{4} Q_0 V_{JJ} P_2(\cos\theta)$

Hyperfine structure: magnetic dipole moment

- yesterday's lecture: fine structure of the nucleus and isotopic shifts

- The nucleus may have a non-zero spin I and therefore a magnetic moment μ.
  It results in a perturbation of the atomic levels due to spin – B field interaction

$$\boxed{-\vec{\mu}.\vec{B}}$$

- Energy shift of the atomic levels depend on the total spin F

$$\vec{F} = \vec{I} + \vec{J}$$

$$|I - J| \leq F \leq I + J$$

- Energy shift

$$\Delta E = \mu B_0 \left\langle \vec{I}.\vec{J} \right\rangle = \frac{A}{2} K$$

$$A = \frac{\mu B_0}{IJ}, \quad K = F(F+1) - I(I+1) - J(J+1)$$

B_0 magnetic field produced by the electron. Note that for I=0, there is no hyperfine structure

Hyperfine structure: magnetic dipole moment

- Typical value for the magnetic moment of a nucleus: nuclear **magneton**

$$\mu_N = \frac{e\hbar}{2m_p} = 3.15\times10^{-8}\ eV.T^{-1}$$

- Typical B field created by an electron orbital:

$$B = \frac{\mu_0 I}{2\pi R}$$

$$I \approx \frac{ev}{2\pi R}$$

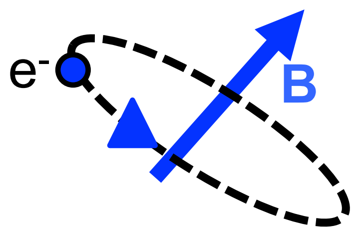

Inner orbital radius $R_n \approx a_0 = 5.2\ 10^{-11}$ m
Bohr velocity ($e^2/\text{hbar}=c\alpha$) $v=2.2\ 10^6\ m.s^{-1}$

$B \approx 4\pi\ 10^{-7}\ 1.6\ 10^{-19}\ 2.2\ 10^6 / (16\pi^2\ 25.\ 10^{-22}) = 1.1$ T

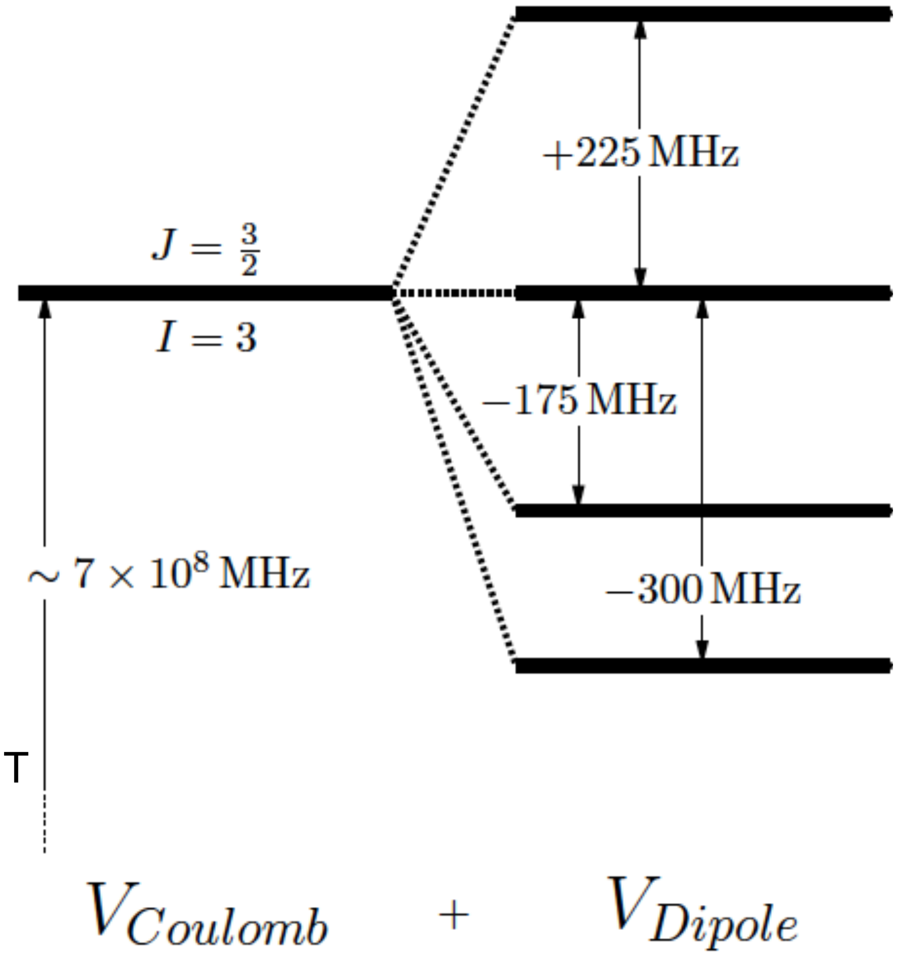

- Estimate of hyperfine energy shift:

$$\Delta E \approx \mu_N B = 3\,10^{-8}\,eV \Rightarrow \omega = \frac{\Delta E}{\hbar} \approx 50\ MHz$$

Hyperfine structure: magnetic dipole moment

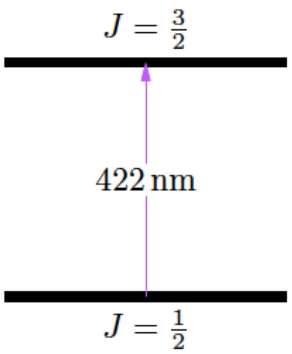

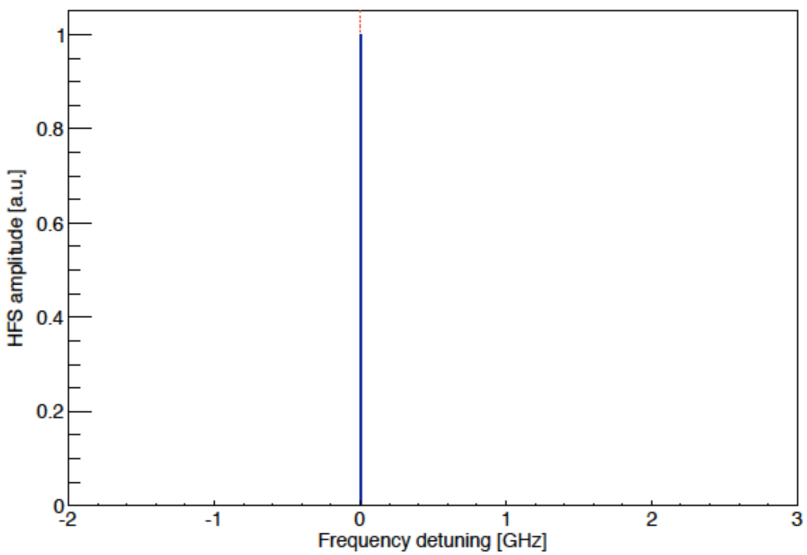

$I = 0$

From T.E. Cocolios, Joliot-Curie school 2015

Hyperfine structure: magnetic dipole moment

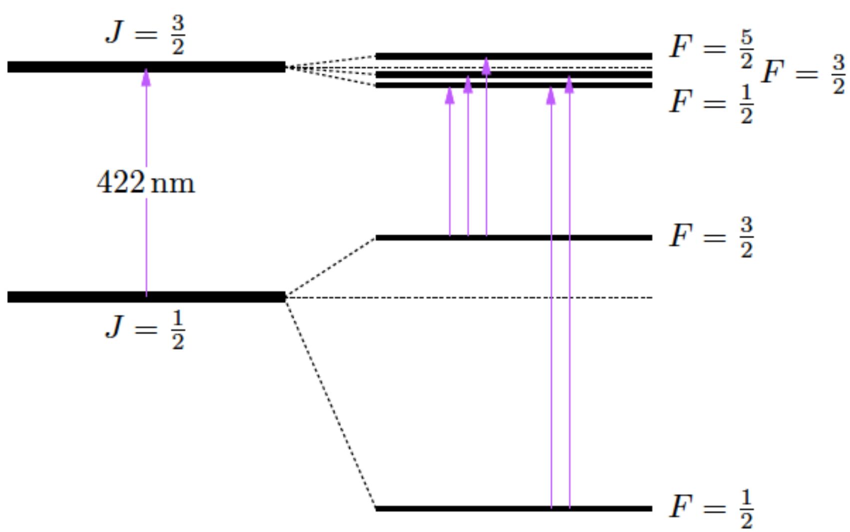

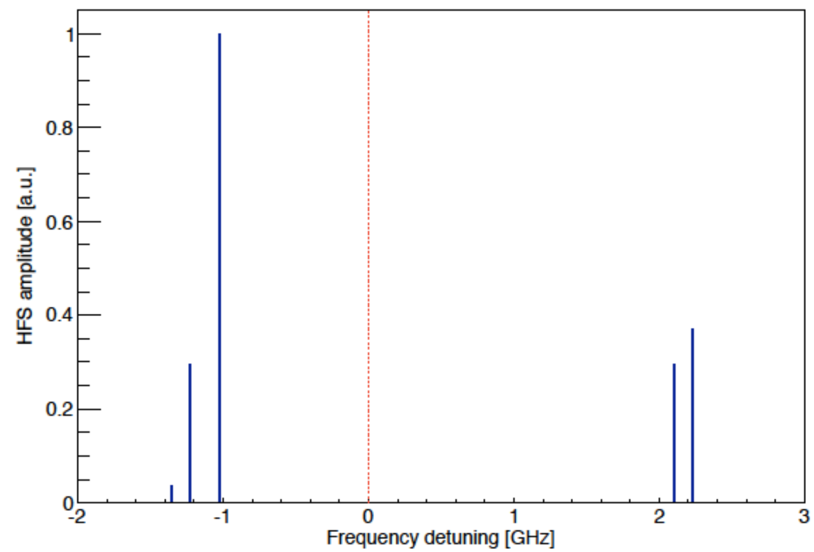

$I = 1$

From T.E. Cocolios, Joliot-Curie school 2015

Hyperfine structure: magnetic dipole moment

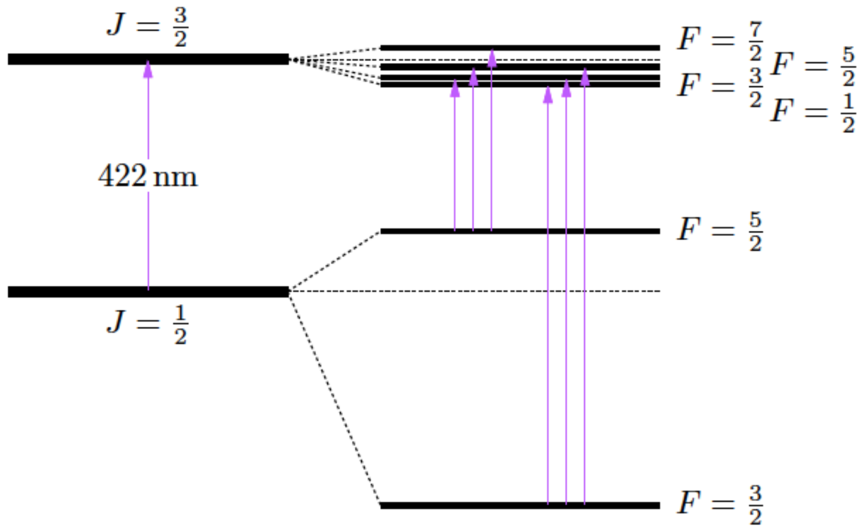

$I = 2$

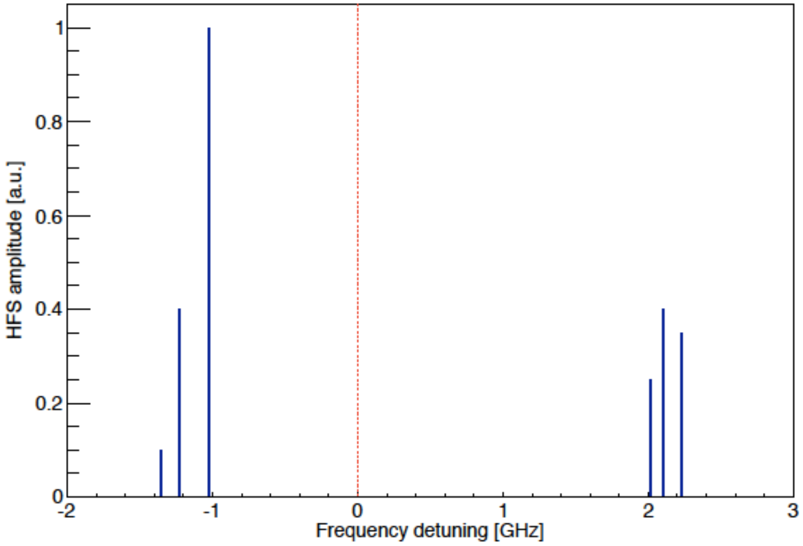

From T.E. Cocolios, Joliot-Curie school 2015

Electric quadrupole moment from hyperfine structure

In a **uniform field**, the energy of a quadrupole moment is independent of the orientation (angle). Therefore there is **no quadrupole interaction.**

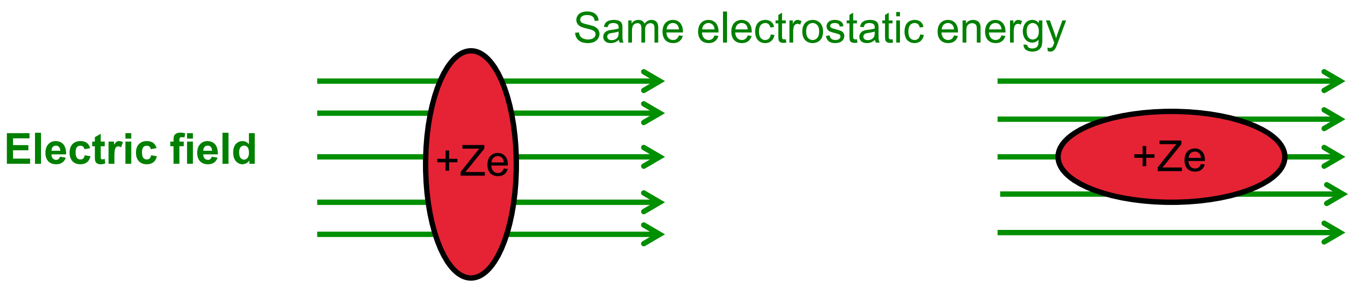

In an **electric field gradient**, there is an **angle dependence** of the energy. Therefore there is a **quarupole interaction**.

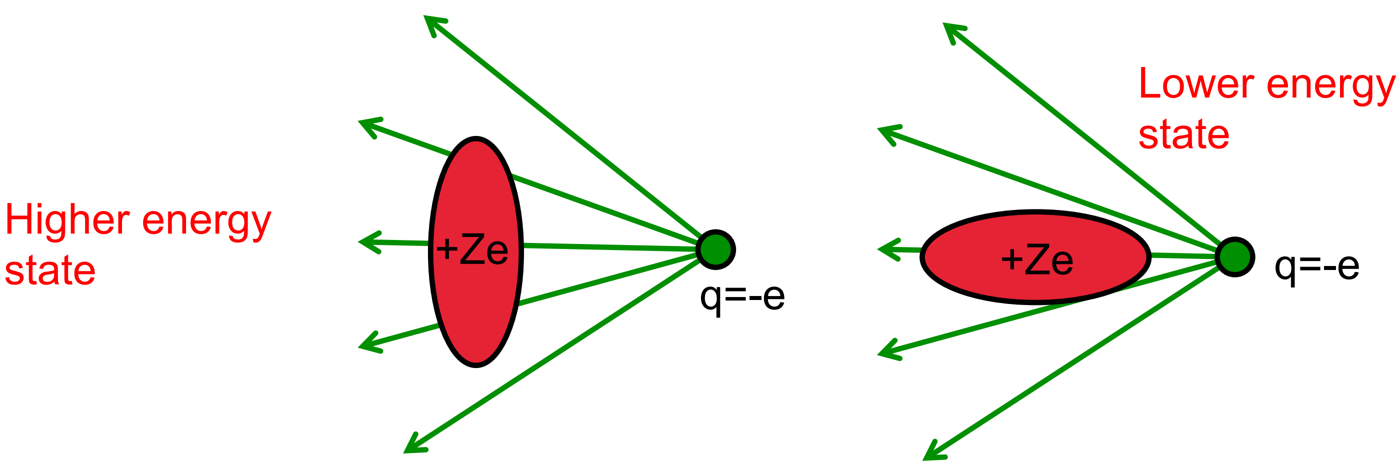

Slide concept from J. Billowes, Balkan school (2004)

Electric quadrupole moment

Electric quadrupole interaction

$$E = \frac{e}{4} Q_0 V_{JJ} P_2(\cos\theta)$$

Electric field gradient along the J direction due to atomic electrons.

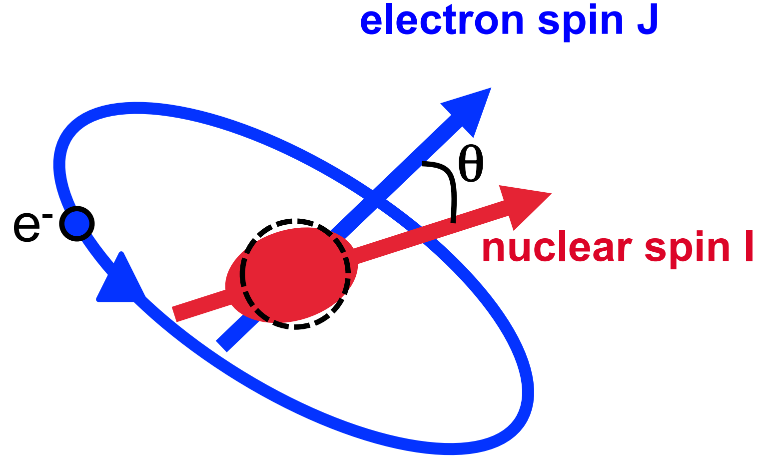

Energy shifts of the F states are then given by

$$\Delta E = \frac{B}{4} \frac{\frac{3}{2}C(C+1) - 2I(I+1)J(J+1)}{I(2I-1)J(2J-1)}$$

$$C = \left[F(F+1) - I(I+1) - J(J+1)\right]$$

$$B = eQ_s \left\langle \frac{\partial^2 V}{\partial z^2} \right\rangle = eQ_s V_{JJ}$$

Where **B** is the hyperfine factor measured in the experiment.
The electric field gradient $\mathbf{V_{JJ}}$ may be obtained from an isotope with known $\mathbf{Q_s}$

Summary: isotope shift and hyperfine structure

Point nucleus + Finite size nucleus + magnetic dipole + electric quadrupole + higher multipoles

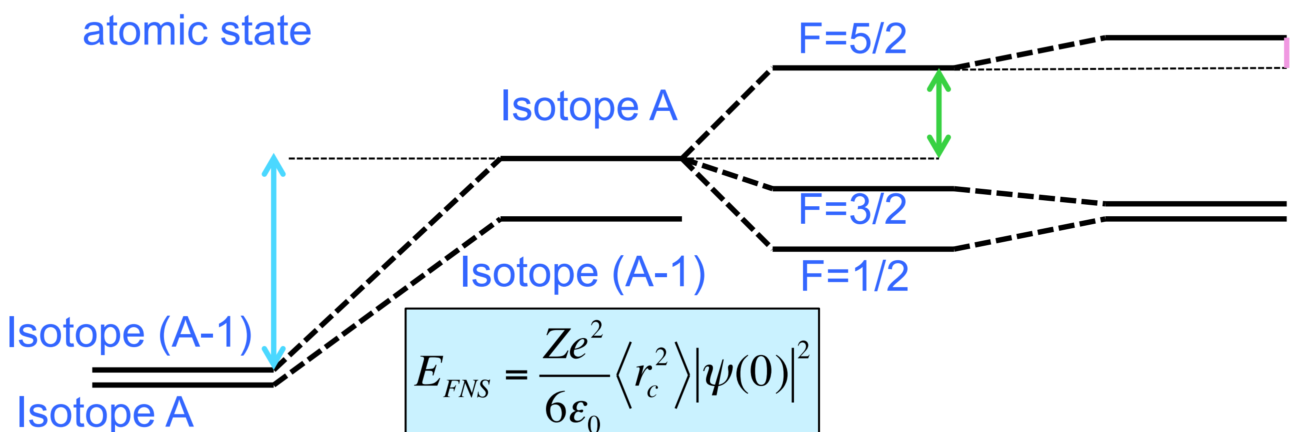

$$E_{FNS} = \frac{Ze^2}{6\varepsilon_0}\left\langle r_c^2 \right\rangle \left|\psi(0)\right|^2$$

$$\Delta E = \mu B_0 \left\langle \vec{I}.\vec{J} \right\rangle = \frac{A}{2}K$$ ≈100 MHz

$$E = \frac{e}{4} Q_0 V_{JJ} P_2(\cos\theta)$$ ≈10 MHz

- ❑ Energy shifts of hyperfine structure can be few ppm of the optical atomic transition energy
- ❑ A single optical transition is split into a number of hyperfine components

Quadrupole moment of Cu isotopes

- Spin, magnetic and Q moments of $^{61-75}$Cu at CERN/ISOLDE
- COLLAPS collinear laser spectroscopy setup
- Beams down to few 10^4 pps
- P. Vingerhoets *et al.*, Phys. Rev. C **82**, 064311 (2011)

- Fit of transition energies with an atomic level splitting given by:

$$E_F = \frac{1}{2}AC + B\frac{\frac{3}{4}C(C+1) - I(I+1)J(J+1)}{2I(2I-1)J(2J-1)}$$

with A proportional to magnetic moment, B to quadrupole moment

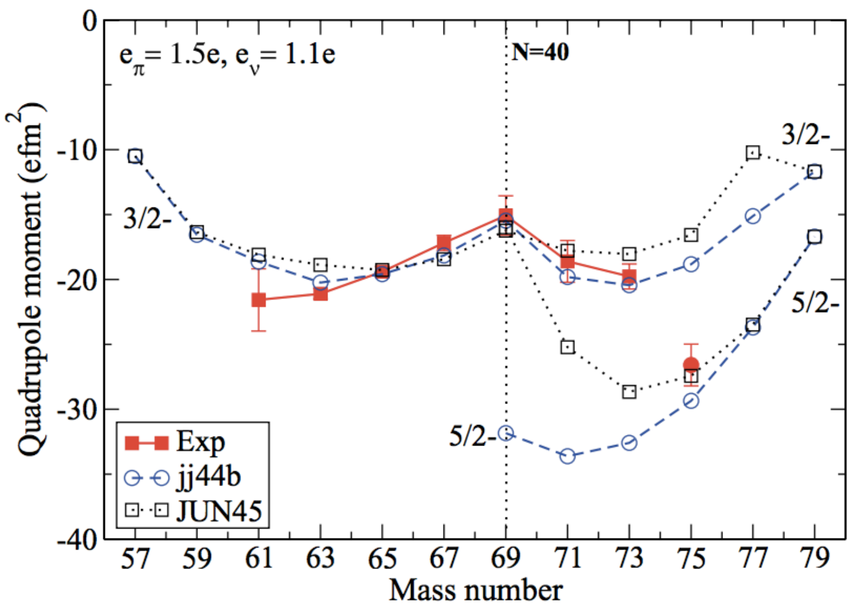

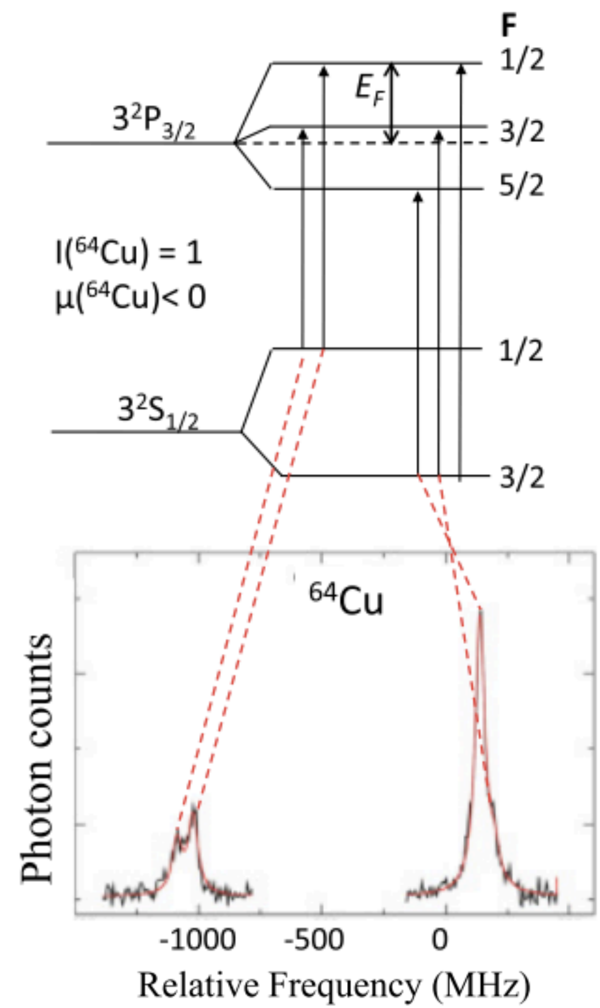

Externally applied fields

- ❑ For light elements where both field gradients and Q moments are small, usually transitions cannot be resolved. Need for **external field**.

- ❑ Different techniques exist (ground state or isomer Q-moment)

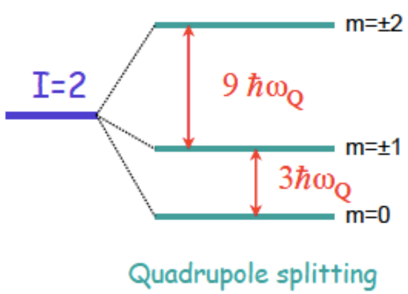

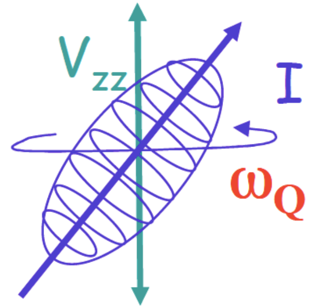

- ❑ **β-NQR** (beta Nuclear Quadrupole Resonance) method (ground state Q moment)
  - Implentation of a **spin-polarized** projectile
  - In a **crystal** where strong electric field gradient exist
  - Beta-decay assymetry is measured
  - **Scan** with a radiofrequency RF magnetic field
  - When RF reaches the quadrupole splitting, energy transitions occur
  - **Asymmetry is cancelled at the resonance**

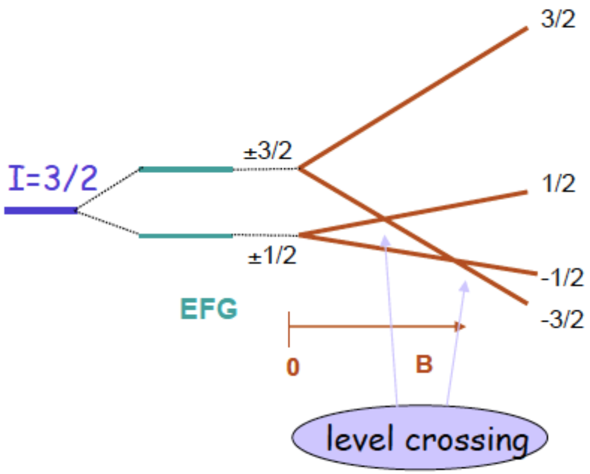

β-NQR with Lithium isotopes

- TRIUMF, A. Voss *et al.,* J. Phys. G: Nucl. Part. Phys. **41**, 015104 (2014)
- SrTiO3 crystal at 295 K
- High polarization of 60%-70%
- Transition frequencies proportional to V_{zz}:

$$\nu_{9,11} = 2\frac{eV_{zz}}{4h}\left|Q_{9,11}\right|$$

- Q_{11}/Q_9=1.0775(12)

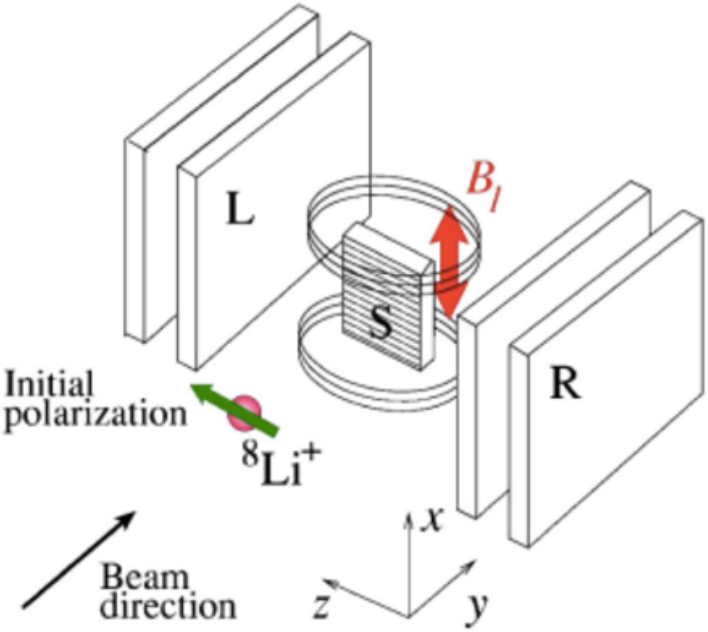

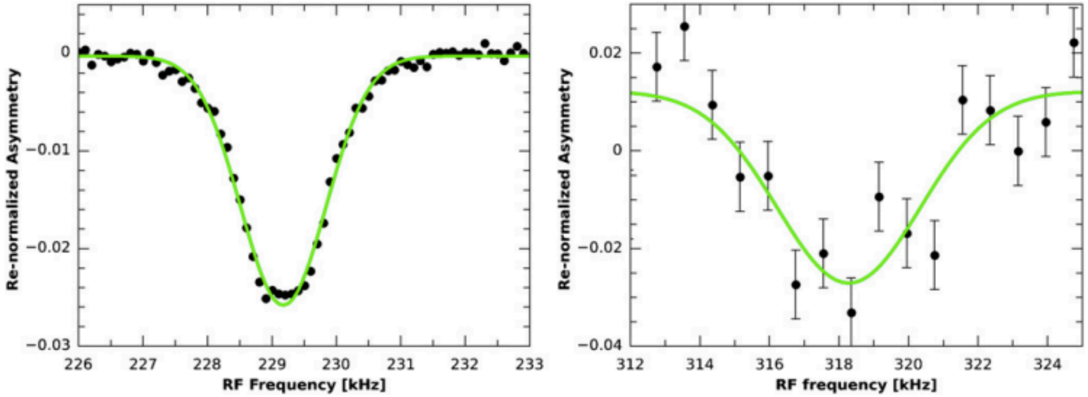

(a) ^{8}Li (b) ^{11}Li

Spectroscopy of axially deformed nuclei

- **Axial rotor** in quantum mechanics: rotation around the symmetry axis does not result in a new state **but** changes only the phase of the wavefunction

- Any rotation excitation involves rotation around an axis **perpendicular to the symmetry axis**

- Rotation and **classical mechanics**:

$$E = \frac{1}{2}\Im\Omega^2$$

$\Im$ moment of inertia

Ω angular velocity

or

$$\boxed{E = \frac{1}{2}\frac{L^2}{\Im}}$$

with $\vec{L} = \Im\vec{\Omega}$ kinetic angular momentum

Continuus $$\Im = \int \left\| \vec{n} \wedge \overrightarrow{OM} \right\|^2 \rho\, d^3 r$$

Discrete $$\Im = \sum m_i r_i^2$$

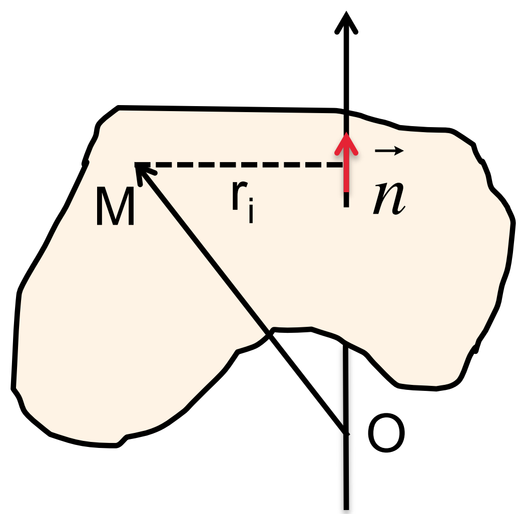

Rotor model for axially deformed nuclei

Quantum mechanics:

$$\boxed{E = E_0 + \frac{\hbar^2}{2\Im} I(I+1)}$$

$$L^2 |\phi\rangle = \hbar^2 I(I+1) |\phi\rangle$$

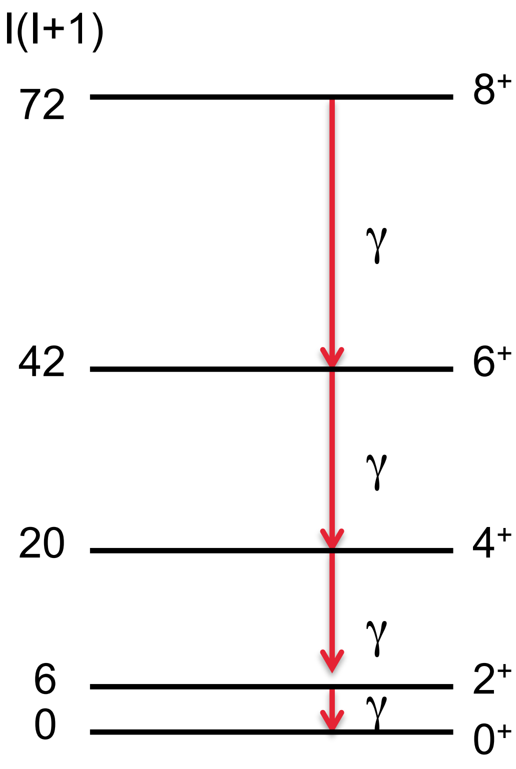

I+2 → I: E2 γ transitions

- for even-even nuclei (0^+ ground state) the collective wavefunction is given by rotational D_{IMK} matrices
- by symmetry, only **even spins with positive parity** are allowed ($0^+, 2^+, 4^+, \ldots$) for a 0^+ ground state
- Decay dominated by γ emission following conservation laws:

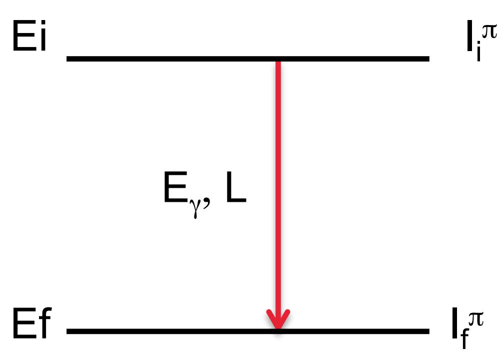

$$E_\gamma = E_i - E_f$$

$$|I_i - I_f| \le L \le I_i + I_f$$

$$\Delta\pi(EL) = (-1)^L$$

$$\Delta\pi(ML) = (-1)^{L+1}$$

Rotor model for axially deformed nuclei

Quantum mechanics:

$$E = E_0 + \frac{\hbar^2}{2\Im} I(I+1)$$

$$L^2 |\phi\rangle = \hbar^2 I(I+1)|\phi\rangle$$

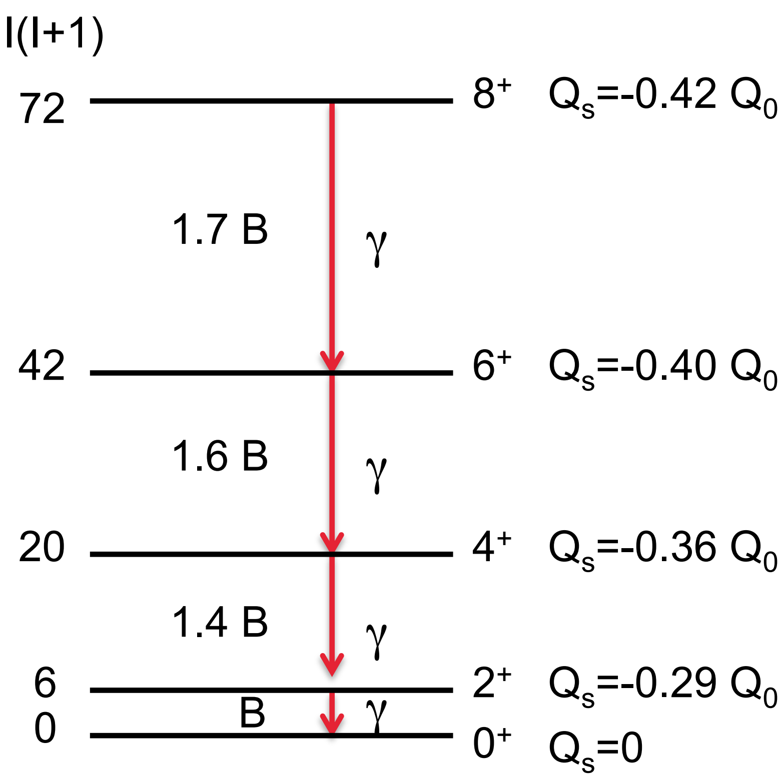

- **Moments of inertia** (from data):

Kinematic: $$\Im^{(1)} = \frac{\hbar^2 (2I+3)}{E_\gamma}$$

Dynamical: $$\Im^{(2)} = \left[\frac{1}{\hbar^2}\frac{d^2E(I)}{dI^2}\right]^{-1} \approx \frac{4\hbar^2}{\Delta E_\gamma}$$

- **Spectroscopic** quadrupole moment:

$$Q_s(I) = -Q_0 \frac{I}{2I+3}$$ (for K=0 band)

- Transition matrix elements B(E2):

$$B(E2; I \rightarrow I-2) = \frac{5}{16\pi} Q_0^2 \frac{3I(I-1)}{2(2I-1)(2I+1)}$$

Spectroscopy of axially deformed nuclei

Example: ^{238}**U** ground-state band

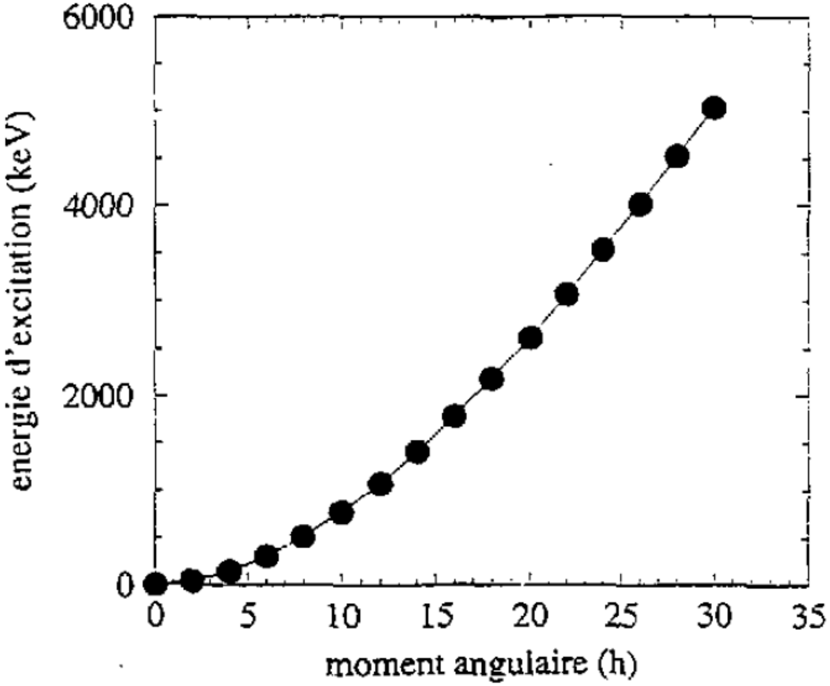

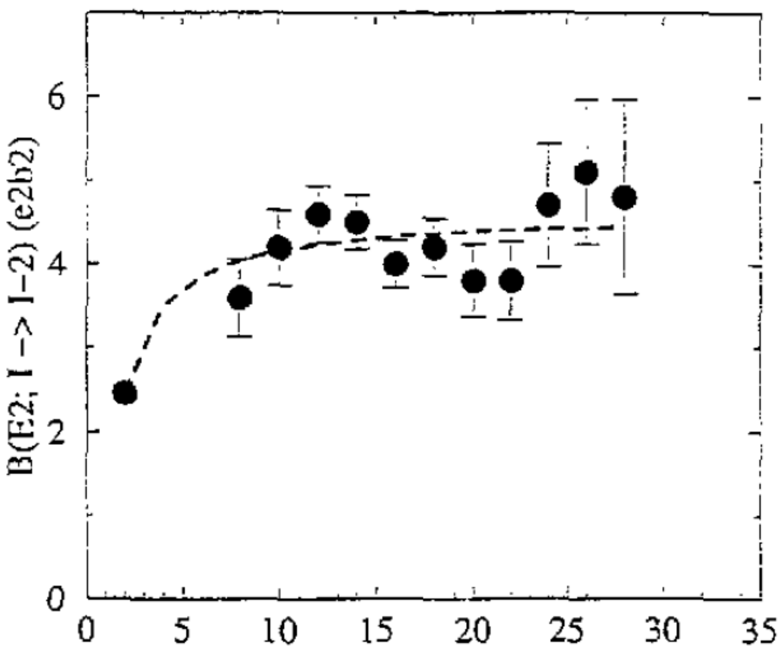

- At high spin, nucleon pairs may break through the **Coriolis** force
  ➔ increase of moment of inertia (**backbending**)

- Very deformed bands are also observed (**superdeformation**, R_z/R_{ortho}≈2)
- **Hyperdeformation** (R_z/R_{ortho}≈3) predicted but still to be evidenced experimentally

Transition matrix elements

Decay rate (s^{-1}):

$$T(\sigma\lambda; I_f \to I_i) = \frac{8\pi(\lambda+1)}{\lambda[(2\lambda+1)!!]^2}\frac{1}{\hbar}\left(\frac{E_\gamma}{\hbar c}\right)^{2\lambda+1} B(\sigma\lambda; I_f \to I_i)$$

$$\frac{1}{\tau_f} = \sum_{\sigma\lambda I_i} T(\sigma\lambda; I_f \to I_i)$$

$$B(E2) \propto \left|\langle \mathrm{I_f} \| \mathrm{M(E2)} \| \mathrm{I_i} \rangle\right|^2$$

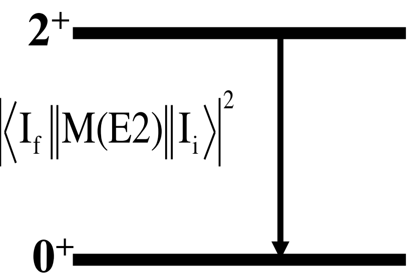

$2^+ \rightarrow 0^+$ decay via E2 transition

$$\tau\,(ns) = \frac{1}{1.22\, E_\gamma^5\, B(E2;\downarrow)}$$

E_γ in Mev, B(E2) in e^2fm^4

Three methods:

- **Low-energy coulomb excitation** (next slides)
- **Lifetime measurement** (see Damian Ralet's lecture)
  - > 100 ns : implantation and timing
  - 10 ps to few 100 ns : in flight (fast) timing
  - 1 ps to 100 ps: plunger, Recoil Distance Doppler Shift method (RDDS)
  - 0.01 ps to 1 ps: Doppler Shift Attenuation method (DSAM)
- **Intermediate-energy coulomb excitation** (suited to low-RIB intensities)

Coulomb excitation

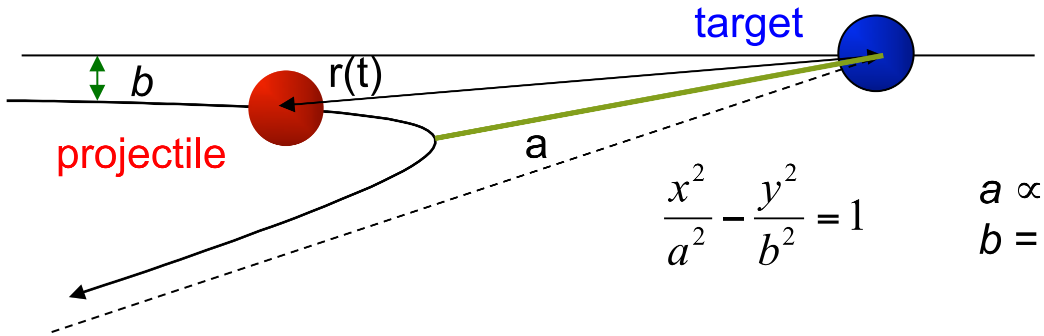

$$\frac{x^2}{a^2} - \frac{y^2}{b^2} = 1$$

$a \propto$ beam energy
b = impact parameter

- **Elastic scattering of charged particles** under the influence of the Coulomb field

$$V_{\text{int}}(t) = \frac{Z_P Z_T e^2}{r} \quad with \quad r(t) = \left| \vec{r}_1(t) - \vec{r}_2(t) \right|$$

➔ hyperbolic relative motion of the reaction partners

- **Rutherford** cross section

$$\frac{d\sigma}{d\Omega} = \frac{Z_1 Z_2 e^2}{E_{cm}^2} \times \frac{1}{\sin^4(\theta_{cm}/2)}$$

valid as long as $E_{cm} = m_0 v^2 = \frac{m_P \cdot m_T}{m_P + m_T} v^2 << V_c = Z_1 Z_2 e^2 / R_{int}$

- **Inelastic cross section**

$$\boxed{\left.\frac{d\sigma}{d\Omega}\right|_{Ruth} \times P_{i \to f}}$$

Coulomb excitation: how to calculate P_{if}?

1) Solving the time-dependent Schrödinger equation:

$$i\hbar\, d\psi(t)/dt = [H_P + H_T + V(r(t))]\, \psi(t)$$

$H_{P/T}$: free Hamiltonian of the projectile/target nucleus
V(t) : the time-dependent electromagnetic interaction

2) Expanding $\psi(t) = \sum_n a_n(t)\, \phi_n$ with ϕ_n as the eigenstates of $H_{P/T}$ leads to a set of coupled equations for the time-dependent excitation amplitudes $a_n(t)$

$$i\hbar\, da_n(t)/dt = \sum_m \langle \phi_n | V(t) | \phi_m \rangle \exp[i/\hbar\, (E_n - E_m)\, t]\, a_m(t)$$

3) The transition amplitude b_{nm} are calculated by the (action) integral

$$b_{nm} = i\hbar^{-1} \int \langle a_n \phi_n | V(t) | a_m \phi_m \rangle \exp[i/\hbar\, (E_n - E_m)\, t]\, dt$$

4) Finally leading to the excitation probability $P(I_n \rightarrow I_m) = (2I_n+1)^{-1} b_{nm}^{2}$

Low-energy Coulomb excitation: first order

First order applicable if only one state is excited, e.g. $0^+ \rightarrow 2^+$ excitation, and for small excitation probability (e.g. semi-magic nuclei)

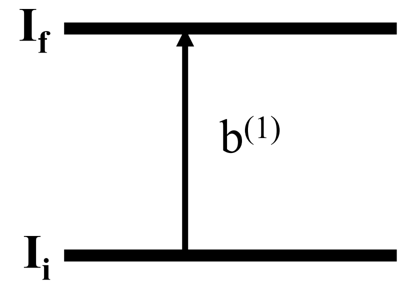

$$b^{(1)} \propto \langle I_f \| M(E2) \| I_i \rangle$$

1st order transition probability for multipolarity λ :

$$P^{(1)}_{i\to f}(\vartheta,\xi) = (2I_i+1)^{-1} |\, b^{(1)}_{i\to f}(\vartheta,\xi)\,|^2 = (2I_i+1)^{-1} |\,\chi^{(\lambda)}_{i\to f}|^2 R^2_\lambda(\vartheta,\xi)$$

with

$$\chi^{\lambda}_{i\to f} = \frac{\sqrt{16\pi}(\lambda-1)!}{(2\lambda+1)!!}\left(\frac{Z_{T/P}e}{\hbar v_i}\right)\frac{\langle i\,|\,M(E\lambda)\,|\,f\rangle}{a^{\lambda}\sqrt{2I_i+1}}$$

Strength parameter

$$R^2_\lambda(\vartheta,\xi) = \sum_\mu |\,R_{\lambda\mu}(\vartheta,\xi)\,|^2$$

Orbital integrals

$$\xi = \xi_{if} = \frac{Z_1 Z_2 e^2}{\hbar}\left(\frac{1}{v_f} - \frac{1}{v_i}\right)$$

Adiabacity parameter

Low-energy Coulex: second order

becomes necessary if **several states** can be excited from the ground state
or when **multiple excitations** are possible, i.e. for larger excitation probabilities

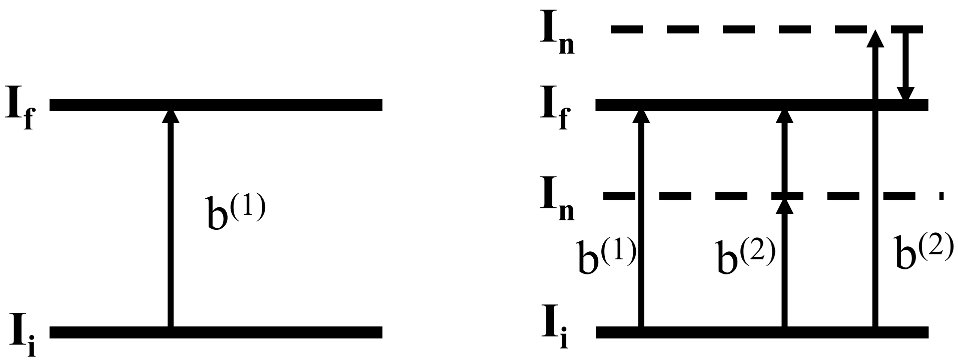

1st order:

$$b^{(1)} \propto \langle I_f \| M(E2) \| I_i \rangle$$

2nd order:

$$b^{(2)} \propto \sum_n \langle I_f \| M(E2) \| I_n \rangle \langle I_n \| M(E2) \| I_i \rangle$$

2nd order transition probability:

$$P^{(2)}_{i \to f}(\vartheta, \xi) = (2I_i + 1)^{-1} \sum_{m_i m_f} | b^{(2)}_{if} |^2 \quad \text{with } b^{(2)}_{if} = b^{(1)}_{if} + \sum_n b_{inf}$$

Low-energy Coulex: second order and re-orientation

Specific case of second order perturbation theory

where the „intermediate“ states are the **m substates** of the state of interest

2^nd order excitation probability for 2^+ state :

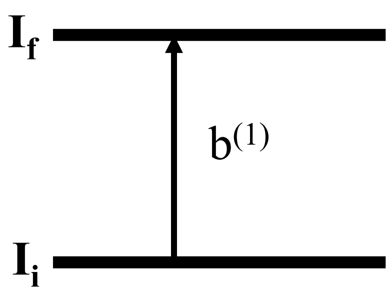

1^st order:

$$b^{(1)} \propto \langle I_f \| M(E2) \| I_i \rangle$$

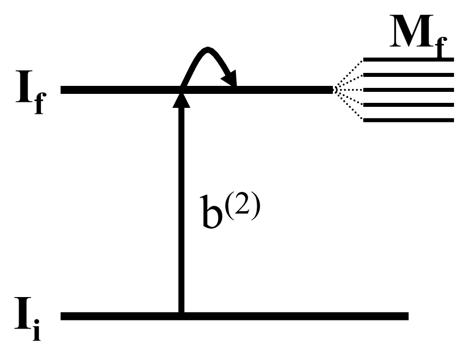

reorientation effect:

$$b^{(2)} \propto \langle I_f \| \boldsymbol{M}(E2) \| I_f \rangle \langle I_f \| \boldsymbol{M}(E2) \| I_i \rangle$$

$$P^{(2)}_{i\to f}(\vartheta,\xi) = |\chi^{(2)}_{i\to f}|^2 R^2_\lambda(\vartheta,\xi) \left[1 + \chi^{(2)}_{f\to f}\, c(\vartheta,\xi)\right]$$

$$\text{with } \chi^{(2)}_{f\to f} = \frac{1}{2}\sqrt{\frac{7}{10}}\,\frac{e^2}{\hbar c}\,\frac{Z_{P/T}}{v_\infty/c}\,\frac{\boxed{Q_f}}{a^2}$$

Spectroscopic quadrupole moment (and **its sign**)

➔ **Disentangle prolate and oblate shapes**

High-resolution gamma spectrometers

Resolving Power
(relative intensity limit)

Scintillator array (*ex.* BaF_2, NaI, Cs(I), $LaBr_3$)

$\sigma_E \approx$ 3-10% FWHM
$\varepsilon_{ph} \approx$ 50%
$\Omega \approx$ 80%
$\Delta\theta \approx 5^o$-15^o

- poor energy resolution
- poor opening angle

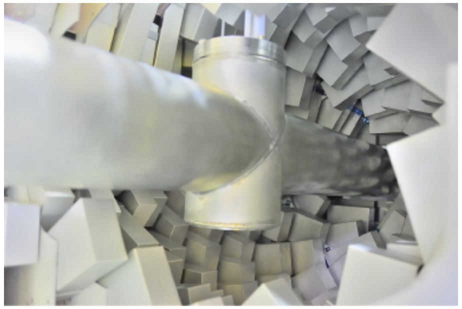

DALI2, RIKEN

1

Compton Shielded Ge

$\sigma_E \approx$ 0.2% FWHM
$\varepsilon_{ph} \approx$ 10%
$\Omega \approx$ 40%
$\Delta\theta \approx 8^o$
ε_{ph} for M_γ=30 :7%

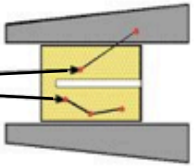

- scattered γ-rays lost
- poor definition of incident angle
- solid angle coverage limited by compton shields

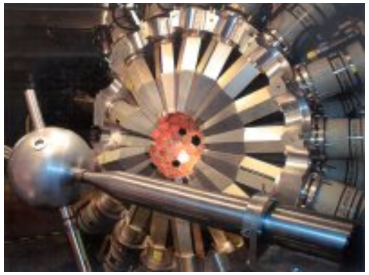

Gammasphere, ANL, USA

10^4

Ge Tracking Array

$\sigma_E \approx$ 0.2% FWHM
$\varepsilon_{ph} \approx$ 50%
$\Omega \approx$ 80%
$\Delta\theta \approx 1^o$
ε_{ph} for M_γ=30 : 40%

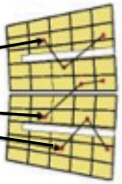

Combination of:
- segmented detectors
- pulse shape analysis
- γ-tracking

AGATA demonstrator, EU

10^7

Physics case: shape coexistence in light Kr isotopes

Energy

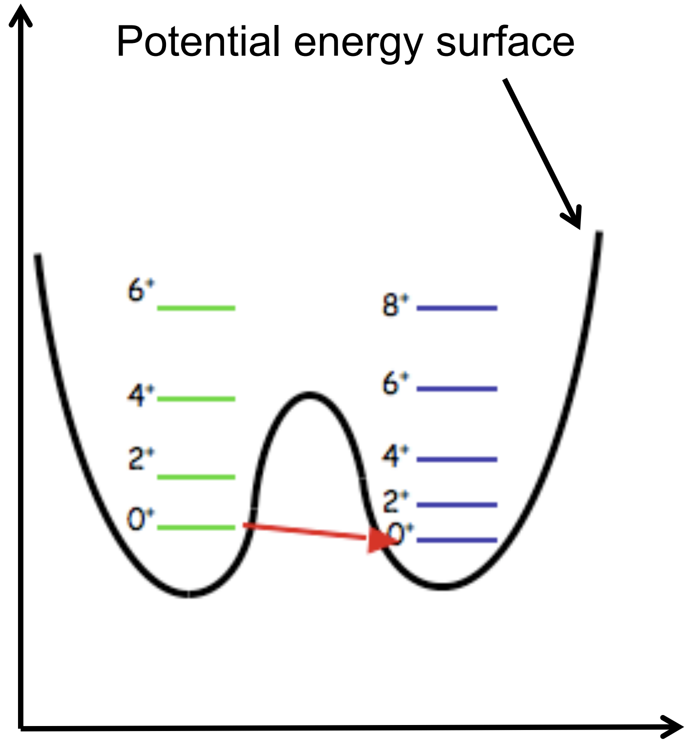

deformation (axial β_2)

Axial symmetry

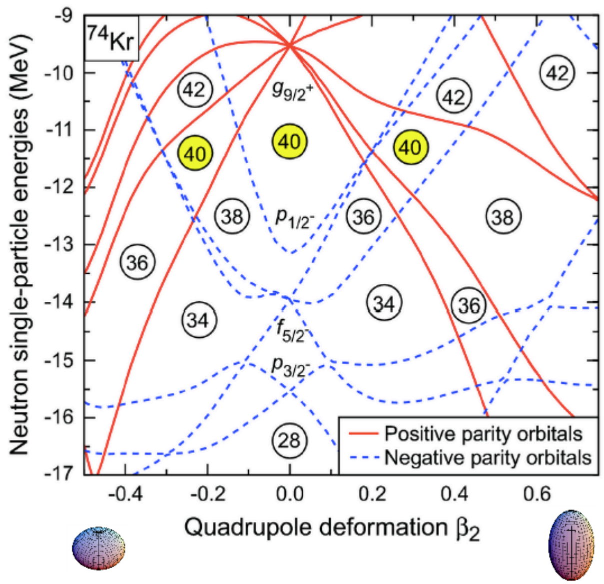

Potential energy surface

Triaxial symmetry

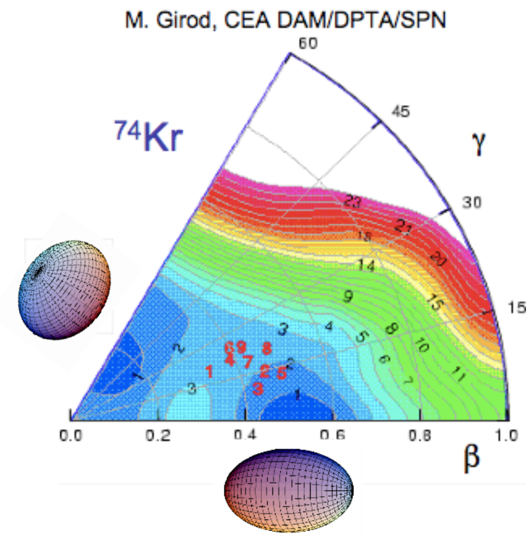

Shape coexistence and low-lying 0^+ states

2-level mixing model

$$|0_1^+\rangle = \cos\theta_0 |0_D^+\rangle + \sin\theta_0 |0_S^+\rangle$$
$$|0_2^+\rangle = -\sin\theta_0 |0_D^+\rangle + \cos\theta_0 |0_S^+\rangle$$

$$\cos^2\theta_0 + \sin^2\theta_0 = 1$$

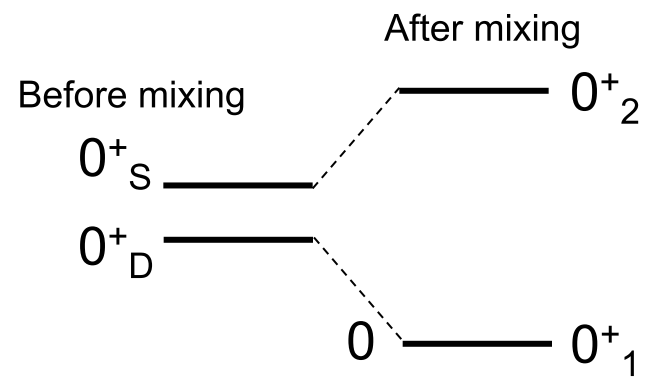

Maximum mixing $\cos^2\theta = \sin^2\theta = 0.5$

Weak mixing $\cos^2\theta \to 1 \quad \sin^2\theta \to 0$

$$|2_1^+\rangle = \cos\theta_2 |2_D^+\rangle + \sin\theta_2 |2_S^+\rangle$$
$$|2_2^+\rangle = -\sin\theta_2 |2_D^+\rangle + \cos\theta_2 |2_S^+\rangle$$

$$B(E2;0_1^+ \to 2_1^+) = \left|\cos\theta_0 \cos\theta_2 \langle 0_D^+ | M(E2) | 2_D^+\rangle + \sin\theta_0 \sin\theta_2 \langle 0_S^+ | M(E2) | 2_S^+\rangle\right|^2$$

$$B(E2;0_2^+ \to 2_1^+) = \left|-\sin\theta_0 \cos\theta_2 \langle 0_D^+ | M(E2) | 2_D^+\rangle + \cos\theta_0 \sin\theta_2 \langle 0_S^+ | M(E2) | 2_S^+\rangle\right|^2$$

Physics case: shape coexistence in light Kr isotopes

E. Bouchez *et al.*, Phys. Rev. Lett. **90**, 082502 (2003).

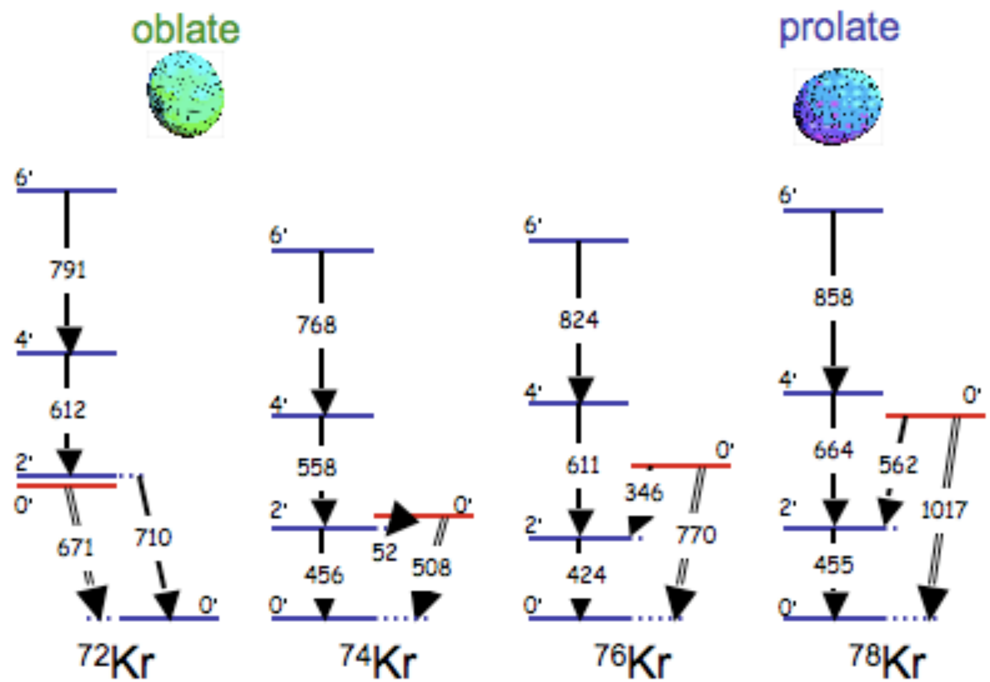

- ❑ energy of excited 0^+ by conversion electron
- ❑ E0 strengths $\rho^2(E0)$

- ❑ Shape coexistence and transition suspected
- ❑ Inversion of ground-state shape in 72Kr

- ❑ Need for Coulomb excitation to verify this scenario

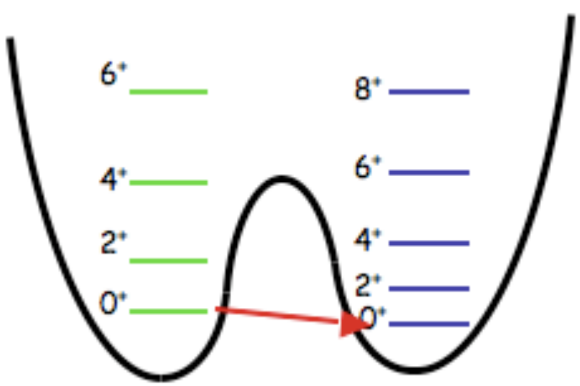

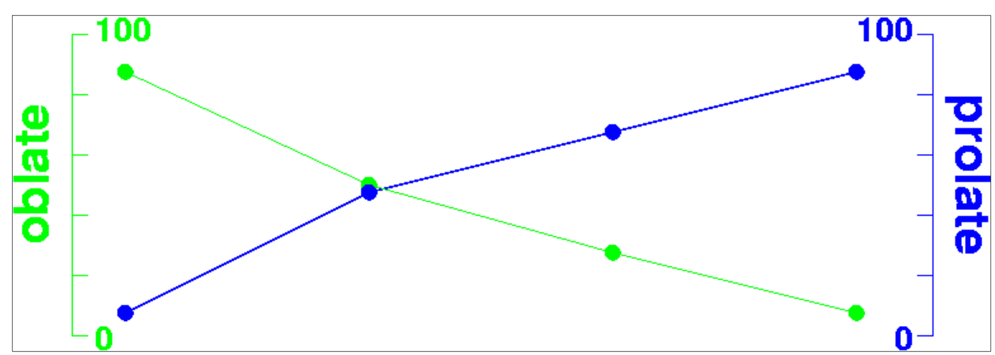

Mixing of the ground state (**two-level mixing** extrapolated from distortion of rotational bands)

Setup for RIB coulomb excitation at SPIRAL, GANIL

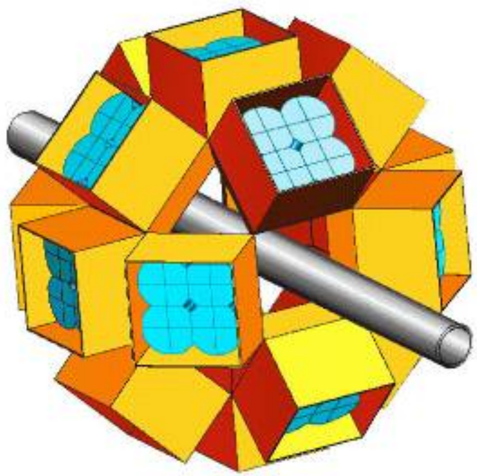

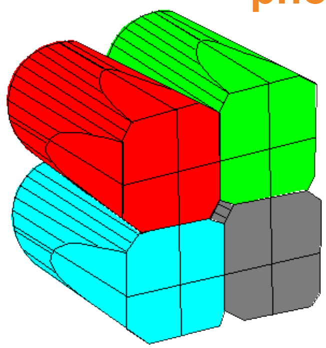

16 large Ge Clover detectors
4 × 4 segmented
photopeak efficiency ε = 20%

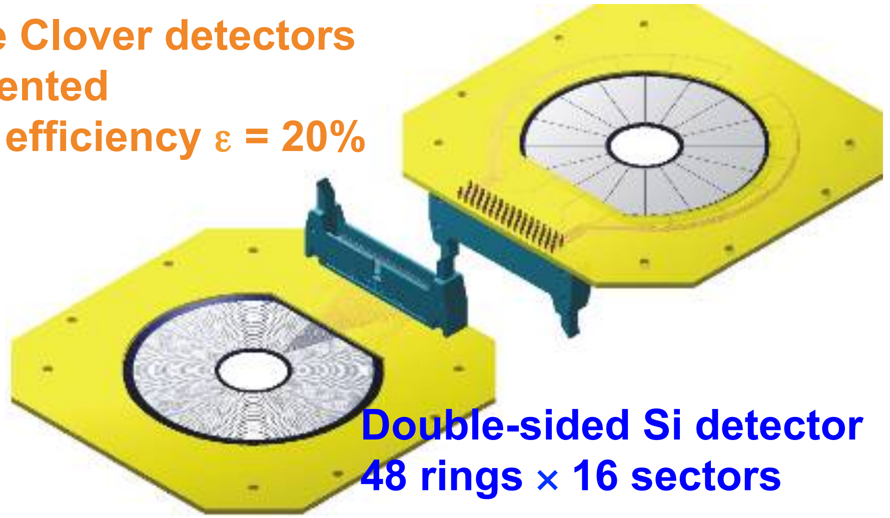

Double-sided Si detector
48 rings × 16 sectors

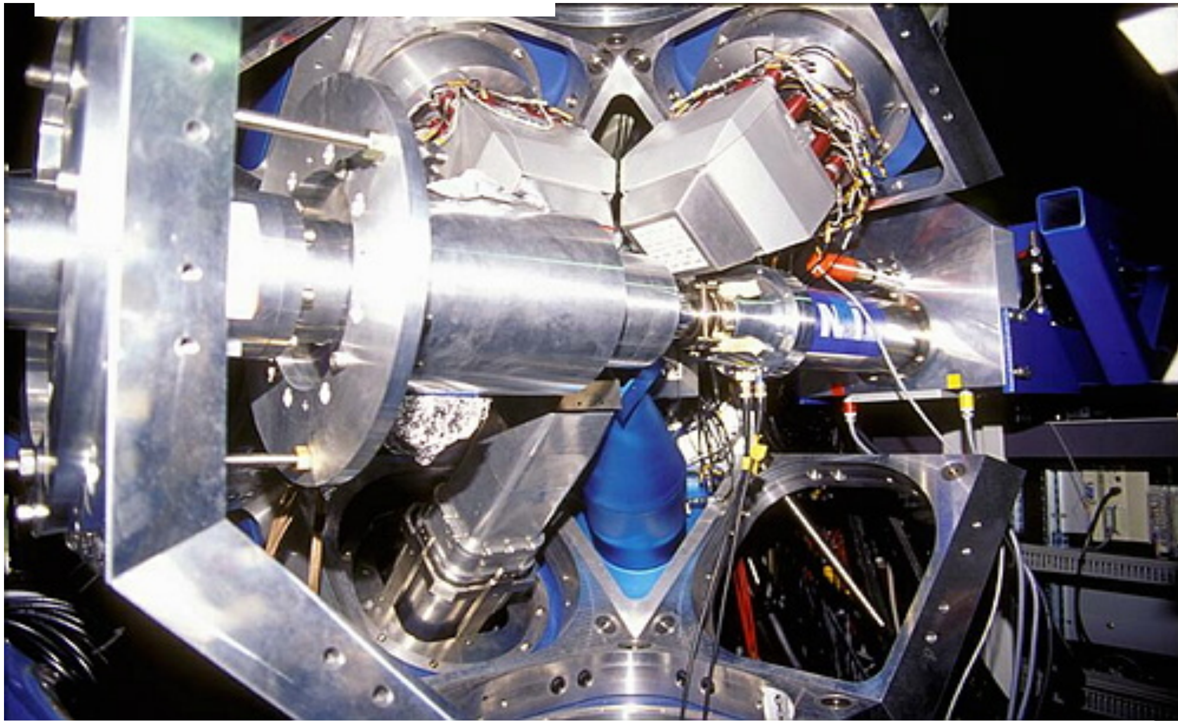

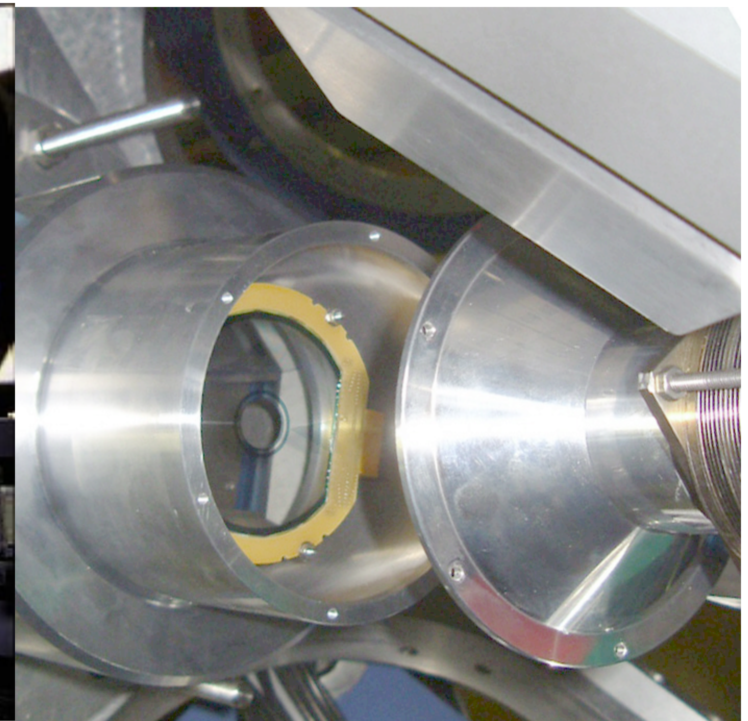

Physics case: shape coexistence in light Kr isotopes

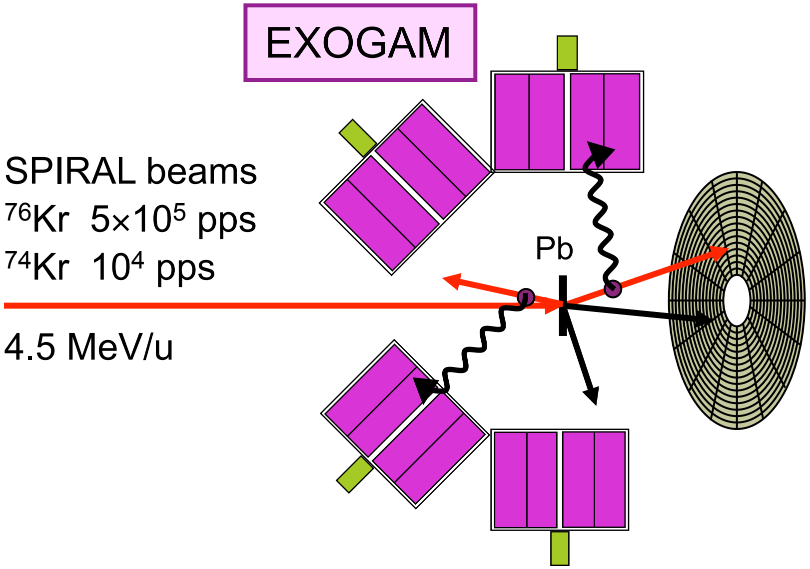

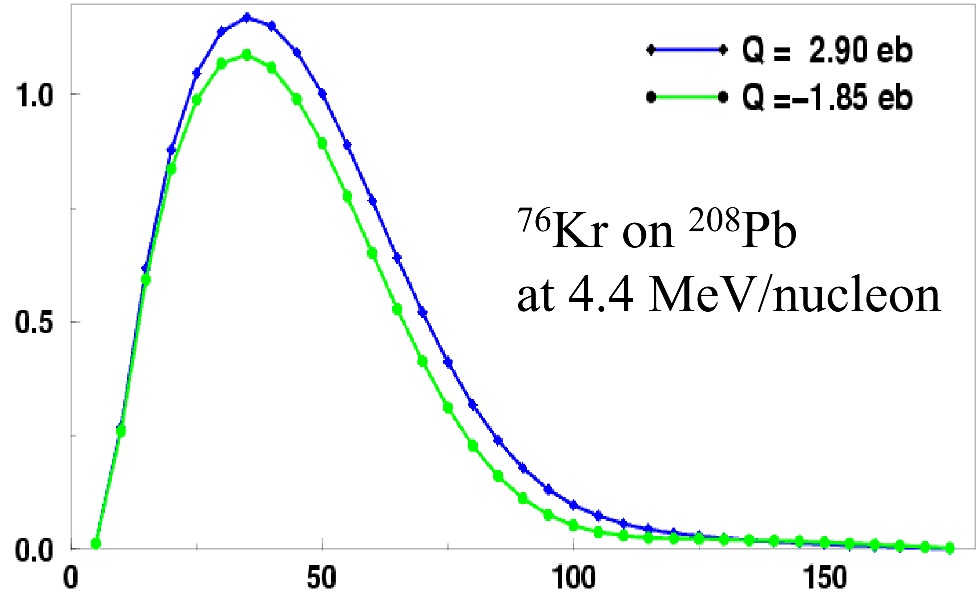

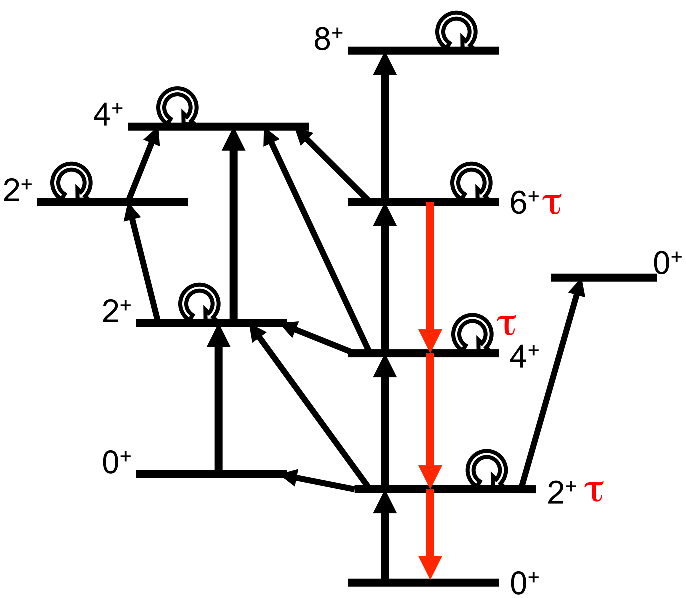

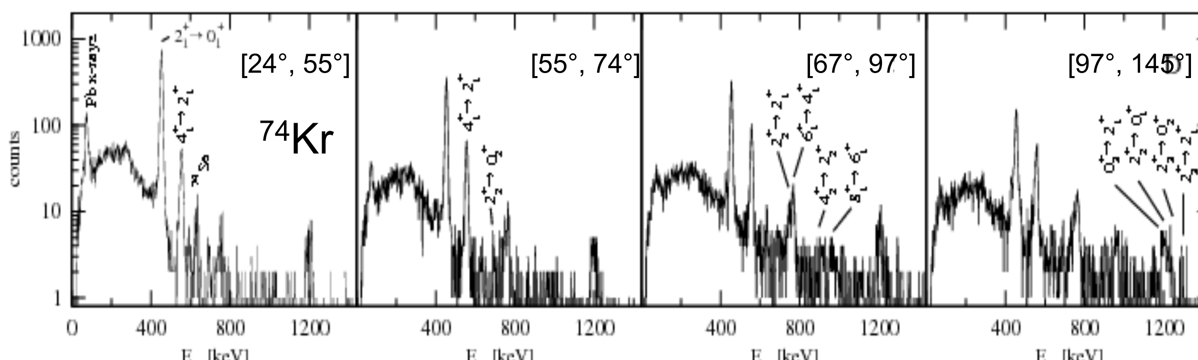

Physics case: shape coexistence in light Kr isotopes

Low-energy Coulomb excitation of ^{74,76}Kr, SPIRAL (GANIL)

E. Clément *et al.*, Phys. Rev. C **75**, 054313 (2007).

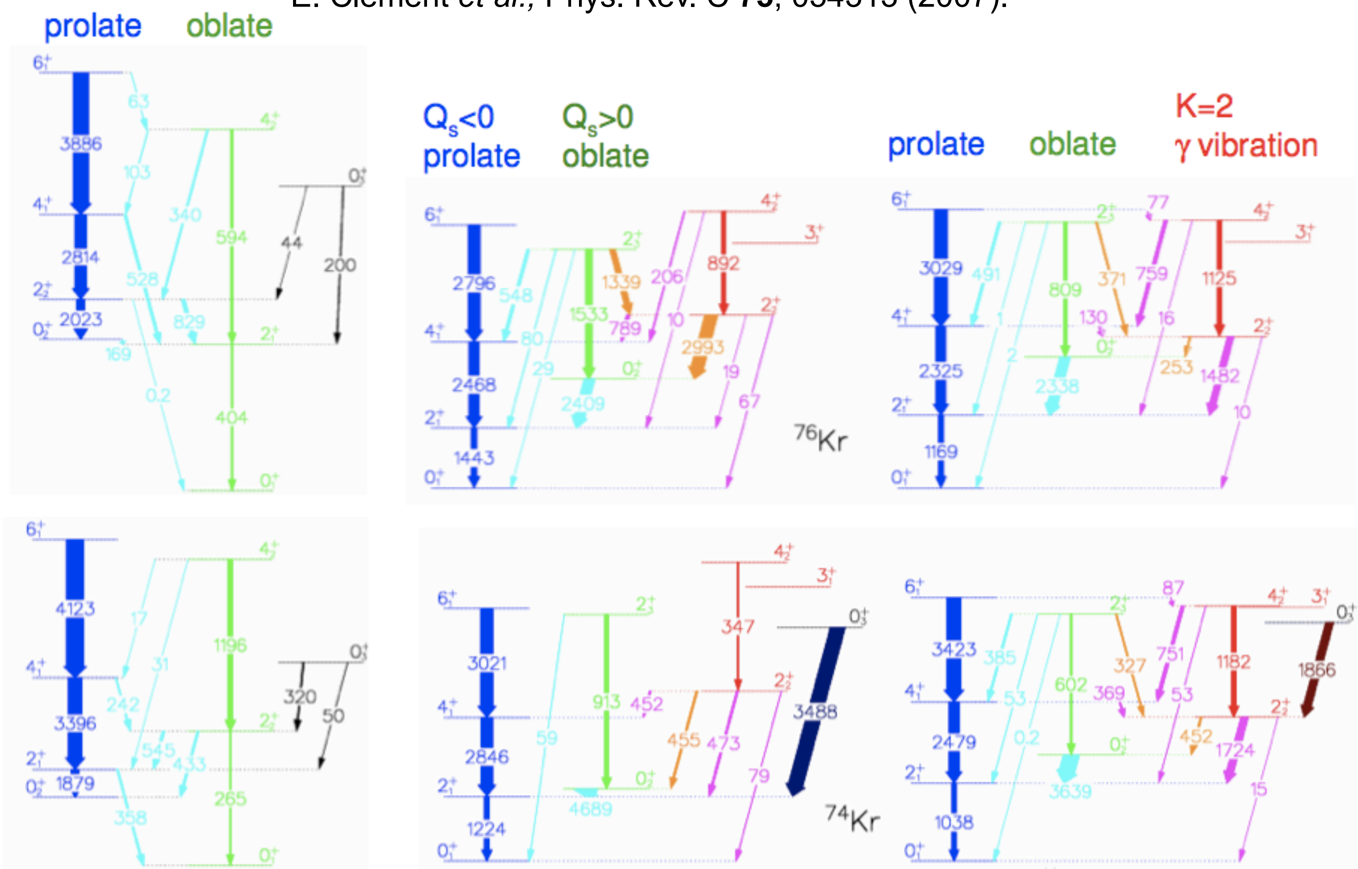

GCM calculation
axial deformation
Skyrme SLy6

M. Bender et al.
PRC 74, 024312 (2006)

experimental B(E2;↓) [e^2fm^4]

GCM (GOA) calculation
q_0, q_2: triaxial deformation
Gogny D1S

Reduced transition matrix element and deformation

- 2^+ **energies** and **B(E2;$2^+ \rightarrow 0^+$)** are often the first observables to characterize shell closures or deformation

- They often mirror each other

- In the rotational model, B(E2) can be used to extract a deformation amplitude β

$$\beta = \frac{4\pi}{3ZR^2}\sqrt{B(E2;0^+ \rightarrow 2^+)/e^2}, \qquad R = 1.2A^{1/3}\ fm$$

- Similarly, the **ratio of 4^+ to 2^+ excitation energies** can be used to infer deformation by comparison to the rotor limit:

$$\frac{E(4^+)}{E(2^+)} = \frac{4(4+1)}{2(2+1)} = \frac{20}{6} = 3.33$$

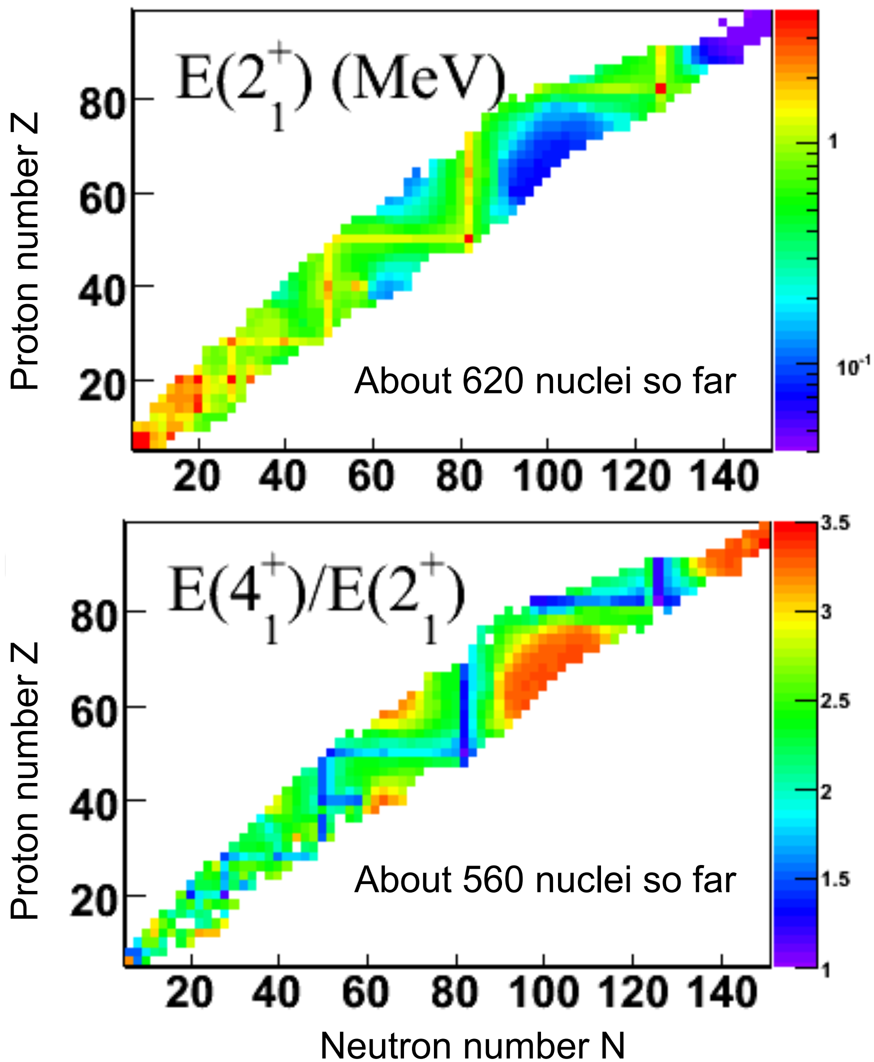

- **Deformation & nuclear shapes**
  - Symmetry breaking and nuclear shapes
  - The deformed harmonic oscillator and Nilsson models
  - Configuration mixing approaches
  - Observables: rotational models and quadrupole moments

- **Ground state deformation from hyperfine structure**

- **Low-energy Coulomb excitation**
  - First order calculation, second order and re-orientation effect
  - Physics case: **shape coexistence** in light Kr isotopes

- **Intermediate-energy Coulomb excitation**
  - Semi-classical description
  - Physics case: **island of inversion** and ^{32}Mg

- **Extreme quadrupole deformations**
  - superdeformation and hyperderformation

- **higher order multipole moments**
  - Octahedral and thetrahedral shapes
  - Physics case: **octupole deformation** in ^{220}Ra

Intermediate-energy Coulomb excitation

- **Advantage**: thick target can be used, measurement at **>10 pps** possible
- **Single-step excitation** is a valid assumption (excitation time >> collision time)
- **Maximum excitation energy**: $\Delta E_{max} = \frac{\hbar c}{a} \beta\gamma$ (*ex.* 10 MeV for Mg+Pb at 50 MeV/u)
- Intermediate energy (above Coulomb barrier): **both Coulomb and nuclear excitations**
  Method: classical equivalence between scattering angle and impact parameter

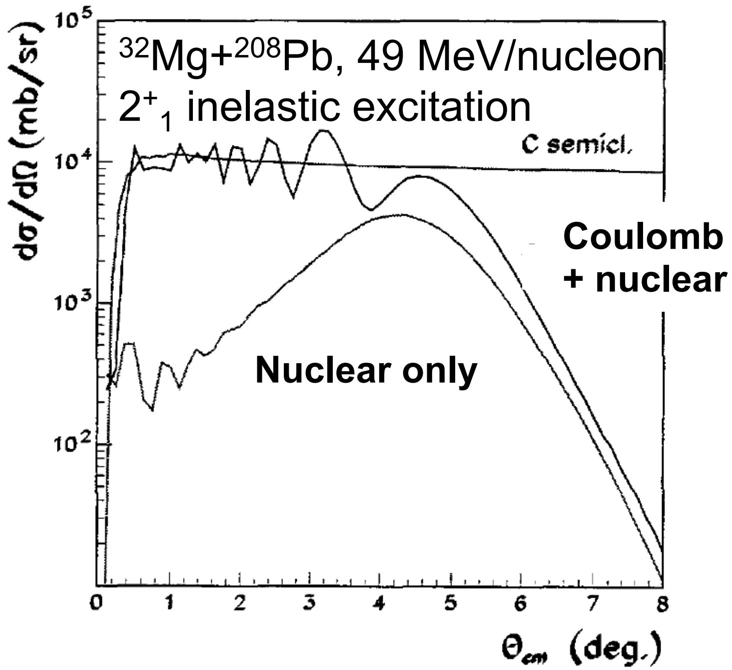

Intermediate-energy Coulomb excitation

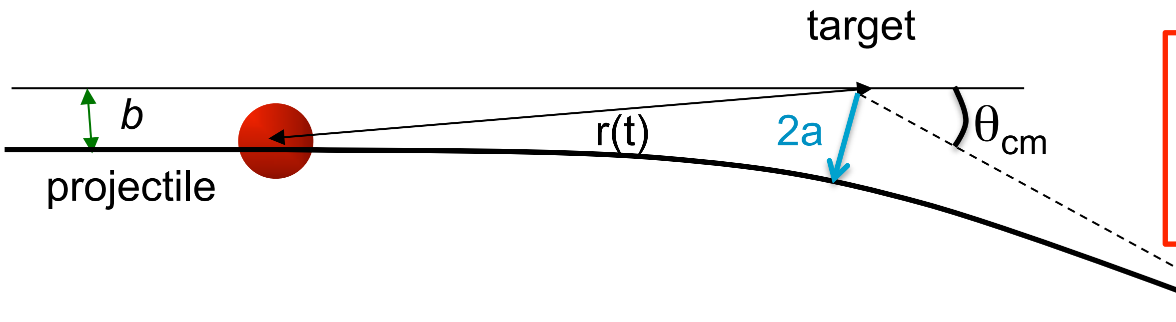

At small impact parameters (nuclear radius distance), nuclear excitations occur.

- Coulomb excitation for $b > b_{min}$ (**cutoff impact parameter** to prevent nuclear contributions):

$$b_{\min} = [C_1 + C_2 + 2]\ fm$$

$$C_i = R_i\left(1 - \frac{1}{R_i^2}\right) \quad with \quad R = 1.28A^{1/3} - 0.76 + 0.8A^{-1/3}$$

- Relation between b_{min} and **maximum scattering angle θ^{max}** (center of mass):

$$b_{\min} = \frac{a}{\gamma}\cot\left(\frac{\theta_{CM}^{\max}}{2}\right) \quad where \quad a = \frac{Z_P Z_T e^2}{m_0 c^2 \beta^2}, \quad \gamma = \frac{1}{\sqrt{1-\beta^2}}$$

- Relation between θ_{cm} and $\boldsymbol{\theta_{lab}}$:

$$\tan(\theta_{lab}) = \frac{\sin(\theta_{CM})}{\gamma\left[\cos(\theta_{CM}) + \frac{\beta_{CM}}{\beta_{proj}}\right]}$$

Physics case: ^{32}Mg and the island of inversion

T. Motobayashi *et al.*, PLB **346**, 9 (1995)

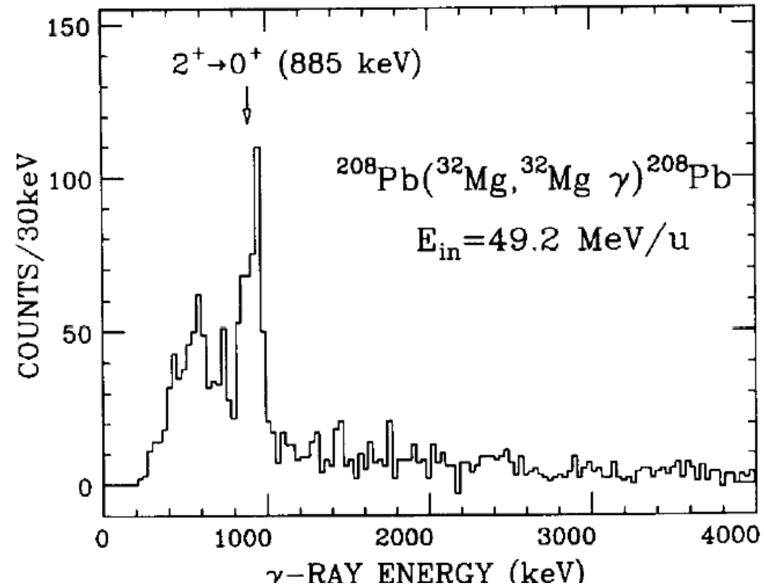

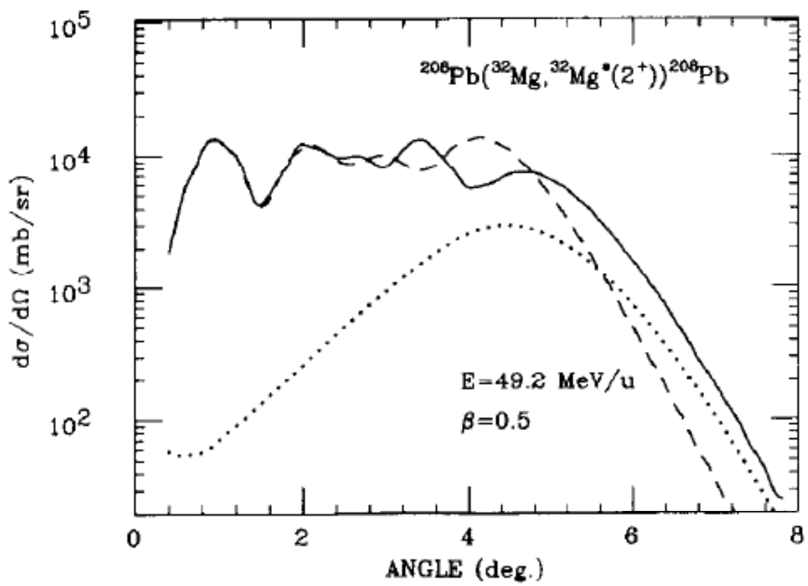

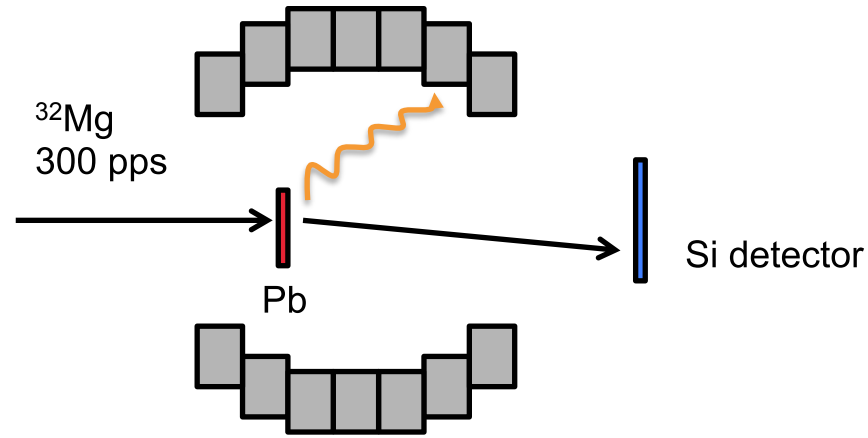

- ❑ inclusive cross section measurement

$$N_\gamma = \sigma_{i \to f} \, N_T \, N_B \, \epsilon,$$

- ❑ **Angular cut** from ^{32}Mg recoil detection to remove nuclear contributions
- ❑ **Unobserved feeding** corrections (20%) leading to « some » uncertainties

$$\sigma_{\pi\lambda} \approx \left(\frac{Z_{pro} e^2}{\hbar c} \right)^2 \frac{\pi}{e^2 \, b_{min}^{2\lambda-2}} B(\pi\lambda, 0 \to \lambda)$$

Physics case: ^{32}Mg and the island of inversion

T. Motobayashi *et al.*, PLB **346**, 9 (1995)

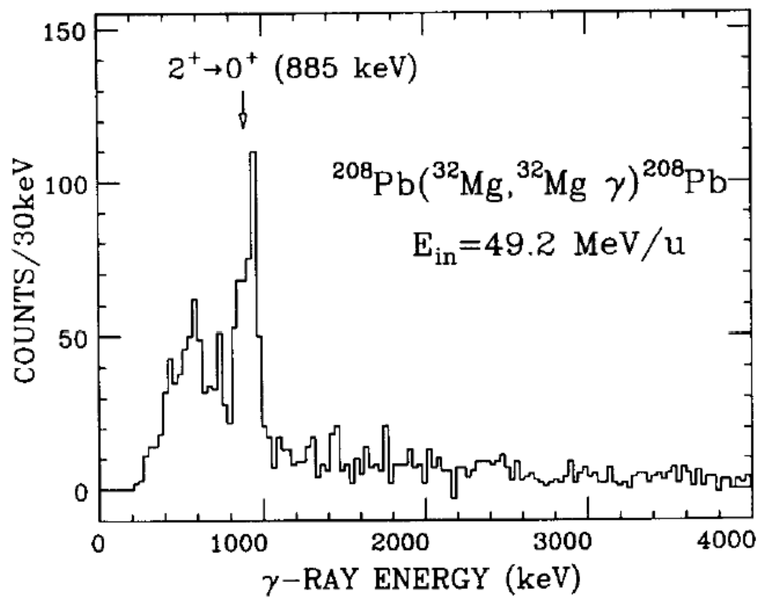

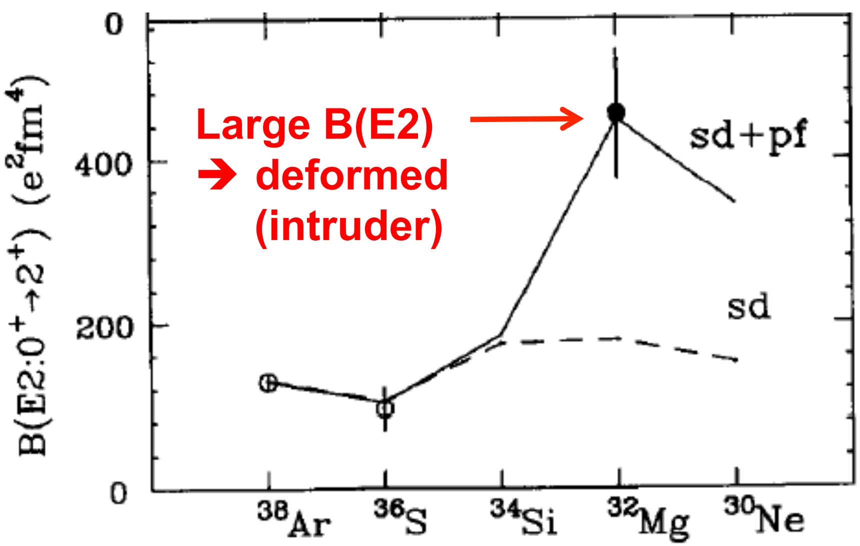

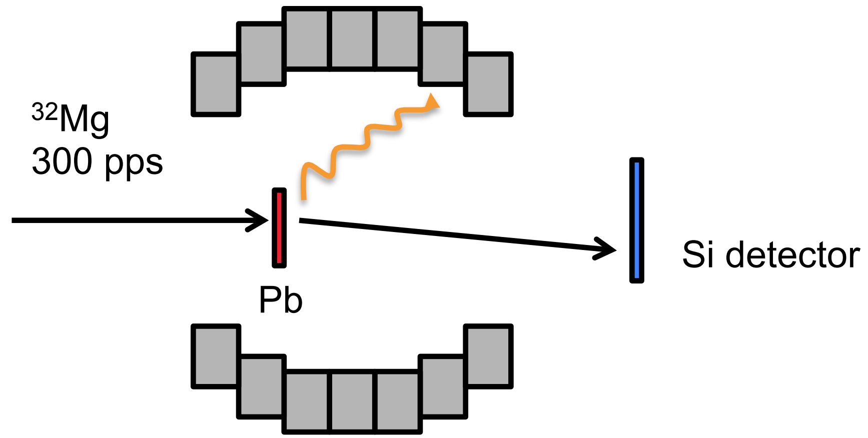

- inclusive cross section measurement

$$N_\gamma = \sigma_{i\rightarrow f}\, N_T\, N_B\, \epsilon,$$

- **Angular cut** from ^{32}Mg recoil detection to remove nuclear contributions

- **Unobserved feeding** corrections (20%) leading to « some » uncertainties

$$\sigma_{\pi\lambda} \approx \left(\frac{Z_{pro}e^2}{\hbar c}\right)^2 \frac{\pi}{e^2\, b_{min}^{2\lambda-2}} B(\pi\lambda, 0\rightarrow\lambda)$$

- **Deformation & nuclear shapes**
  - Symmetry breaking and nuclear shapes
  - The deformed harmonic oscillator and Nilsson models
  - Configuration mixing approaches
  - Observables: rotational models and quadrupole moments

- **Ground state deformation from hyperfine structure**

- **Low-energy Coulomb excitation**
  - First order calculation, second order and re-orientation effect
  - Physics case: **shape coexistence** in light Kr isotopes

- **Intermediate-energy Coulomb excitation**
  - Semi-classical description
  - Physics case: **island of inversion** and ^{32}Mg

- **Extreme quadrupole deformations**
  - superdeformation and hyperderformation

- **higher order multipole moments**
  - Octahedral and thetrahedral shapes
  - Physics case: **octupole deformation** in ^{220}Ra

Extreme deformations

Fusion-evaporation reaction

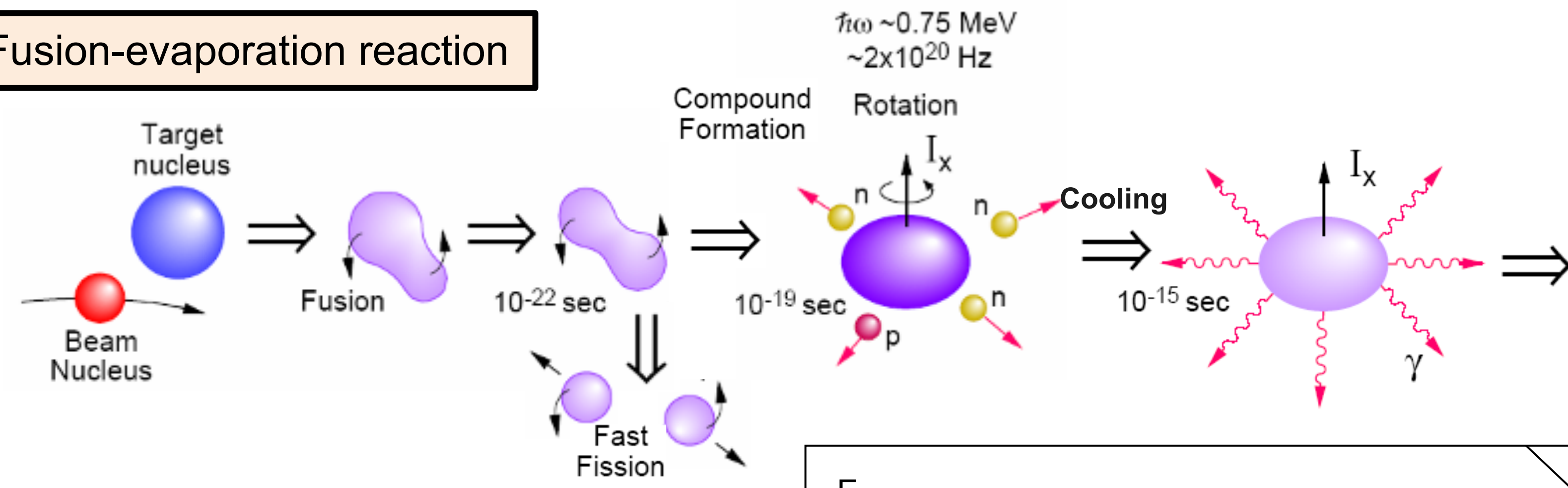

- ❑ large cross section (~1 barn)
- ❑ predominantly proton-rich nuclei (no Coulomb barrier for neutrons)
- ❑ large angular momentum transfer → many γ rays

gamma-ray spectrometer with
- ❑ high resolution (keV)
- ❑ large efficiency (~10% at 1 MeV)
- ❑ high granularity ($N_{Det} >> M_{\gamma}$)
- ❑ good Photopeak-to-Compton ratio

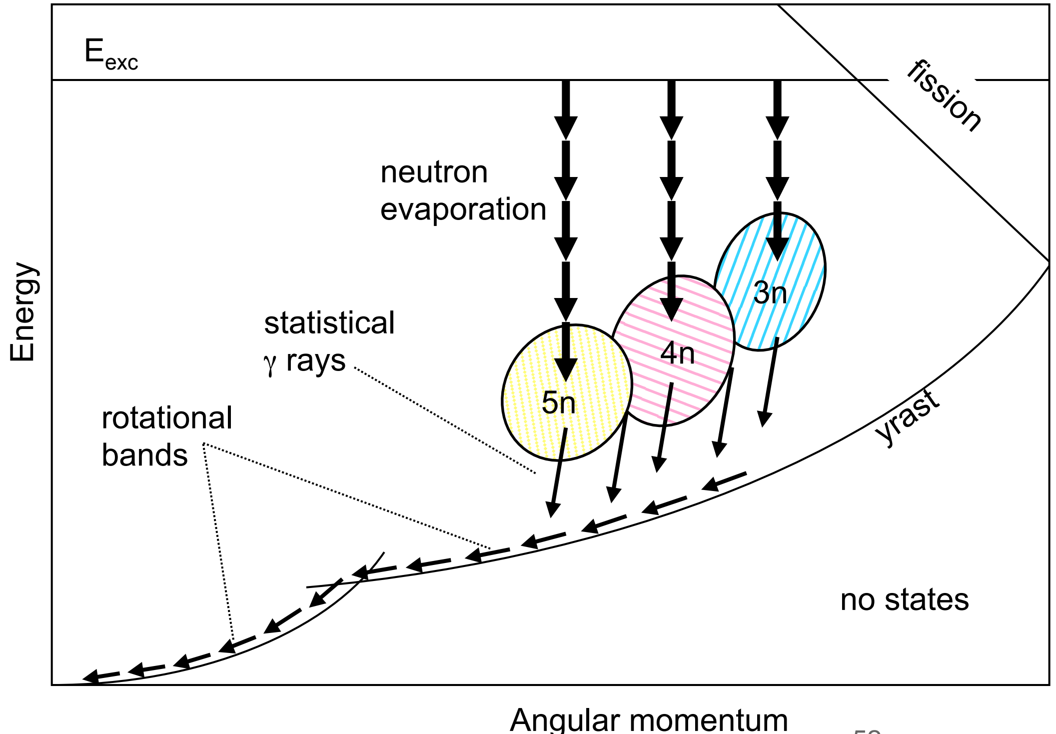

γ-ray spectrum from a fusion-evaporation reaction

Many superimposed gamma cascades, complicated singles spectra

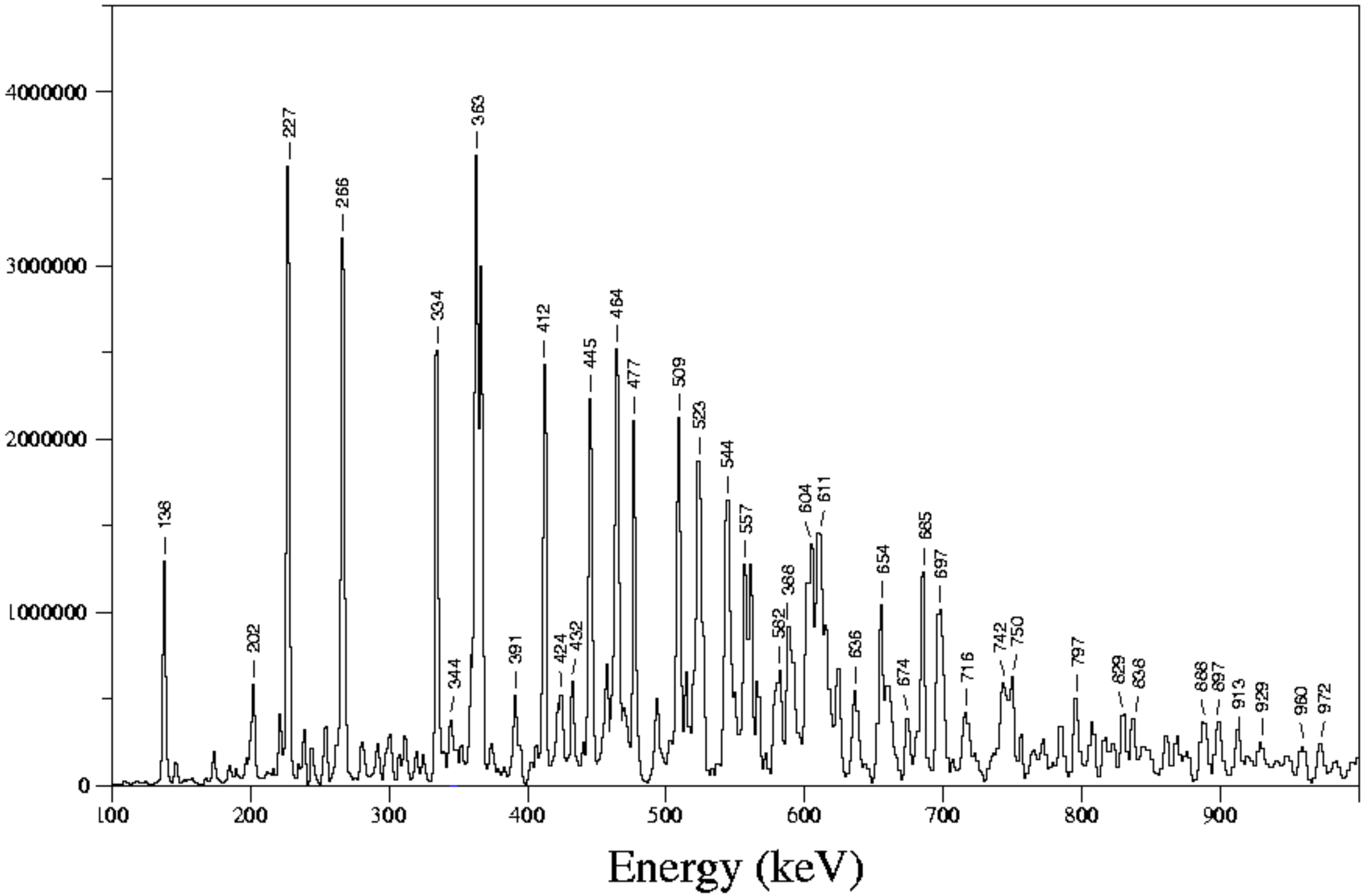

Resolving Power

Cascade of interest Populated with relative intensity α

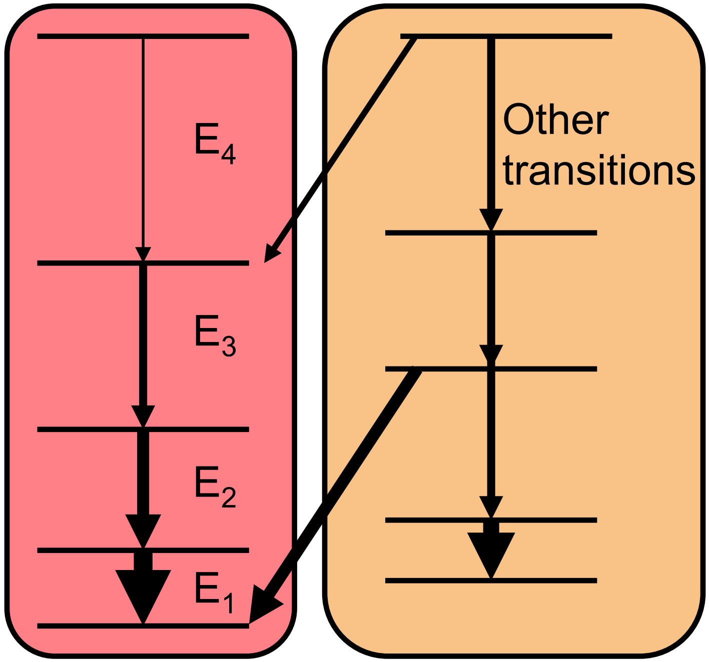

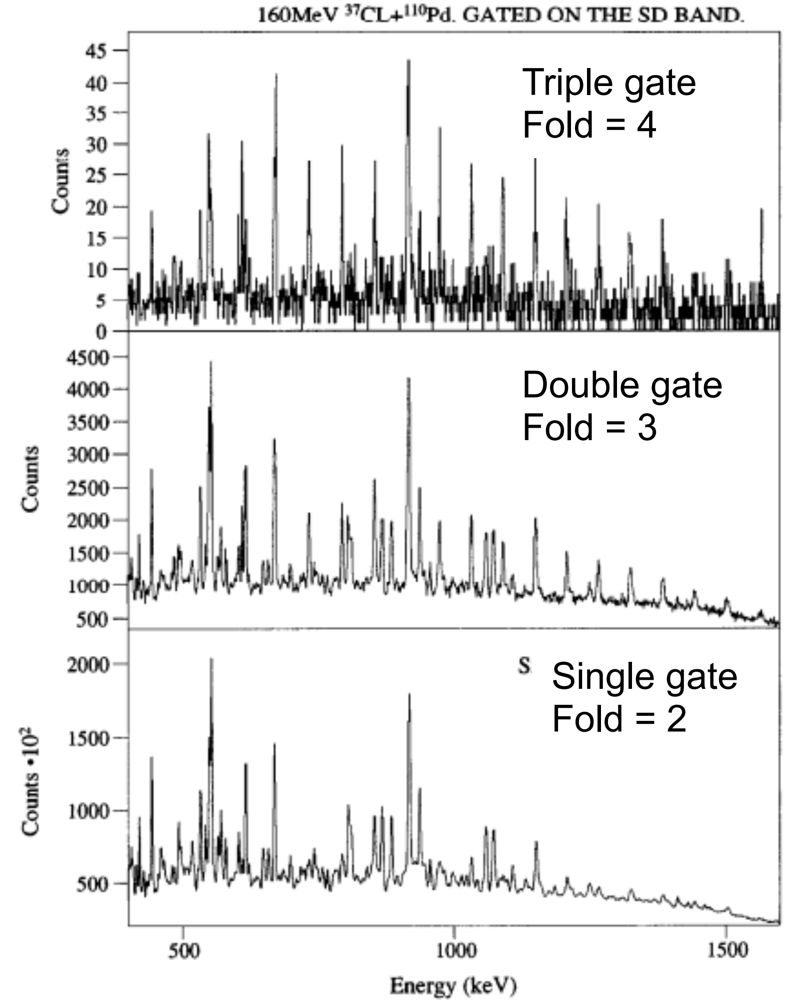

- ❑ Mesure **high-fold coincidences** F
- ❑ Apply (F-1) **gates on energies** $E_1 \ldots E_{F-1}$

- ❑ **Resolution** and **efficiency** are very important

- How do efficiency and resolution impact the sensitivity of the measurement?
- How the gating improves the peak-over-Total ratio (P/T)?
- What is the best fold F to consider?

A. Ataç *et al.*, Nucl. Phys. A 557, 109 (1993)

Resolving Power

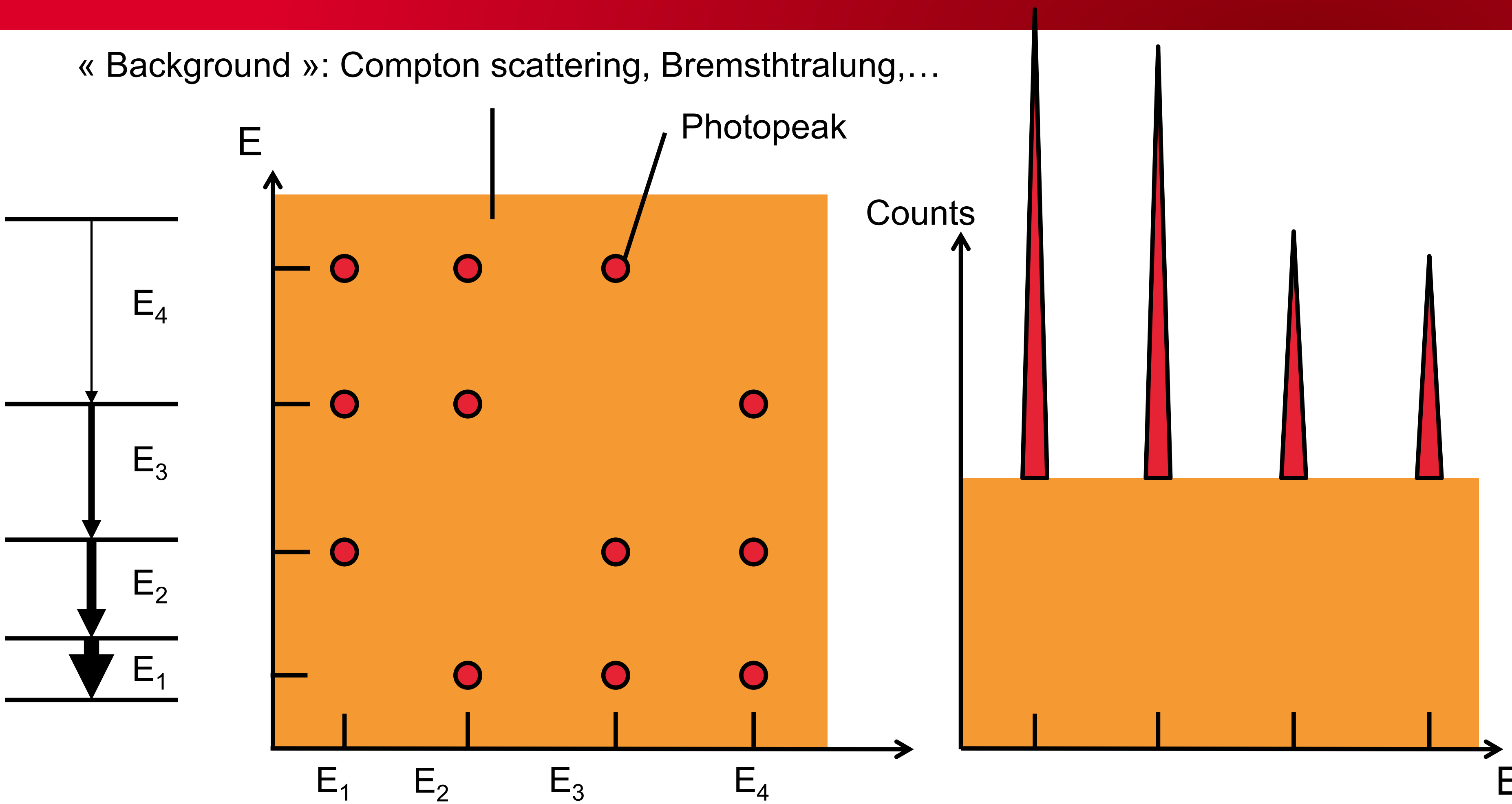

level scheme

Two-dimensional plot (Fold = 2) gamma-gamma coincidences

Projected gamma spectrum

Slide inspired by D. Weisshar, NSCL

Resolving Power

S(E): average energy spacing

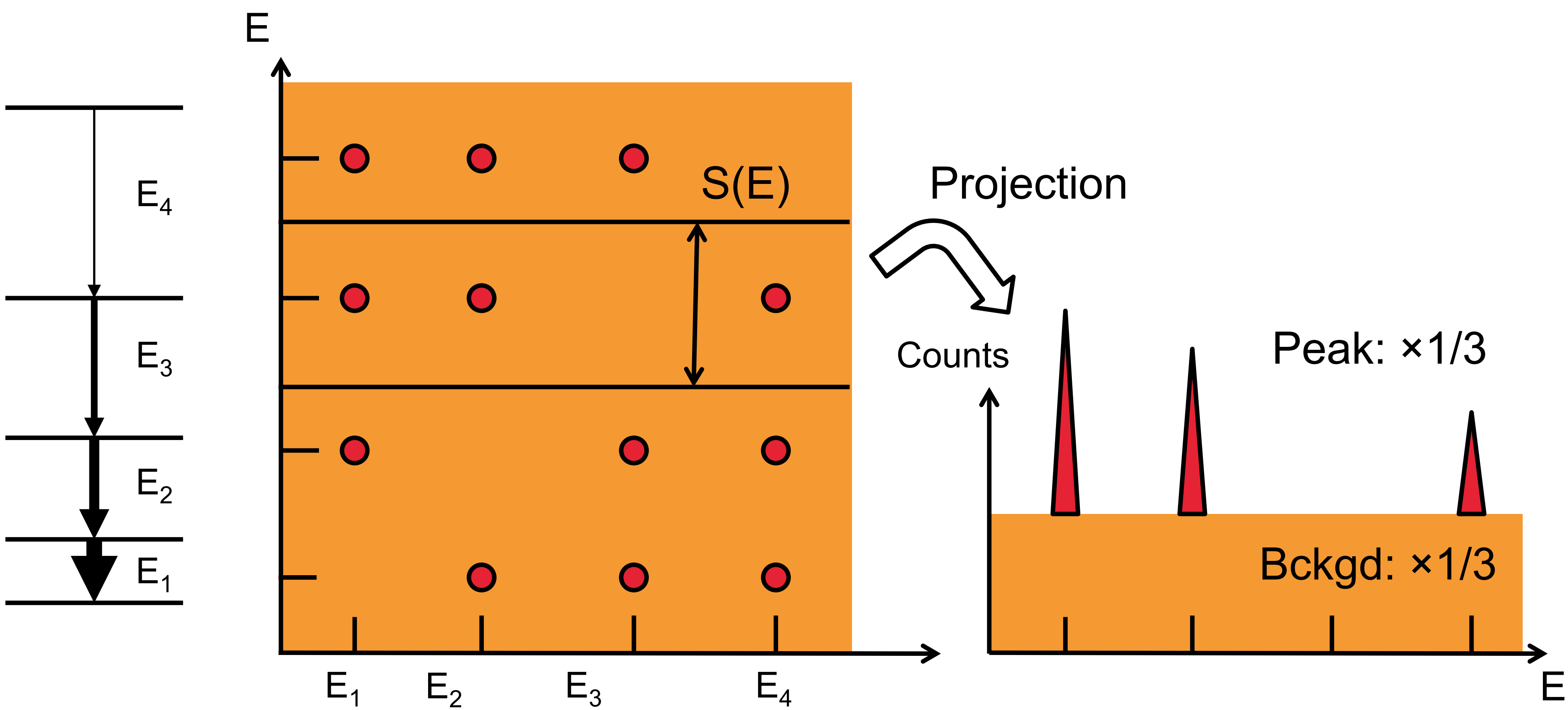

level scheme

Two-dimensional plot (Fold = 2) gamma-gamma coincidences

Projected gamma spectrum

Slide inspired by D. Weisshar, NSCL

Resolving Power

S(E): average energy spacing
δ(E): energy resolution

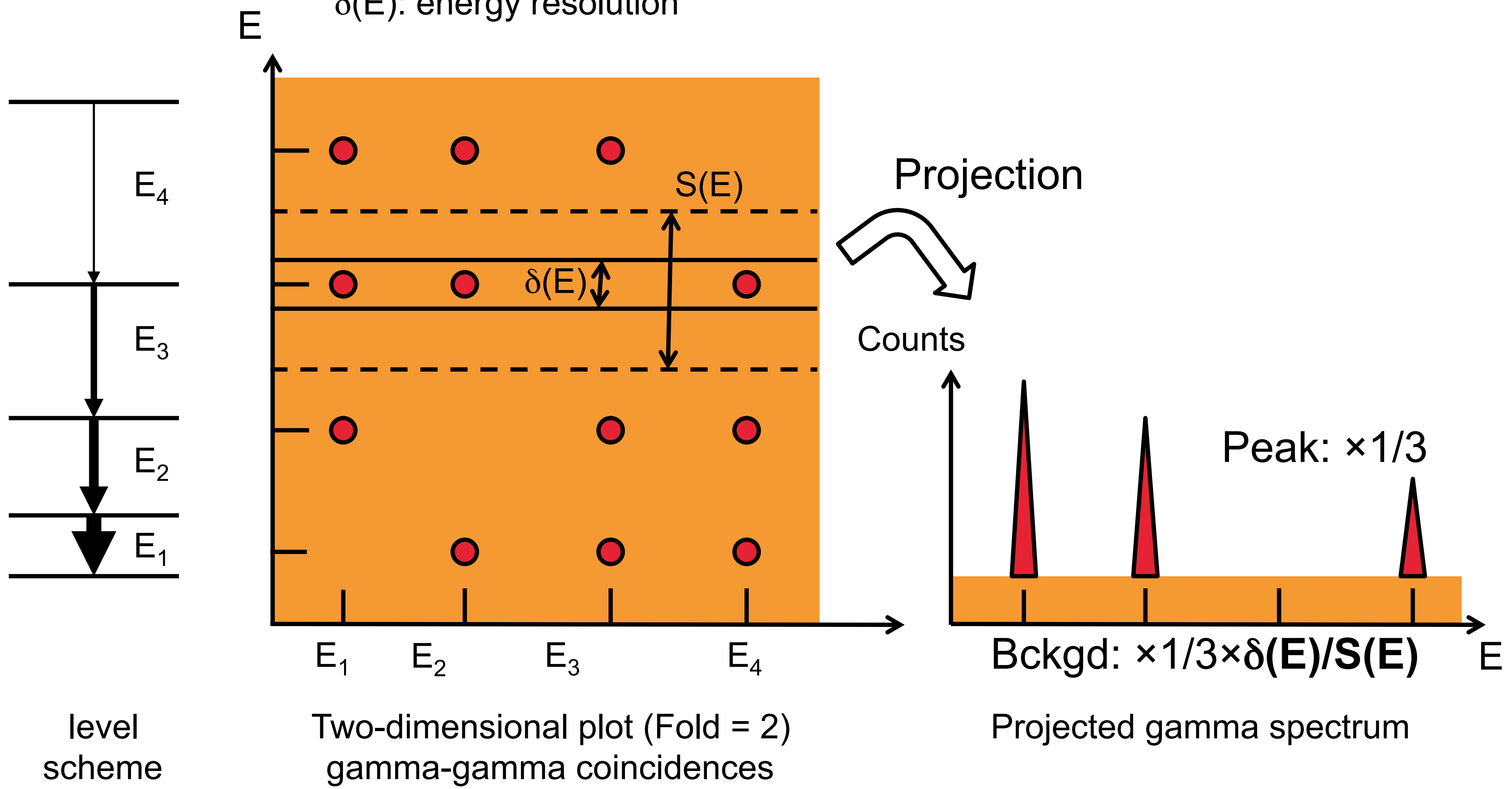

Slide inspired by D. Weisshar, NSCL

Peak-over-Total (P/T)

- P/T: probability to get a gamma in the photopeak and not in the Compton plateau

- Example: P/T=0.2, 2 gammas, 100 detected events
  - Both detected in photopeaks: P×P=4%
  - 1 Peak, 1 Compton: P×C=32%
  - Both detected as Compton: C×C=64%

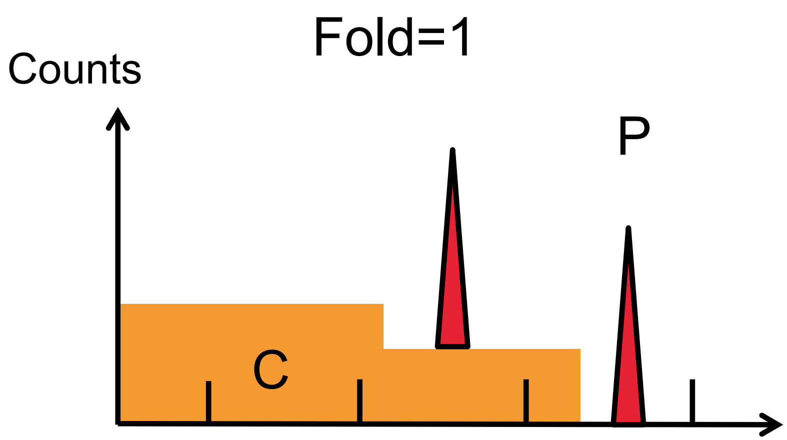

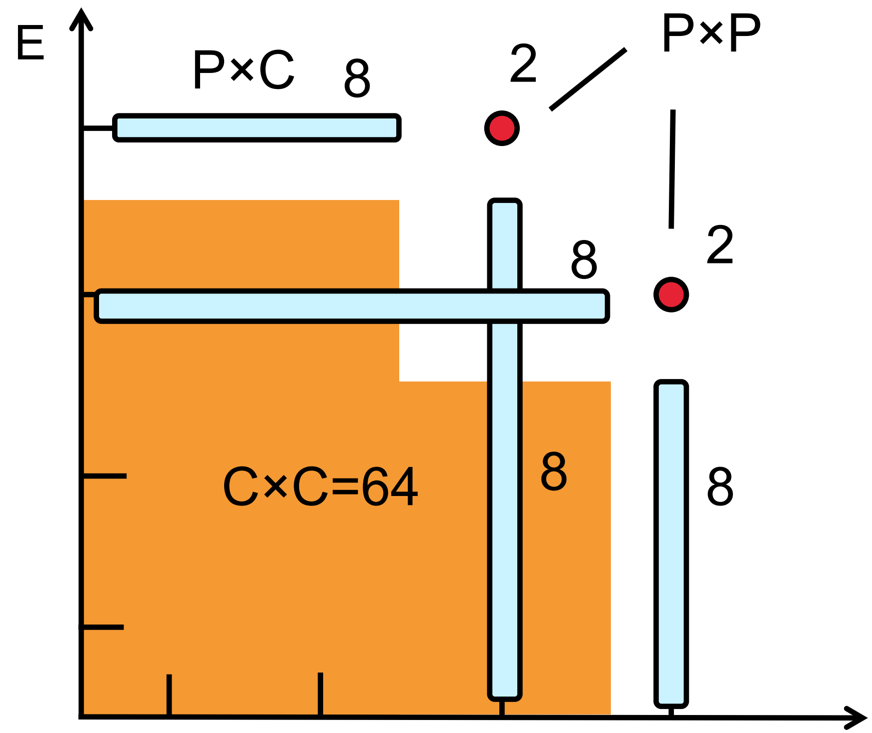

Fold=1: 10 events in photopeaks

Fold=2: 2 (10×P/T) events in photopeaks after cut

Each time the fold is increased by 1, the statistics is lowered by a factor P/T

Slide inspired by D. Weisshar, NSCL

Resolving Power

- Background reduction factor is **R=P/T×S(E)/δ(E)×0.76**
- For fold F=1 the **Peak-to-Background ratio** for a branch with intensity **α** is **αR**.
- For a **higher fold F** the Peak-to-Background ratio changes to **αR^F**.
- If N_0 is the total number of events, the amount of detected counts N in the peak is

$$N = \alpha N_0 \varepsilon^F$$

ε: full-energy-peak efficiency of spectrometer

- A minimum intensity α_0 is resolvable if $\alpha_0 R^F = 1$
- The **RESOLVING POWER** (RP) is defined as $RP = 1/\alpha_0$
- The above gives

$$\boxed{RP = \exp\left[\ln\left(\frac{N_0}{N}\right)\frac{1}{1-\ln(\varepsilon)/\ln(R)}\right]}$$

Resolving Power of gamma-ray detectors

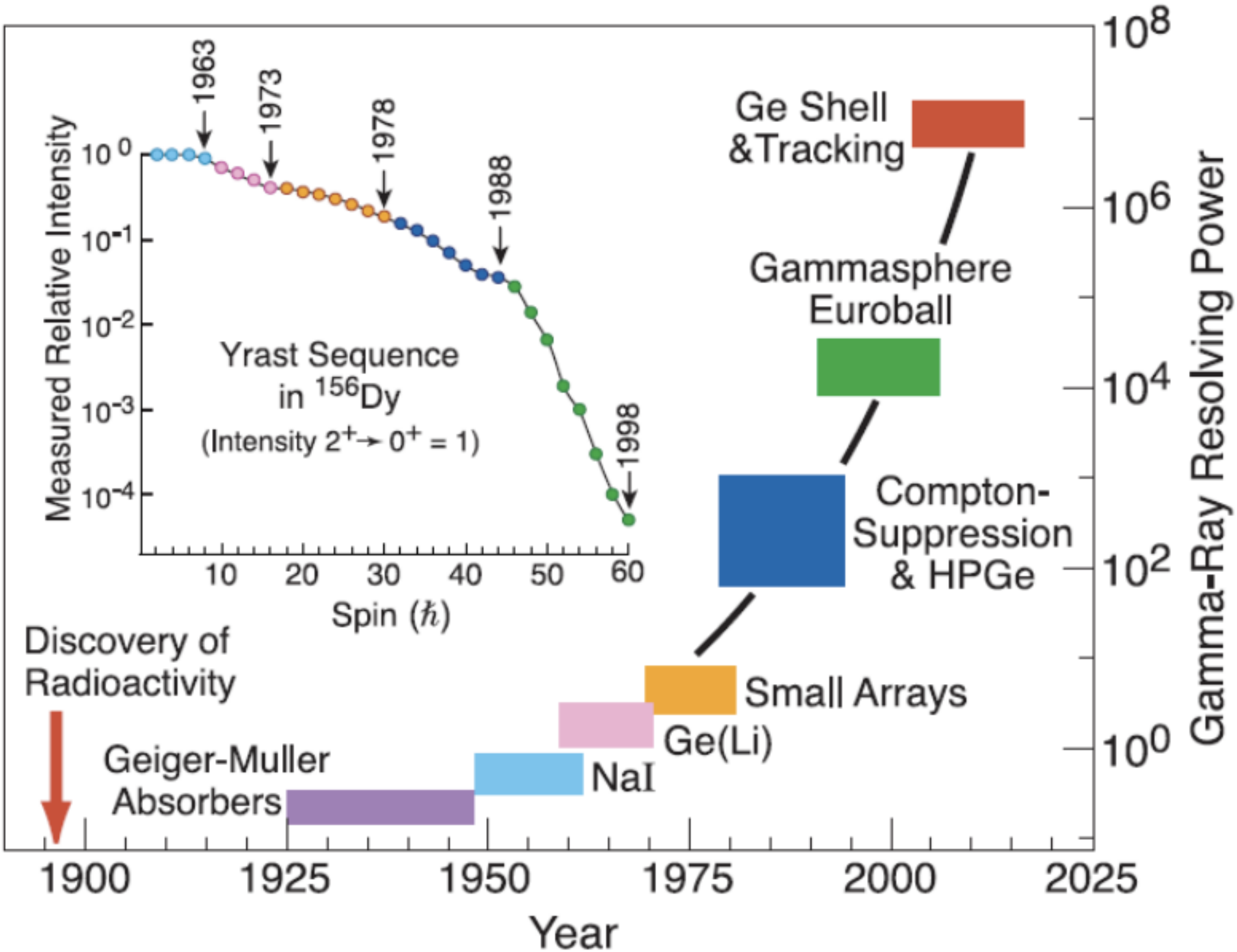

AGATA

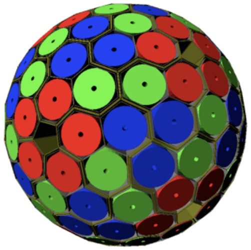

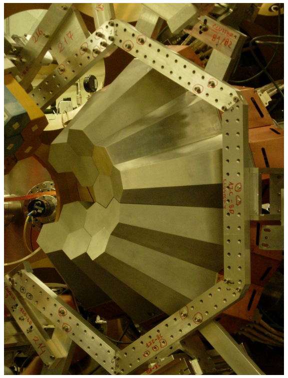

Band termination at high spin

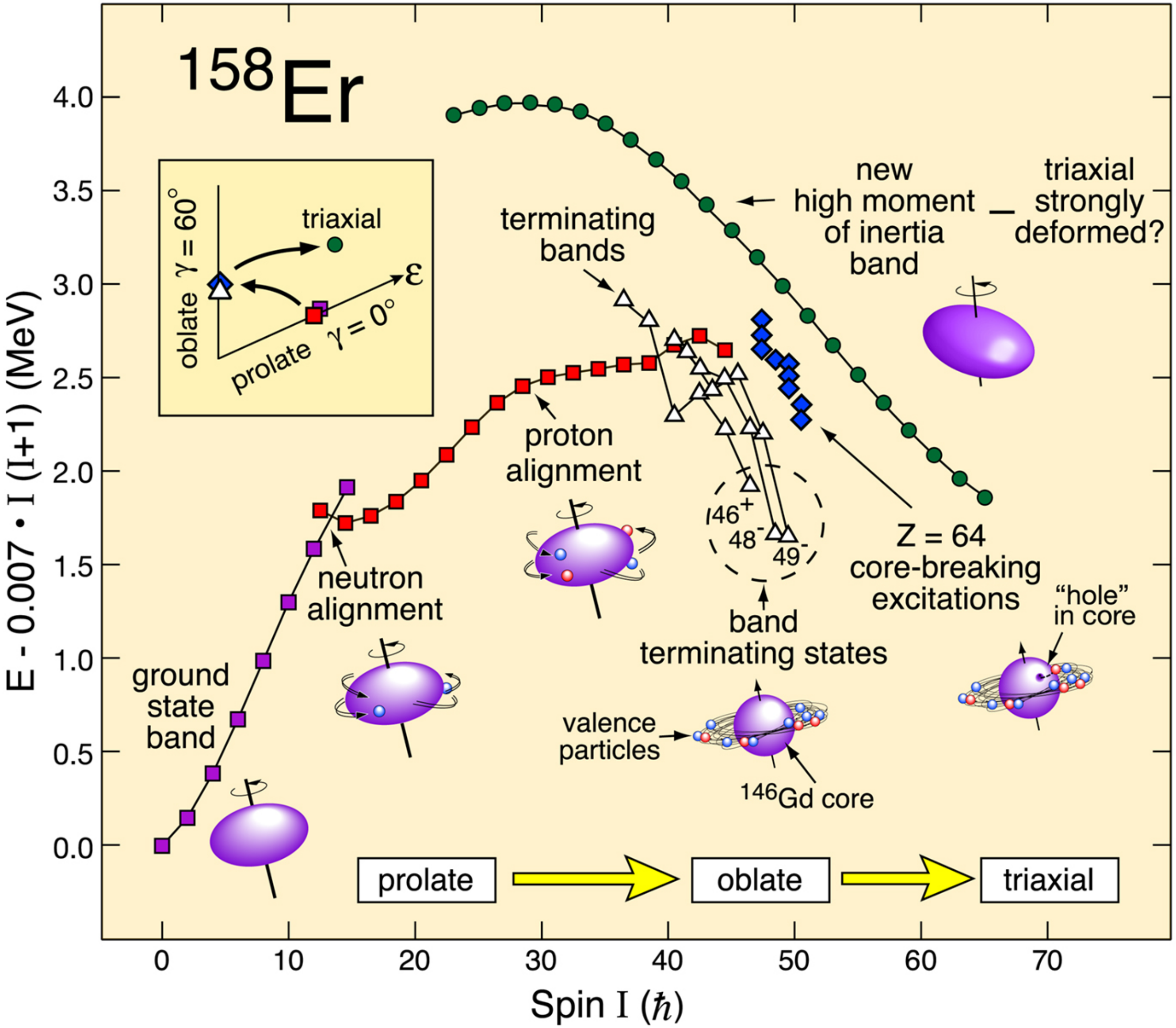

Shapes and intruder orbitals

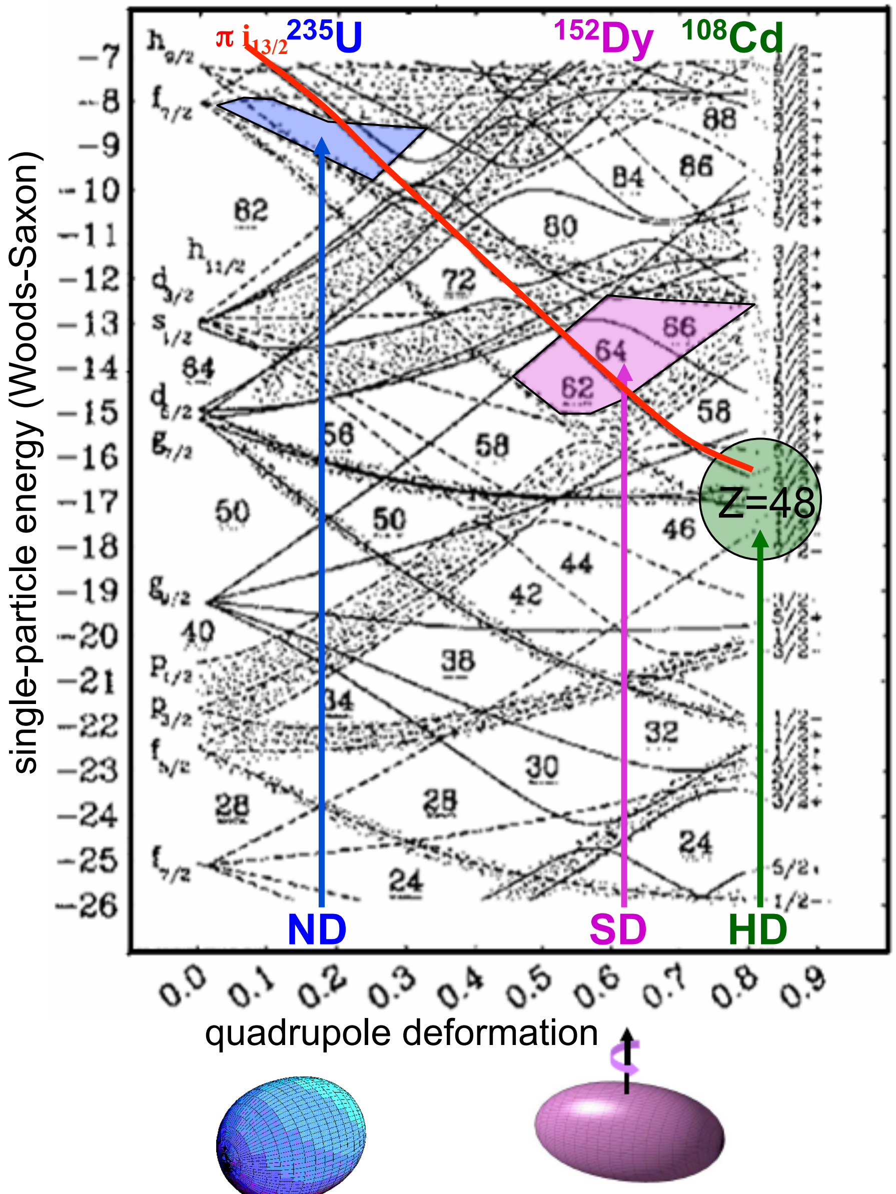

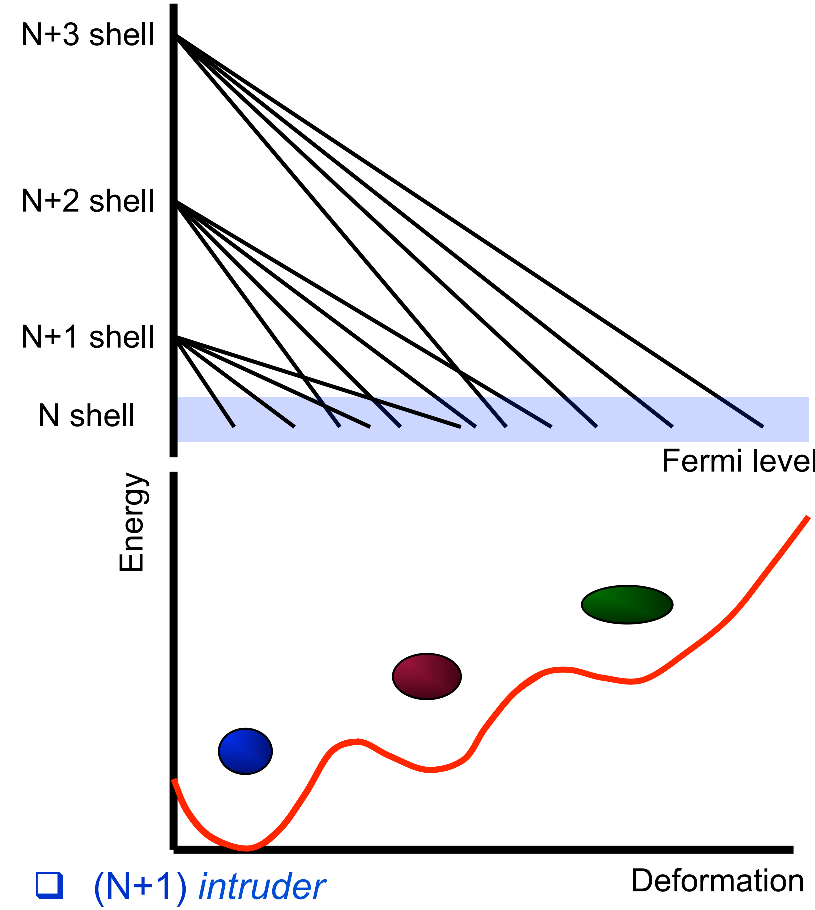

- (N+1) *intruder*
  ⇒ normal deformed, e.g. ^{235}U
- (N+2) *super-intruder*
  ⇒ Superdeformation, e.g. ^{152}Dy, ^{80}Zr
  ⇒ Fission isomers in actinides, e.g. ^{235}U
- (N+3) *hyper-intruder*
  ⇒ Hyperdeformation, e.g. in ^{108}Cd ?
  ⇒ Fission resonances in actinides

Superdeformation: history

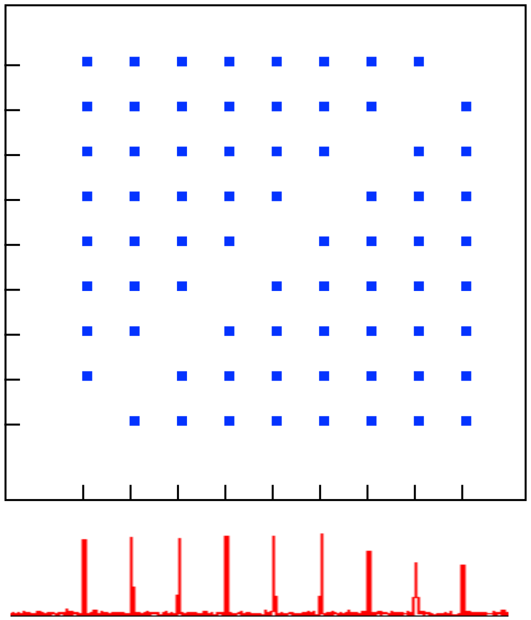

B.M. Nyako *et al.*, PRL **52**, 507 (1984)

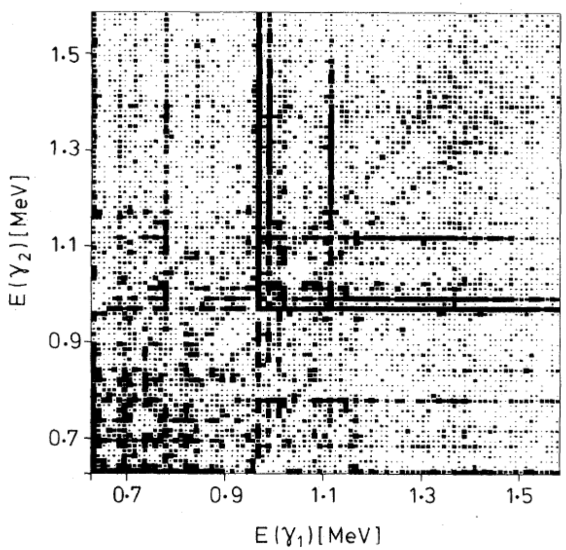

P.J. Twin *et al.*, PRL **57**, 811 (1986)

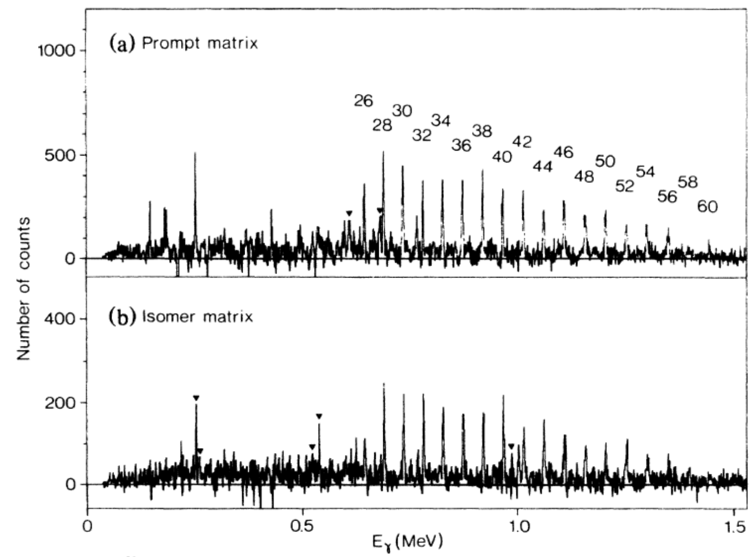

- ❑ **1984**: unresolved gamma band in ^{152}Dy due to too low statistics, but « ridge » observed
- ❑ Ridge is the sign of the spacing between two transitions of the same band
- ❑ **1986**: observation of the first rotational superdeformed band in ^{152}Dy

- ❑ Extracted moment of inertia is: $\Im^{(2)} = 85\hbar^2 MeV^{-1}$

Superdeformation: state of the art

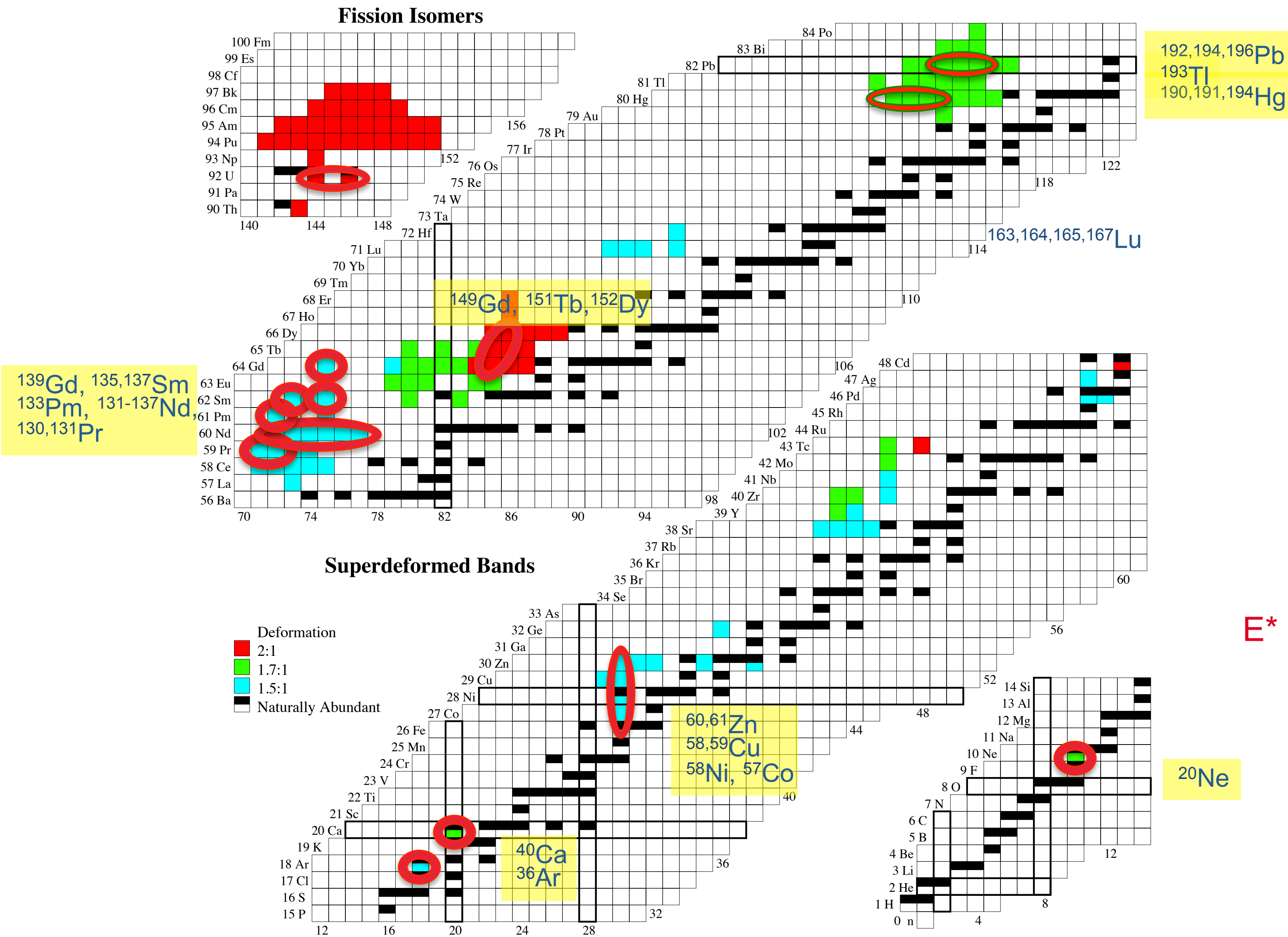

E* and I known

RIBs and hyperdeformation

- Theoretical prediction for extreme deformation (**hyperdeformation**) with 3:1 ratio
- Hyperdeformation favored at high-spin ⇒ Competes with **fission**
- **intense neutron-rich** beams would:
  - increase the fission barrier
  - favor Yrast hyperdeformed structures at high spin

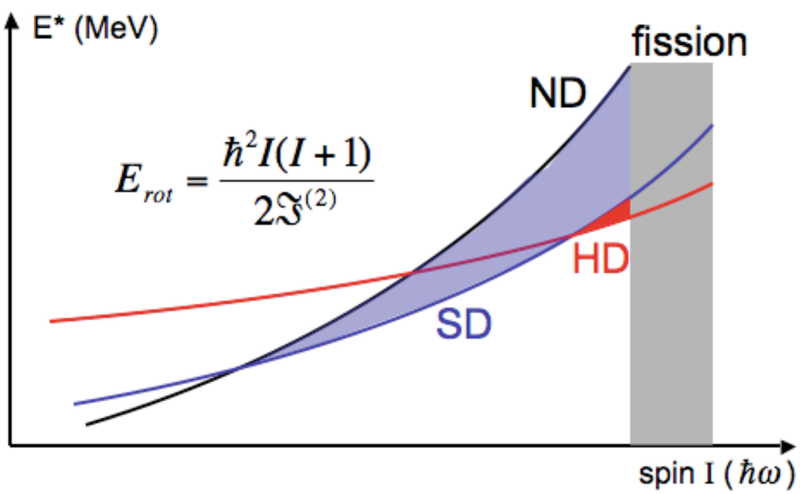

Fission barrier vs. High spin

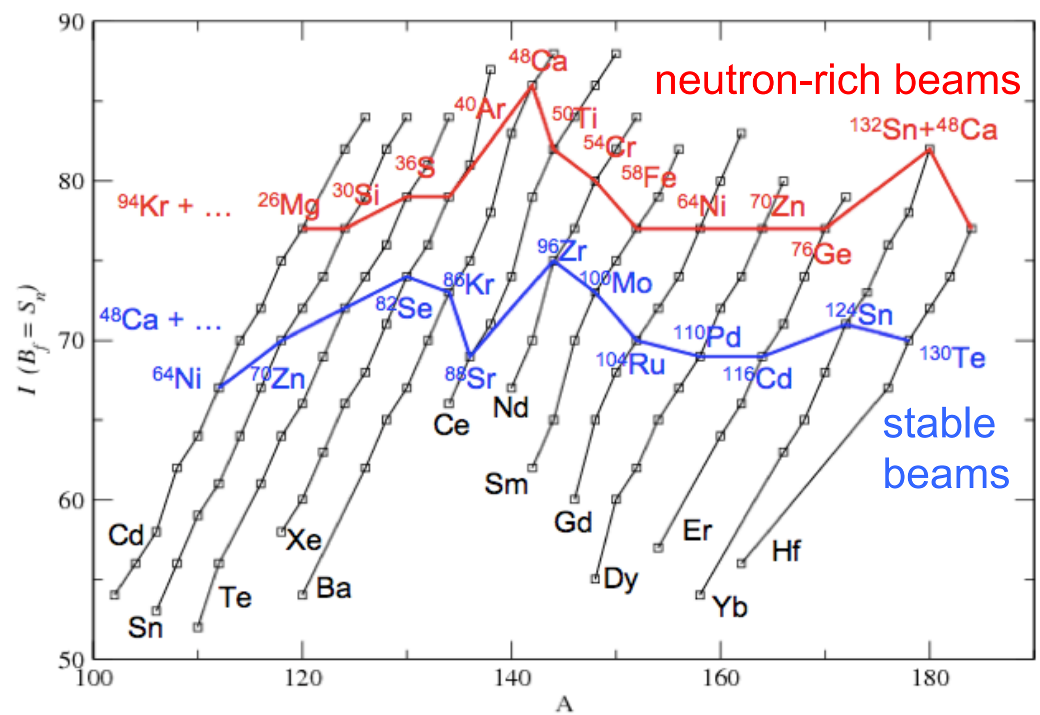

First hints of hyperdeformation

- $^{64}Ni+^{64}Ni$ @ 255, 261 MeV
- 4 weeks beam time
- Euroball IV, Strasbourg
- spins above 70 ħ populated

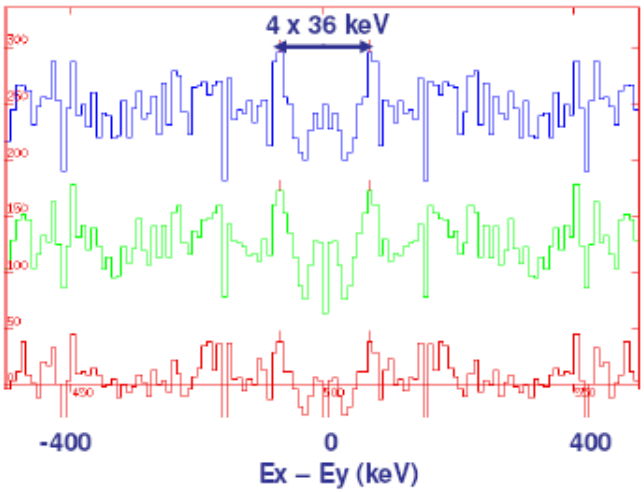

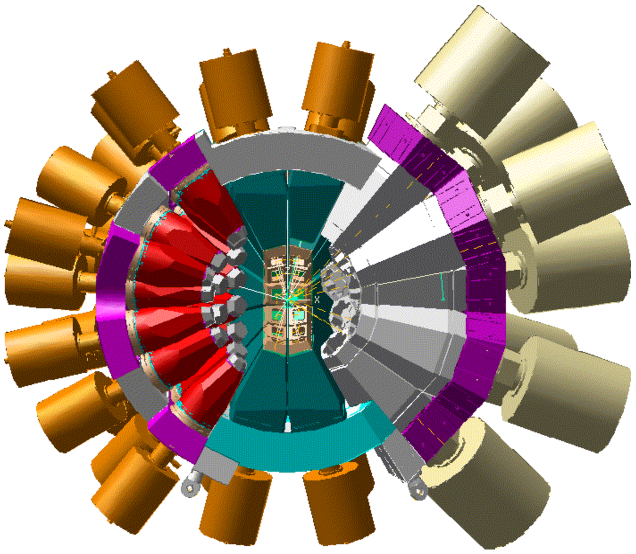

- Ridges observed, corresponding to large $J^{(2)} = 110$ -120 $\hbar^2 MeV^{-1}$, but no discrete bands

D. R. Lafosse *et al.*, Phys. Rev. Lett. **71**, 231 (1995).

- Other claims from resonances produced in (d,p)-followed-by-fission measurements interpreted as rotational bands in hyperdeformed potential well

A. Krasznahorkay *et al.*, Phys. Rev. Lett. **80**, 2073 (1998)

Higher multipole moments: octupole deformation

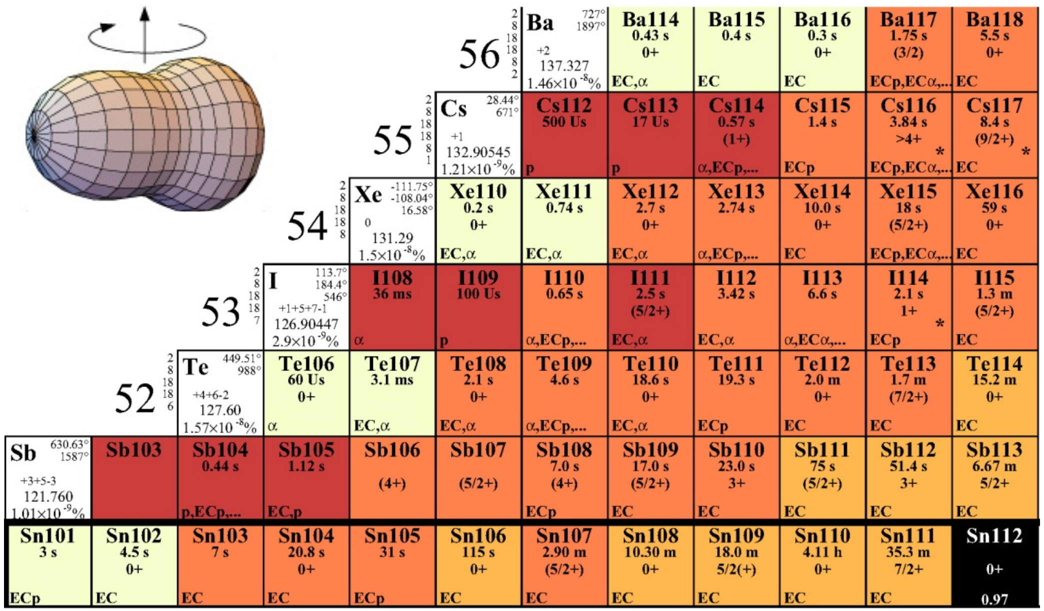

$$R(\vartheta,\phi) = R_0\left[1+\sum_{\lambda}\sum_{\mu=-\lambda}^{+\lambda} a_{\lambda\mu}\, Y_{\lambda\mu}(\vartheta,\phi)\right]$$

- ❑ Octupole deformation: **axial symmetry** and **$\alpha_{30}\neq 0$**
- ❑ In regions of the nuclear chart with ΔI=3 and parity change at the Fermi surface
  Ex. Xe region, close to the N=Z line

- ❑ Characterized by:
- ▪ **Strong static octupole moment Q_{30}**
- ▪ **low-lying 3^-** excitations (even-even nuclei)
- ▪ **strong B(E3)** strength

Predictions for ground-state octupole deformation

P. Möller et al. / Atomic Data and Nuclear Data Tables 94 (2008) 758–780

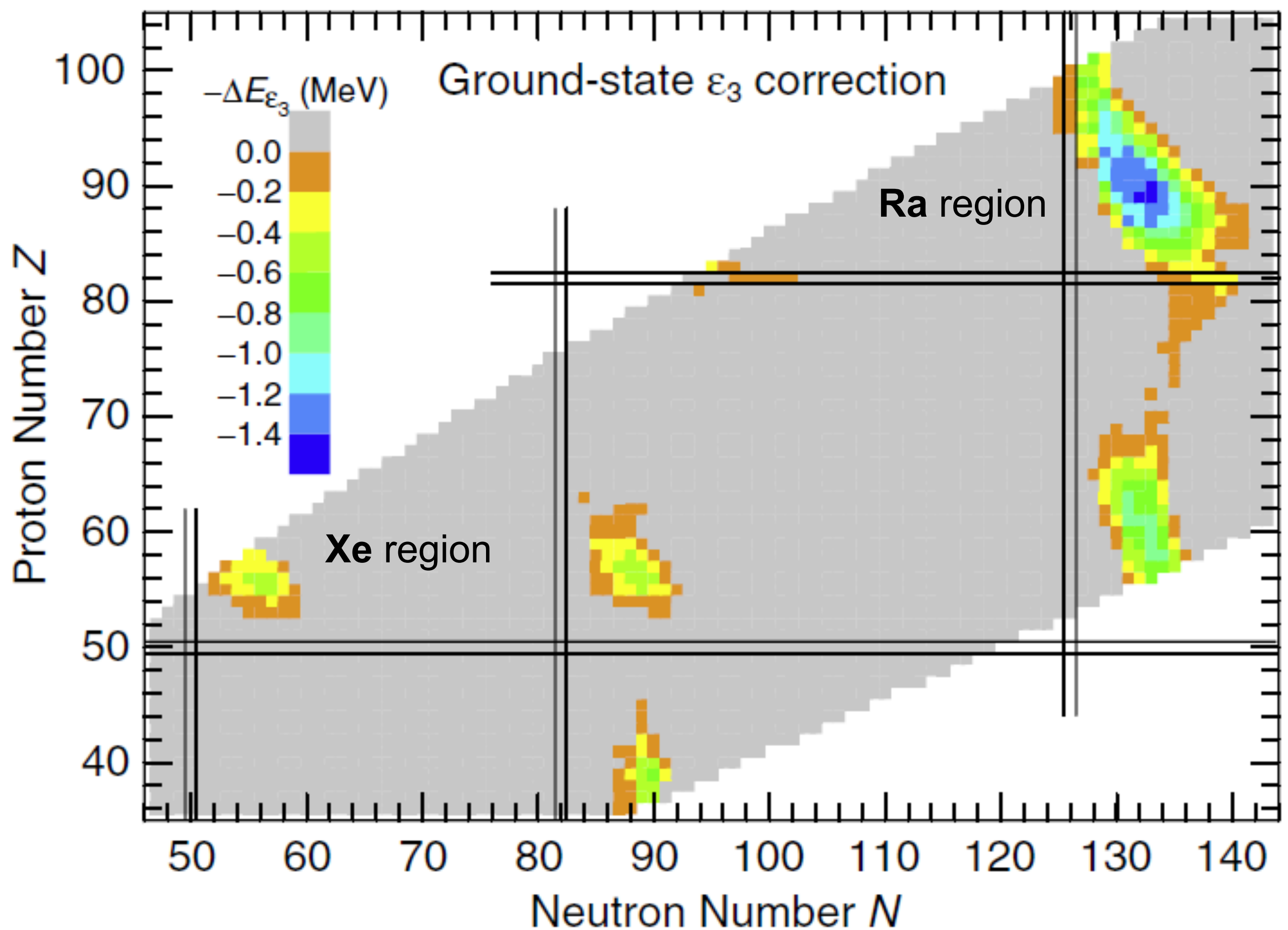

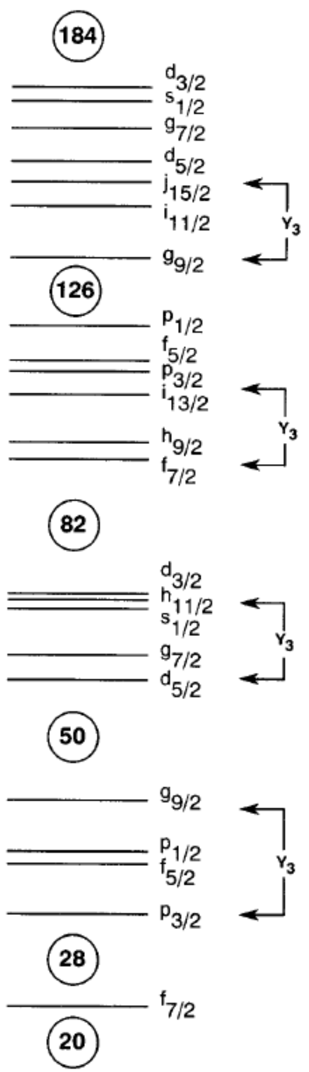

Higher multipole moments: octupolar deformation

ARTICLE
doi:10.1038/nature12073

L. P. Gaffney *et al.*, Nature 497, 204 (2013)

Studies of pear-shaped nuclei using accelerated radioactive beams

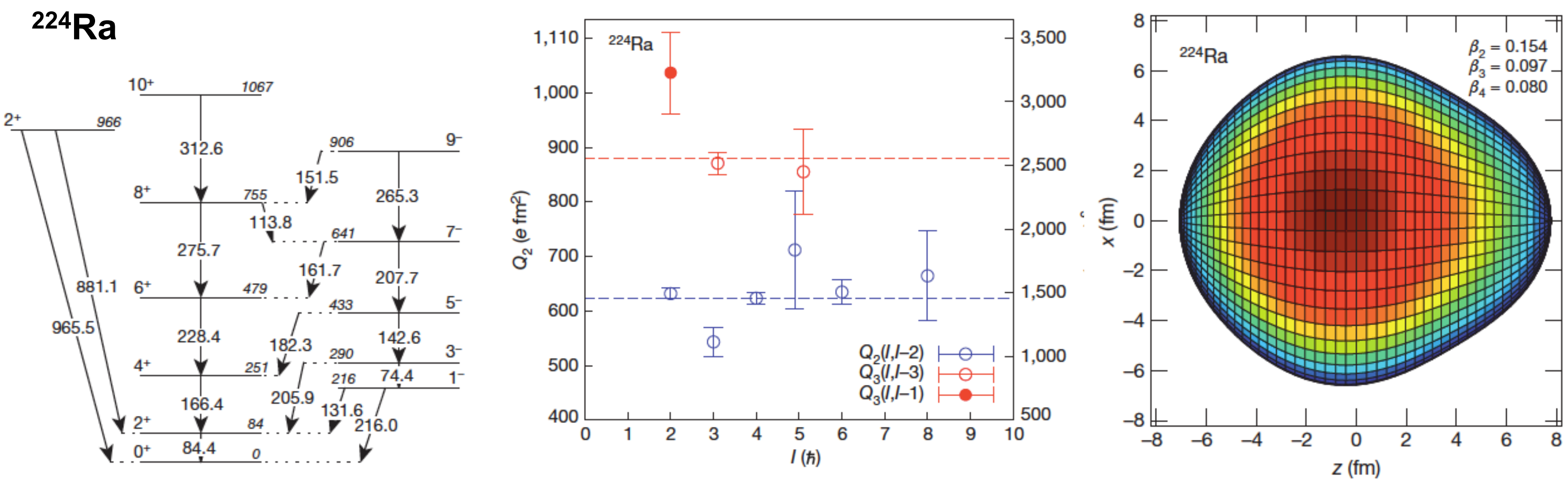

- ❑ Low-energy Coulomb excitation of ^{220}Rn and ^{224}Ra at REX-Isolde, CERN
- ❑ Incident energy of 2.8 MeV/nucleon, Ni and Sn secondary targets
- ❑ Quadrupole Q_2 and octupole Q_3 moments measured
- ❑ ^{224}Ra shows a strong octupole deformation

Octahedral and Tetrahedral Symmetries

- Spontaneous symmetry breaking may lead to high level degeneracies in deformed nuclei

- Group theory gives such high symmetry configurations

$$R(\vartheta,\phi) = R_0\left[1 + \sum_{\lambda}\sum_{\mu=-\lambda}^{+\lambda} a_{\lambda\mu}\, Y_{\lambda\mu}(\vartheta,\phi)\right]$$

- Two symmetries lead to **4-fold degeneracies in nucleonic levels**

Octahedral symmetry

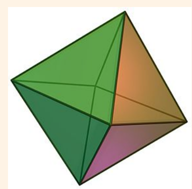

Lowest order: $\alpha_{40} \neq 0$

$$\alpha_{4,\pm 4} = \pm\sqrt{\frac{5}{14}} \times \alpha_{40}$$

Figure from J.Dudek

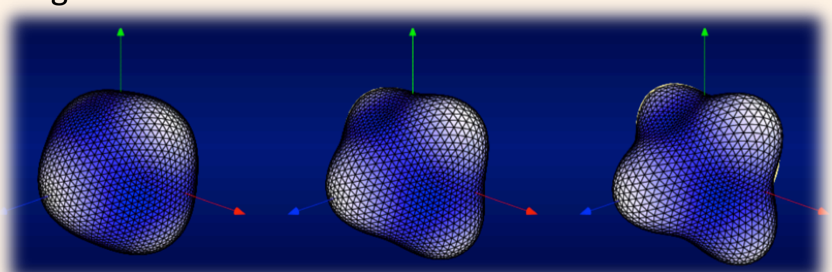

$\alpha_{40} = 0.1$ $\alpha_{40} = 0.2$ $\alpha_{40} = 0.3$

Tetrahedral symmetry

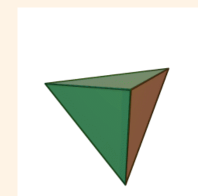

Lowest order: $\alpha_{32} \neq 0$

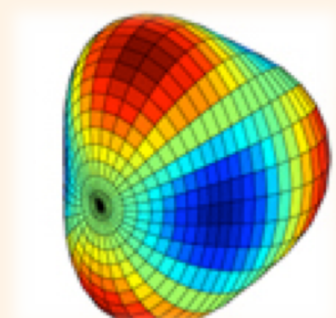

Tetrahedral Signatures

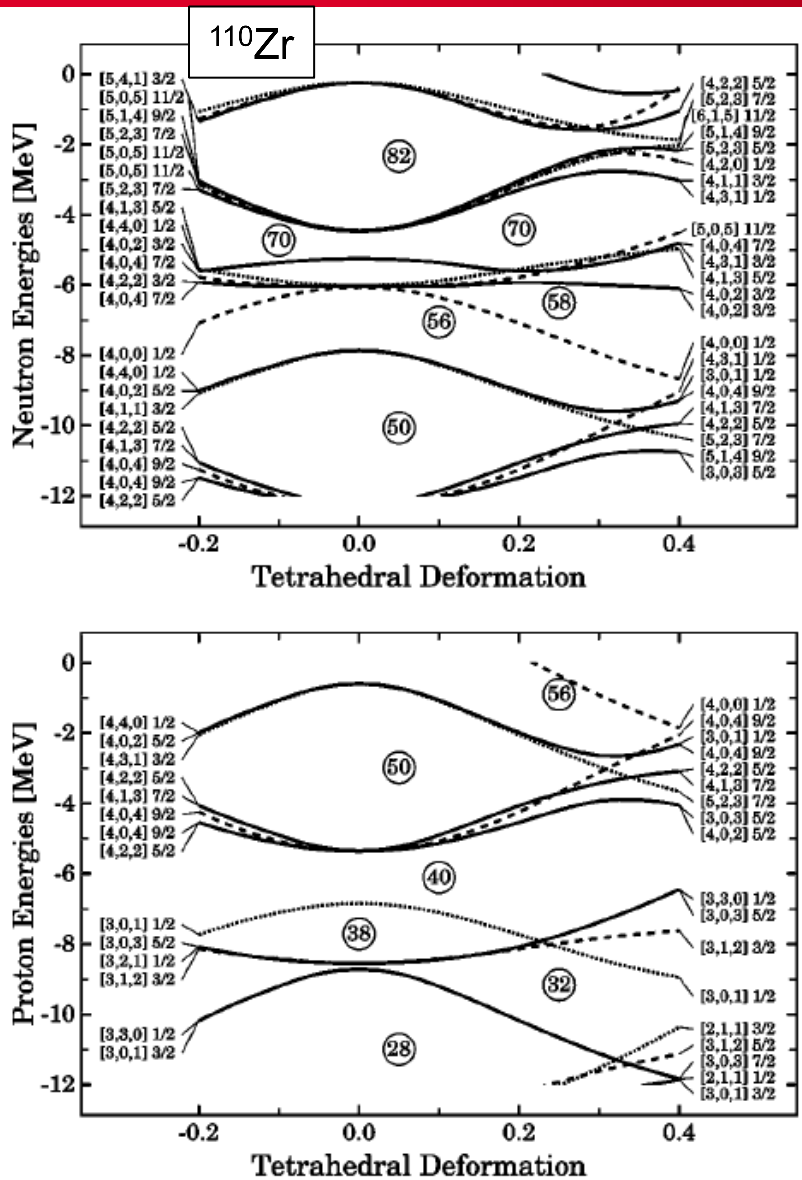

P. Schunck *et al.,* PRC 69 (2004)

Tetrahedral magic numbers: 32, 40, 56, 64, 70,90,132-136

Predicted tetrahedral nuclei: $^{64,72,88}Ge$, $^{80,110}Zr$, $^{112,126,146}Ba$, $^{134,154}Gd$, ^{160}Yb, ^{222}Th

Signatures:

- ❑ **level ordering:** $3^-, 4^+, 6^+, 6^-, 8^+$…
- ❑ Decay pattern of specific groups of states

- ❑ Never evidenced experimentally

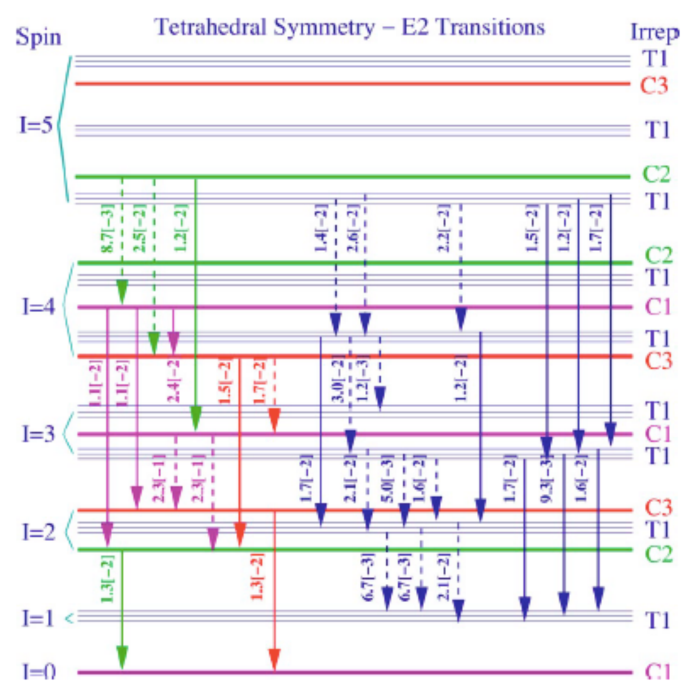

Spectroscopy of ^{110}Zr

- 40 protons 70 neutrons: tetrahedral magic numbers
- Some calculations predict tetrahedral minimum preferred over spherical or deformed minima
- Most calculations predict prolate deformed minimum
- ^{110}Zr was claimed of astrophysical interest (r process)

Tetrahedral minimum

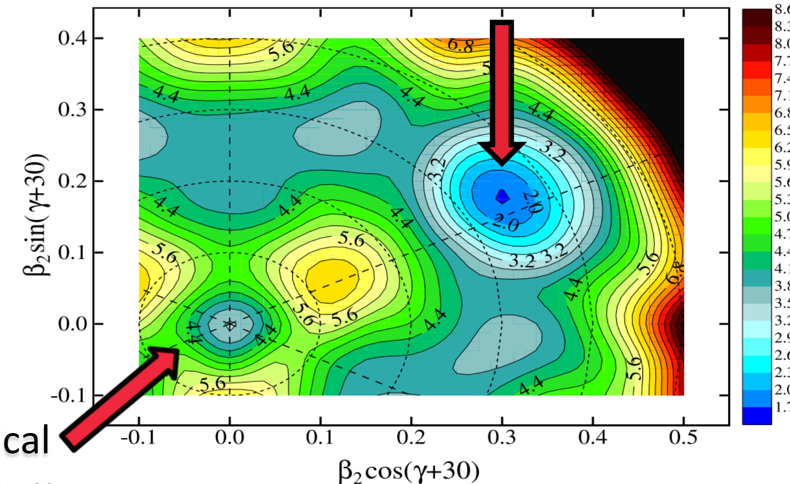

Spherical minimum

Figure from N. Schunck *et al*, PRC 69 (2004)

In-beam gamma Spectroscopy, RIKEN (2015)

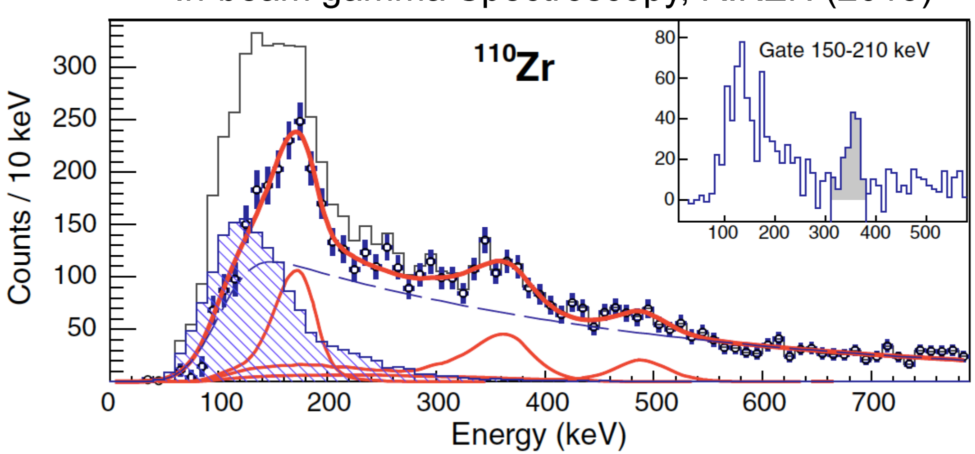

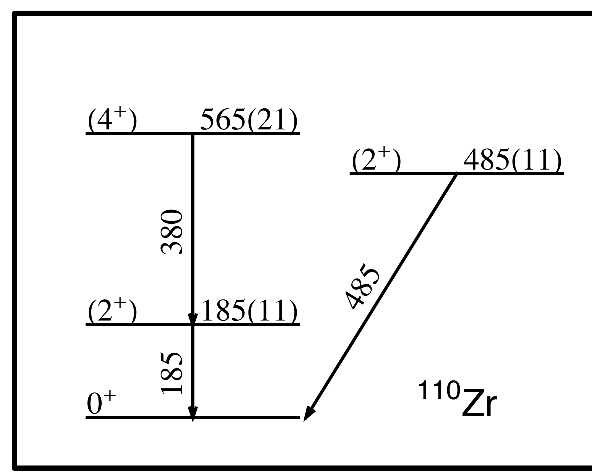

N. Paul *et al.*, PRL 118, 032501 (2017)

Experimental vs theory level scheme comparison

- ❑ Low-lying spectroscopy in agreement with prolate predictions
- ❑ Rejection of a static tetrahedral deformation

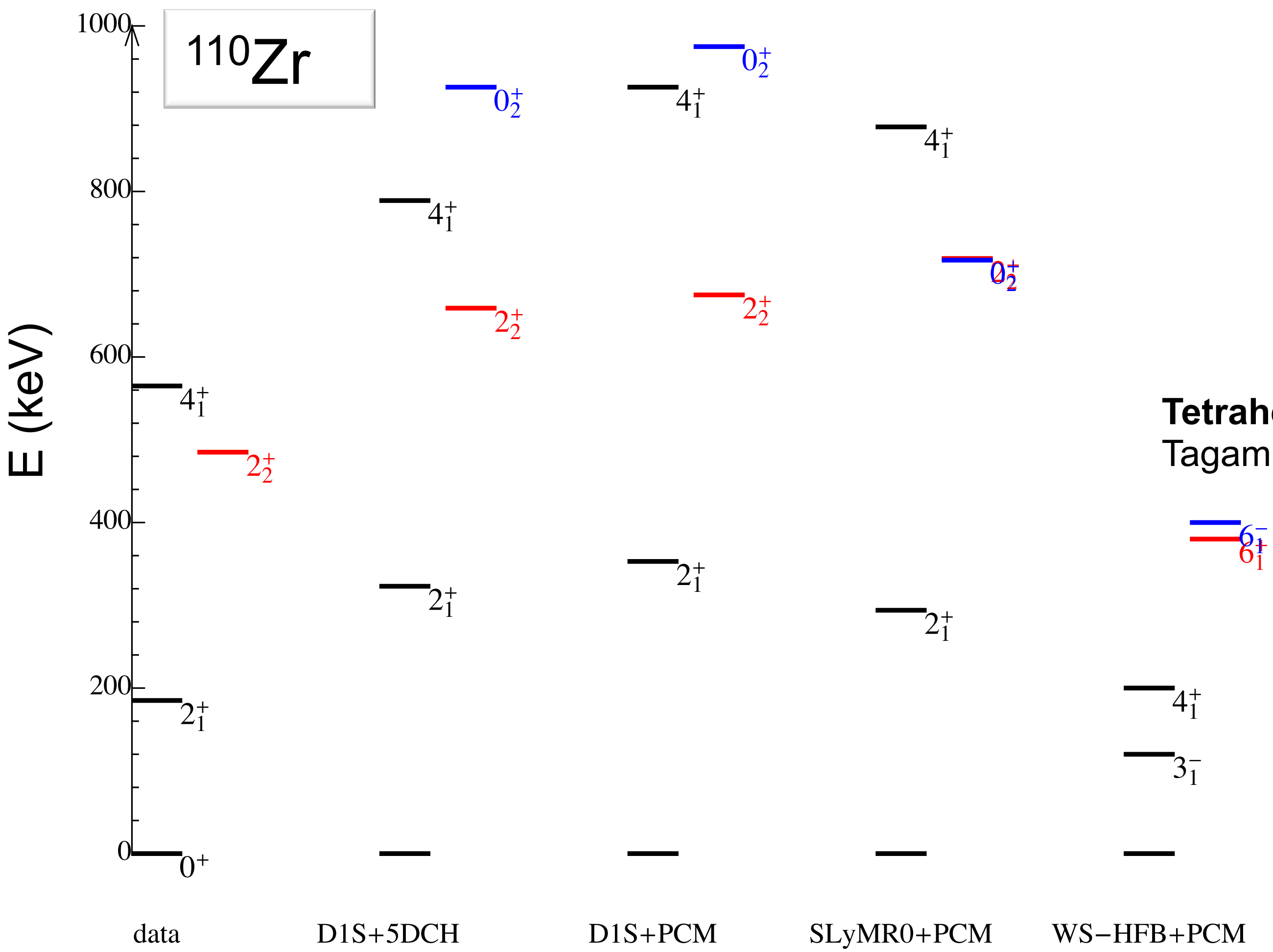

Tetrahedral predictions
Tagami et al, PRC 87 (2013)

2^+ and R_{42} systematics along the N=70 isotonic chain

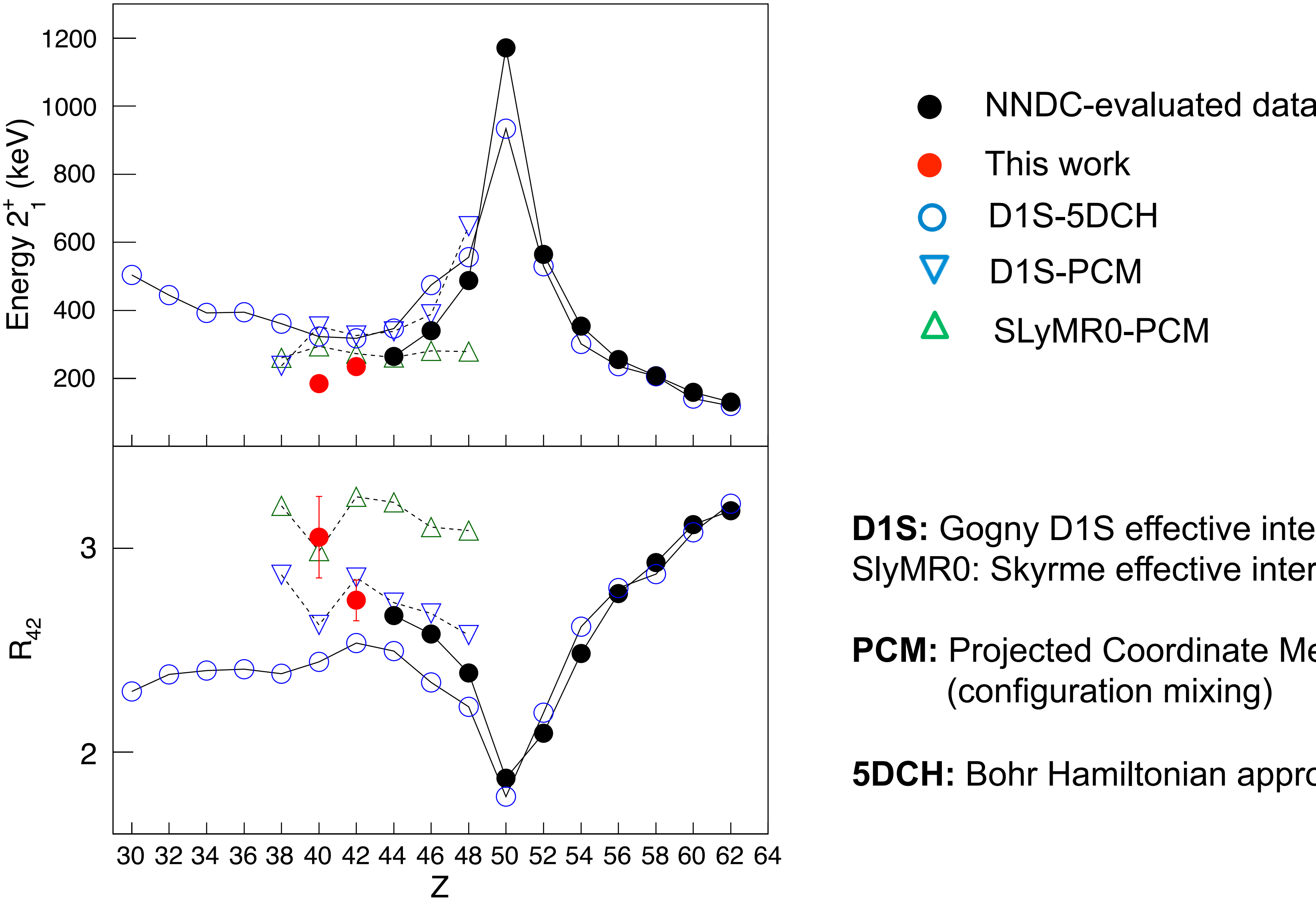

D1S: Gogny D1S effective interaction
SlyMR0: Skyrme effective interaction

PCM: Projected Coordinate Method
(configuration mixing)

5DCH: Bohr Hamiltonian approximation